

University of Montana

ScholarWorks at University of Montana

Graduate Student Theses, Dissertations, &
Professional Papers

Graduate School

1988

The geology and mineralization at the Omar Copper Prospect Baird Mountains Quadrangle Alaska

Peter F. Folger
The University of Montana

Follow this and additional works at: <https://scholarworks.umt.edu/etd>

Let us know how access to this document benefits you.

Recommended Citation

Folger, Peter F., "The geology and mineralization at the Omar Copper Prospect Baird Mountains Quadrangle Alaska" (1988). *Graduate Student Theses, Dissertations, & Professional Papers*. 7440.
<https://scholarworks.umt.edu/etd/7440>

This Thesis is brought to you for free and open access by the Graduate School at ScholarWorks at University of Montana. It has been accepted for inclusion in Graduate Student Theses, Dissertations, & Professional Papers by an authorized administrator of ScholarWorks at University of Montana. For more information, please contact scholarworks@mso.umt.edu.

COPYRIGHT ACT OF 1976

THIS IS AN UNPUBLISHED MANUSCRIPT IN WHICH COPYRIGHT
SUBSISTS. ANY FURTHER REPRINTING OF ITS CONTENTS MUST BE
APPROVED BY THE AUTHOR.

MANSFIELD LIBRARY
UNIVERSITY OF MONTANA
DATE: 1988

THE GEOLOGY AND MINERALIZATION AT THE OMAR COPPER
PROSPECT, BAIRD MOUNTAINS QUADRANGLE, ALASKA

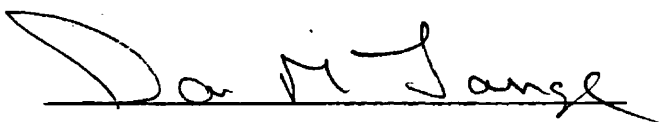
by

Peter F. Folger

A.B. Dartmouth College, 1982

Presented in partial fulfillment of the requirements
for the degree of
Master of Science
University of Montana
1988

Approved by



Chairman, Board of Examiners



Dean, Graduate School



Date

UMI Number: EP38241

All rights reserved

INFORMATION TO ALL USERS

The quality of this reproduction is dependent upon the quality of the copy submitted.

In the unlikely event that the author did not send a complete manuscript and there are missing pages, these will be noted. Also, if material had to be removed, a note will indicate the deletion.



UMI EP38241

Published by ProQuest LLC (2013). Copyright in the Dissertation held by the Author.

Microform Edition © ProQuest LLC.

All rights reserved. This work is protected against unauthorized copying under Title 17, United States Code



ProQuest LLC.
789 East Eisenhower Parkway
P.O. Box 1346
Ann Arbor, MI 48106 - 1346

Folger, Peter Franklin, M.S., March 1988 Geology

The Geology and Mineralization at the Omar
Copper Prospect, Baird Mountains, Alaska

Director: Ian Muirhead Lange 

Copper sulfide mineralization is stratabound and discordant within Devonian dolostone host rocks at the Omar Prospect, 100 km northeast of Kotzebue, Alaska. Pyrite and chalcopyrite are disseminated within organic/insoluble-rich zones in bioclastic wackestone to packstone. The organic material may have been the loci for bacterial reduction of seawater sulfate, which provided reduced sulfur that reacted with iron and copper to form early pyrite and chalcopyrite. Chalcopyrite, tennantite/tetrahedrite, and bornite replaced pyrite within the organic/insoluble-rich zones. Discordant veins comprised of commonly euhedral dolomite and chalcopyrite and bornite cut earlier mineralization and form a stockwork or breccia. Some breccia textures resemble incipient solution collapse, and may have formed as a result of dissolution by meteoric waters, hydrothermal fluids, or acids generated by thermal degradation of kerogen. Late calcite-quartz-malachite-chalcopyrite veins crosscut earlier textures and may represent remobilization of copper during deformation and metamorphism associated with the mid-Jurassic to Cretaceous Brooks Range orogeny.

Conodont alteration indexes suggest all lithologies at Omar reached a minimum of 300-350°C, corresponding to lower greenschist facies metamorphic temperatures. Conodonts from mineralized dolostones do not reflect anomalously high temperatures, suggesting hydrothermal fluids were below 300-350°C. Pyrobitumen blebs spatially associated with mineralization suggest that hydrothermal fluids may have generated and transported liquid hydrocarbons; however, hydrocarbons were not genetically associated with sulfide precipitation.

Copper, lead, zinc, cobalt, arsenic, silver, +/- manganese constitute a trace element suite useful as a pathfinder for Omar-type mineralization. Omar shares many characteristics with some Mississippi Valley-type deposits, particularly deposits in southeast Missouri, but is most similar to carbonate-hosted discordant copper deposits like Ruby Creek, Alaska, and the Cooley and Ridge deposits in Australia.

Table of Contents

Abstract.....	p.ii
Introduction and Previous Work.....	p.1
Regional Geology.....	p.4
Stratigraphy at Omar.....	p.7
Ordovician Lithologies.....	p.8
Devonian Lithologies.....	p.18
Lithologies of Unknown Age.....	p.21
Structure.....	p.21
Mineralization.....	p.30
Introduction.....	p.30
Subsurface Mineralization.....	p.31
Surface Mineralization.....	p.37
Cathodoluminescence Studies.....	p.65
Maturation of Organic Material in Mineralized and Unmineralized Rocks.....	p.74
ROCK-EVAL Pyrolysis Study.....	p.82
Carbonate Staining.....	p.87
Trace Element Geochemistry of Rocks, Soils, and Stream Sediments.....	p.90
Statistical Methods.....	p.90
Rocks.....	p.92
Soil and Stream Sediments.....	p.101
Lead Isotopes.....	p.110
Fluid Inclusions.....	p.112
Discussion.....	p.114
The Relationship Between Organic Material and Mineralization.....	p.114
Stratabound Mineralization.....	p.119
Sources of Metals and Fluids.....	p.121
Comparison to Other Deposits.....	p.122
Suggestions for Exploration.....	p.126
Summary.....	p.127
Conclusions.....	p.131

References.....p.132

Appendix A. Trace Element Geochemical Data.....p.142

Appendix B. Analytical Procedure and Equipment for
ROCK-EVAL Pyrolysis by EXLOG Laboratories, Anchorage,
Alaska.....p.152

List of Figures

Figure 1	Location map showing northwest Alaska.....	p.2
Figure 2	Geologic map of the Omar Copper Prospect (pocket)	
Figure 3	Photographs and photomicrograph of kink folding in Ordovician metalimestone.....	p.23
Figure 4	Geologic cross sections A-A' and B-B'.....	p.27
Figure 5	Thrust/reverse fault showing metalimestone thrust over dolostone.....	p.29
Figure 6	Simplified geologic logs from Bear Creek Mining Company and interpretive correlation..	p.35
Figure 7	Photomicrographs of organic-rich zones in Devonian dolostone and association of sulfides to organic material.....	p.41
Figure 8	Photomicrographs of copper and iron sulfide textures showing replacement and exsolution textures.....	p.44
Figure 9	Photomicrographs of copper sulfide veinlets cutting earlier disseminated mineralization..	p.48
Figure 10	Photomicrograph of copper sulfide veinlet cutting dolostone.....	p.49
Figure 11	Photomicrograph of copper sulfide veinlet with euhedral dolomite gangue.....	p.49
Figure 12	Photomicrograph of copper sulfide vein with slightly corroded dolomite gangue.....	p.50
Figure 13	Photomicrographs of bornite and chalcopyrite exsolution textures.....	p.53
Figure 14	Breccia texture in Devonian dolostone.....	p.55
Figure 15	Comparison between mineralized and unmineralized breccias.....	p.56
Figure 16	Photomicrographs of coated grains with bornite filling the grain core.....	p.57
Figure 17	Contoured Pi diagram of vein orientations from Copper Hill.....	p.60
Figure 18	Photographs of late calcite and quartz veins cutting Devonian dolostone.....	p.61
Figure 19	Photograph of silicified outcrop of Devonian dolostone.....	p.62
Figure 20	Photograph of dolostone gossan.....	p.64
Figure 21	Photograph of late calcite quartz vein crosscutting foliation in metalimestone.....	p.64

Figure 22	Photomicrographs of gangue dolomite within copper sulfide veinlets under plane polarized light and cathodoluminescence showing growth zoning in the dolomite.....	p.67
Figure 23	Photomicrographs of gangue dolomite showing growth zoning under cathodoluminescence.....	p.69
Figure 24	Photomicrographs of zoned dolomite in quartz and dolomite-filled cavity.....	p.72
Figure 25	Photograph of pyrobitumen in dolomite and calcite veinlets within Devonian dolostone..	p.77
Figure 26	Photomicrographs of zoned dolomite under cathodoluminescence within pyrobitumen-filled veinlets.....	p.78
Figure 27	Photomicrographs of spheroidal pyrobitumen blebs partially replaced by pyrite and chalcopyrite within dolomite and quartz-filled vugs.....	p.81
Figure 28	Geochemical factor map of rock samples.....	p.98
Figure 29	Geochemical factor map of soil samples.....	p.104
Figure 30	Geochemical factor map of stream sediment samples.....	p.107
Figure 31	Schematic diagram showing mineralizing events and postmineralizing veining and remobilization.....	p.130

List of Tables

Table 1	Ages, CAIs, and paleoenvironmental interpretations from conodont samples.....	p.10
Table 2	CAIs and corresponding minimum temperatures.....	p.13
Table 3	Summary of BCMC drill logs for drill holes 5, 6, 16, 17.....	p.32
Table 4	Mineral occurrence chart.....	p.39
Table 5	Results from ROCK-EVAL pyrolysis.....	p.83
Table 6	Results of Alizirin Red-s/Potassium ferricyanide staining.....	p.88
Table 7	Univariate statistics for rock data.....	p.93
Table 8	Factor loadings for rock data.....	p.96
Table 9	Geochemical values for rocks samples with high factor loadings on factors 2 and 4.....	p.100
Table 10	Univariate statistics for soil data.....	p.102
Table 11	Factor loadings for soil data.....	p.105
Table 12	Factor loadings for stream sediment data.....	p.108
Table 13	Univariate statistics for stream sediment data.....	p.109
Table 14	Lead isotope data.....	p.111
Table 15	Fluid inclusion data.....	p.113

Acknowledgements

I thank many people in the U.S.G.S for their help with this project. Sue Karl gave me the initial funding and encouragement with the thesis. Jeanine Schmidt spent days in the field and probably more days poring over the manuscript. Julie Dumoulin helped me with carbonates and conodonts. Anita Harris identified conodonts which helped enormously with the stratigraphy. Rich Goldfarb shoveled dirt and gave the manuscript his very careful attention. Randy Baker survived my cooking. Lanier Rowan provided invaluable advice about cathodoluminescence and fluid inclusions, as well as giving me the benefit of her knowledge of carbonate-hosted deposits. Dave Leach also provided much information on mid-continent ore deposits. Joel Leventhal was very helpful with interpreting the organic material, as well as explaining the pros and cons of rock-eval pyrolysis. John Gray carried rocks like a trooper and helped out with the fieldwork, and the entertainment.

I would like to especially thank Ian Lange, chairman of the thesis committee, and the other members of my committee: Arnie Silverman, Don Loftsgaarden, and Stan Church.

I would also like to thank Jay Hammett of Kennecott Exploration for company reports and maps.

And, of course, Rick Zehner provided spiritual, as well as intellectual, guidance.

Introduction and Previous Work

The Omar copper prospect, approximately 100 km northeast of Kotzebue, Alaska, is in the Baird Mountains 10 x 30 quadrangle (67° 30'N, 160° 55'W; Fig. 1). Discontinuously mineralized dolostones are exposed within a 1 by 3 km area (Fig. 2) between the western fork of the Omar river and the North Fork of the Squirrel River. Chalcopyrite, bornite, lesser covellite and pyrite, minor chalcocite and tennantite-tetrahedrite, and rare galena, together with supergene copper carbonates and iron oxides are exposed at the surface. Lesser amounts of chalcocite occur in the subsurface than are exposed at the surface.

Subsurface information is limited to Bear Creek Mining Company (BCMC) drill logs. Petrography on polished and regular thin sections and cathodoluminescence provided information about the mineralization history at Omar. Conodont alteration indexes (CAIs) and a study of the maturity of organic material gave some information on the thermal history of Omar host rocks. Staining of the host rocks with alizarin red-s and potassium ferricyanide

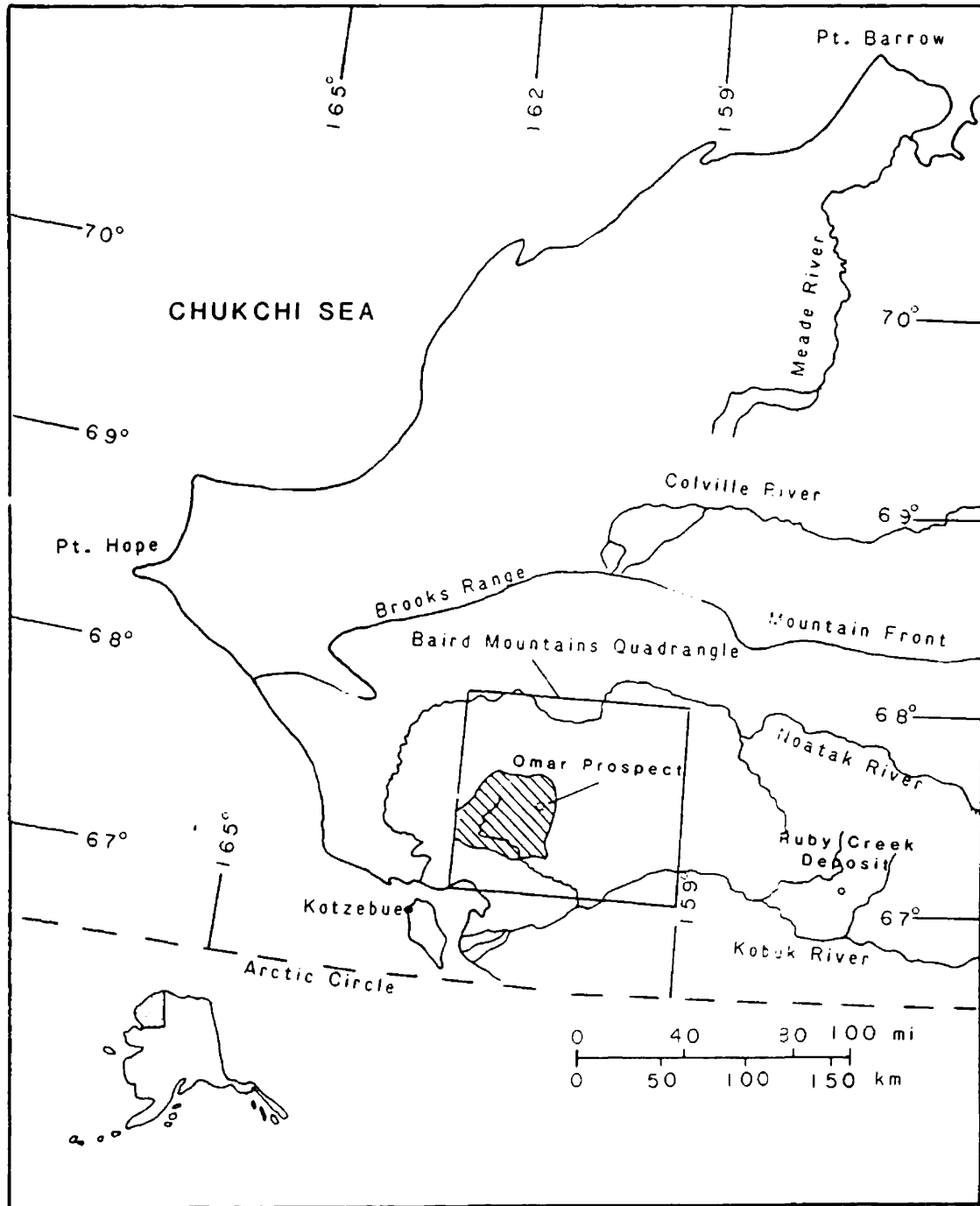


Fig. 1. Location of the Omar Copper Prospect. The shaded area in the Baird Mountains quadrangle marks the approximate boundary of the Squirrel/Omar River carbonate rocks.

revealed variations in the iron content of calcite and dolomite that may be related to mineralization.

I describe the textural relationships between sulfide minerals and gangue minerals, the host carbonate rocks, and timing and controls of mineralization. The trace element lithogeochemical characteristics, and secondary geochemical dispersion halos in both stream sediment and soils are discussed to aid in the development of exploration models.

Bear Creek Mining Company (BCMC) discovered significant copper sulfide mineralization at Omar in 1962 after a regional stream sediment reconnaissance, drilled 19 diamond drill holes between 1966 and 1967, and continued assessment work until 1972. Unfortunately, this core was discarded at the headwaters of Omar Creek (Fig. 2) and only fragments remain.

Watts, Griffith, and McQuat (WGM Inc.), under contract to the U.S. Bureau of Mines, conducted geologic mapping and soil sampling in 1977 (Degenhart and others, 1978), and Jansons (1982) determined the cobalt content of rock, stream sediment, and soil samples from the prospect. Folger and others (1985) compared the use of insoluble residues from stream sediments to conventional untreated samples from Omar Creek in an attempt to enhance dispersion halos. New conodont dates and conodont

alteration indexes (CAIs) collected during this study and by A. Harris and J. Dumoulin (written communication, 1985, 1986) are included in this report. This paper results from 23 days of field work during the summers of 1984 and 1985, and subsequent petrographic and lab work at the University of Montana and the U.S. Geological Survey, Branch of Exploration Geochemistry, Golden, Co.

Regional Geology

The Omar Prospect lies within the western Brooks Range fold and thrust belt, an area of complexly folded and faulted Lower Paleozoic (and Precambrian?) to Lower Mesozoic metasedimentary and metaigneous rocks (Fig. 1; Tailleux and Snelson, 1968; Martin, 1970; Mayfield and others, 1983). The central and western Brooks Range is characterized by extensive thrust faulting and crustal shortening of up to 580 km in places, possibly as a result of opening of the Canada Basin to the north (Tailleux and Snelson, 1969; Mull, 1982). In contrast, the northeastern Brooks Range experienced mainly vertical basement-involved uplift with much less horizontal movement (Detterman, 1970; Mull, 1982). Sedimentological evidence from Neocomian to Albian flysch deposited in a foreland deep north of the thrust belt suggests a

mid-Jurassic (?) to Cretaceous age for deformation and thrusting (Mull, 1982).

Predominate rock types within the Baird Mountains quadrangle include highly deformed Lower Paleozoic (and Precambrian?) phyllites and schists in the central and eastern parts of the quadrangle, Devonian and Mississippian Endicott Group metasediments and phyllites (Mull, 1982) in the northern part of the quadrangle, and Lower to Middle Paleozoic carbonate rocks in the west-central (including Omar host rocks) and northeastern parts of the quadrangle. Tailleux and others (1977) suggested Endicott Group clastic rocks and the Paleozoic carbonate rocks are tectonically juxtaposed. Mineralogical evidence (Mayfield, 1976) and conodont alteration indexes from samples collected during the Baird Mountains Alaska Mineral Resources Assessment Program (1983-1985) suggest most rocks in the Baird Mountains quadrangle underwent greenschist and blueschist facies metamorphism (Dumoulin and Harris, 1986).

The previously undifferentiated carbonate rocks of the Squirrel River Basin were presumed to be Silurian to Devonian in age (Fig. 1; Beikman, 1980). More recent studies of the Squirrel River carbonates (Dumoulin and Harris, 1985, 1986), identified both Ordovician and Devonian dolostones and metalimestones that are present

at Omar. As per their classification, the terms dolostone and metalimestone are used here to describe recrystallized carbonate rocks that retain some pre-metamorphic textures. Marbles are rocks that have been totally recrystallized to calcite.

Lower and lower Middle Ordovician rocks are thick sequences of platformal carbonates deposited under slightly restricted to normal marine conditions, in very shallow to intermediate water depths. Up to 250 m of carbonate was deposited in 5 million years (Dumoulin and Harris, 1985, 1986). Normal to slightly ferroan dolostone, commonly finely laminated and displaying fenestral fabric, was deposited both in lower and upper intertidal environments. Some of the fenestrae may reflect original algal laminations, but others were probably produced by penecontemporaneous evaporite growth and later dissolution or replacement (Dumoulin and Harris, 1986). Dolomitic to argillaceous metalimestone was deposited under deeper water conditions. Lower Ordovician rocks near the Omar deposit are locally bioturbated packstone and grainstone with laminated and scoured beds.

Distinctly different Lower to lower Middle Devonian dolostone, metalimestone, and lesser marble are also found in the Squirrel/Omar River drainages. The Devonian

dolostone, locally cherty and consisting mostly of bioclastic packstone, was deposited over a range of normal marine shelfal depositional environments. In contrast to Ordovician rocks, the Devonian rocks contain a sparse to abundant megafauna of corals, stromatoporoids, gastropods, brachiopods, and bryozoans (Dumoulin and Harris, 1986).

Minor amounts of basaltic(?) sills, dikes, and flows within the Squirrel River carbonate rocks, occur 8 to 15 km north and east of Omar. Their age is unknown but probably Paleozoic based on field relations with Ordovician and Devonian carbonate rocks.

Stratigraphy at Omar

The stratigraphy at the Omar prospect (3 km²) consists of unnamed metalimestones and dolostones included within the Devonian and Ordovician carbonate rocks described by Dumoulin and Harris (1986). Previous work (BCMC, unpublished reports; Degenhart and others, 1978), defined a number of carbonate lithologies of unknown, but presume Devonian age.

The stratigraphic units used in this paper were defined by field and petrographic observations; ages were

determined by conodonts (A. Harris, written communication, 1985,1986). Similar-looking Lower to Middle and Middle to Upper Ordovician dolostones were distinguished primarily by conodonts ages. Silurian lithologies are rare in the Squirrel River drainage basin, and no Silurian lithologies were identified at Omar. An unconformity of Late Ordovician and/or Early Silurian time is suspected to occur in the Squirrel River basin (Dumoulin and Harris, 1986).

Ordovician Lithologies

Although recrystallization has obscured many primary features, conodont assemblages as well as sedimentary textures in some well-preserved dolostones lend insight into the original depositional environment. Ordovician rocks contain few megafossils are generally more recrystallized than Devonian lithologies at Omar. Conodont species associations from Ordovician rocks, however, have suggested specific depositional environments. Table 1 contains the paleoenvironmental interpretations provided by A. Harris (written communication, 1985,1986). Ordovician dolostones were deposited under warm and shallow water conditions.

Ordovician metalimestone may be a deeper water facies although the particular conodont fauna recovered at Omar are not diagnostic paleoenvironmental indicators (OM154, Table 1).

Table 1. Ages, CAI values, and paleoenvironmental association from conodont faunal association (all data from A. Harris, written communication, 1985-1986).

Sample #	Age	CAI	Paleoenvironment	Unit
8-13-83H	Early Devonian	5-6	----	5
OM55	Early Devonian	5-5.5	----	5
OM60	Early Devonian	5	----	5
OM63	Early Devonian	5-5.5	----	5
OM67	Early Devonian	5.5-6	----	5
OM156	Early Devonian	5-5.5	----	5
OM118	Early Devonian	5	Warm, shallow water, high energy	5
OM64	Middle Devonian	5-5.5	----	5
OM60	Middle Devonian	5	----	5
OM160	Middle Devonian	5	----	5
OM54	Early Devonian- Early Mississippian	7-8	----	5
OM88	Early to Middle Devonian	5.5	----	5
OM136	Middle to Late Ordovician	7-8	Restricted, warm, shallow water, innermost platform association	4
OM100	Middle to Late Ordovician	5.5-7	Restricted, warm, innermost platform association.	4
OM146	Middle to Late Ordovician	5.5 and 7-8	Restricted, warm, innermost platform association.	4
OM147	Middle to Late Ordovician	7-8	Restricted, warm, innermost platform association.	4
OM145	Middle Ordovician	7-8	Restricted, warm, innermost platform association.	4

Table 1 (continued)

OM86	early Middle Ordovician	6-7	Restricted to normal marine, shallow to very shallow platform association.	2
OM102	Early to early Middle Ordovician	5.5-6	Normal marine shelfal or platformal.	2
OM51	Early to early Middle Ordovician	5.5	Normal marine, open shelf	2
OM63	late Early Ordovician	6	----	2
8-13-83E	late Early Ordovician	5.5-6.5	Warm, shallow water biofacies	2
OM151	late Early Ordovician	7-8	Warm, shallow water biofacies	2
OM57	late Early Ordovician	5.5-6	Warm, shallow water biofacies	2
OM87	late Early Ordovician	5.5-6	Shallow to mid-shelf, normal marine	2
OM106	early Early Ordovician	5.5-6	----	2
OM112	early Early Ordovician	5.5	Normal, marine shelfal to platformal species.	2
OM155	early Early Ordovician	5-5.5	Warm, shallow water association	2
OM154	early Early Ordovician	5.5	Pelagic fauna, no water temperature interpretation.	1

Most Ordovician rocks at Omar are dolostones, with a generally fine-grained matrix of interlocking dolomite crystals and sparse calcite crystals. The rocks are commonly bleached, often changing from medium or dark gray to light gray along strike. Anomalously high Conodont Alteration Indexes (CAIs) from some samples of Ordovician dolostone record apparent temperatures of up to 490° C (Tables 1 and 2) and probably indicate hydrothermal (and oxidizing) fluids interacted locally with the rocks. (A. Harris, written communication, 1986). CAIs correspond to progressive and irreversible color changes of conodonts, usually in response to temperature and duration of burial (Epstein and others, 1977). Epstein and others (1977) established temperature and time intervals for each color based on experimental and field evidence (Table 2).

Table 2. Minimum Temperatures of Heating
 Corresponding to Conodont Alteration Indexes
 (Epstein and others, 1977; A. Harris, written
 communication, 1985-1986)

CAI	Minimum Temperature ° C
5	300
5-5.5	300-350
5.5	350
5.5-6	350-400
6	400
6-7	400-500
7-8	490+

Because CAIs (5-6) for most carbonates in the Omar area reflect minimum burial temperatures of 300-350o C (Table 1), CAIs of 7-8 probably recorded very local, and relatively shorter, interactions with hydrothermal fluids that may have bleached the rocks, and altered conodont colors to give misleading temperature estimations (A. Harris, written communication, 1985,1986). Bleached areas and high CAIs do not correspond to areas of copper sulfide mineralization; their origin is unknown.

The two varieties of Ordovician dolostone are distinguished by conodont microfossils and field relationships. Conodont fauna from dolostones fall into three age groups: early Early Ordovician, late Early to early Middle Ordovician, and Middle to Late Ordovician (Table 1). Lower Lower Ordovician and upper Lower to lower Middle Ordovician dolostone were mapped as one unit because both units were texturally indistinguishable in the field. The Middle to Upper Ordovician dolostone locally displayed more distinctive light and dark laminations than older dolostone units.

Veinlets of coarser dolomite or calcite cut the matrix of all Ordovician dolostones, and lesser amounts of quartz fills both veinlets and small pockets within the matrix. Stylolites are generally present but not

abundant, and are commonly sutured (interpenetrating pillar and socket surfaces; Wanless, 1979). Both veins and sutured stylolites probably formed after lithification of the carbonate.

One sample of platy-weathering metalimestone at Omar yielded an early Early Ordovician age, and is the oldest mappable unit recognized at Omar. Samples from a similar platy-weathering brown to orange to gray metalimestone that lies in apparent stratigraphic contact above the Lower to Middle Ordovician dolostone contained unrecognizable conodonts (A. Harris, written communication, 1985, 1986). Hence, based on field relations, I assigned an Earliest Ordovician age to one platy-weathering metalimestone (unit 1) and an uncertain, though probably Ordovician age, to the other platy-weathering metalimestone unit (unit 3; Fig. 2). The platy-weathering brown to orange to gray metalimestone is a common lithology in the western Baird Mountains quadrangle, probably representing a single depositional environment, though not necessarily a single age.

Unit 1-Lower Lower Ordovician Metalimestone. A brown-gray to orange-gray weathering metalimestone is fine to coarsely crystalline (.2 to .8 mm) and is commonly platy-weathering. It contains laminae of dark and light

carbonate ranging from <1mm to 6cm thick. Laminae are occasionally disrupted by oval blobs of coarse, crystalline white calcite, that were stretched and deformed during metamorphism.

The metalimestone varies from a fairly uniform texture of interlocking calcite crystals with scattered dolomite crystals to a consistently banded texture with layers of coarse (<1 to 3 mm), sparry, calcite crystals and thinner laminae of opaque insoluble material containing small (.04 to .1 mm) dolomite crystals. The insoluble material may be either original compositional variation, or resulted from compaction and carbonate dissolution during diagenesis (Shinn and Robbin, 1983). These laminae commonly contain pyrite, are continuous for at least 2 to 5 cm, and are .5 to 1 mm thick. Quartz (<.2 mm across) occurs with the organic/insoluble-rich layers; less commonly with the coarser calcite. White mica and chlorite occur on some partings between calcite layers (J. Dumoulin, oral communication, 1986).

Unit 2-Lower Lower to Lower Middle Ordovician Dolostone.

Lower Lower to lower Middle Ordovician dolostone is light gray, less commonly medium to dark gray, mostly fine-grained (.2 to .5 mm), and massive to less commonly laminated (1-2 cm laminations). The dolostone contains

rare, relict megafossils (I recognized one gastropod), and scattered pyrite grains. Where massive, the dolostone is variably pinkish-white and sugary-textured.

Unit 3-Metalimestone, Uncertain Age although Probably Ordovician. The brown to gray to orange platy-weathering metalimestone is similar to unit 1. It is thinly banded and contains coarsely crystalline (1 to 3 mm) calcite layers. Field relationships suggest this metalimestone is younger than lower Lower to lower Middle Ordovician dolostone. Conodonts recovered from samples are too deformed for accurate age determinations (A. Harris, written communication., 1986).

Unit 4-Middle to Upper Ordovician Dolostone. Middle to Upper Ordovician dolostone is medium to light gray, massive to finely laminated (.5-.7 cm laminations of light and dark gray carbonate), locally sugary-textured dolostone. Locally preserved spheres, irregular and elongate clasts are visible in thin section, and possibly represent fenestrae or burrows (J. Dumoulin, oral commun., 1986). The locally abundant spheres and clasts indicate that the dolostone was probably originally a bioclastic packstone or grainstone. The dolostone contains rare, disseminated pyrite.

Devonian Lithologies

Devonian age rocks from the Omar area include both dolostones and metalimestones. Conodonts from dolostones and metalimestones range between Early and Middle Devonian. The Devonian dolostone contains relatively more organic material than Ordovician dolostones, commonly preserves textures suggestive of encrusting and boring algae (G. Stanley, oral communication, 1986), and hosts a variety of fossil forms. Rugosan and colonial coral patches, 10-20 m wide, may represent bioherms or patch reefs. BCMC drilled over 400' of "reef core" material at Copper Hill*, indicating locally abundant carbonate buildups or patch reefs. In addition, BCMC drill logs report "reef" or "talus" breccia, possibly representing local reef front or fore reef environments. Abundant stromatoporoids and coral buildups are typical of Devonian, shallow water, carbonate environments (James, 1983).

*Informal names: Copper Hill, Blind Spot, Trail Mountain, Omar Mountain, Hump Mountain, Everclear Ridge, South Saddle, C Ridge are both from BCMC unpublished data and this study, and are shown in Fig. 2.

Unit 5-Devonian Dolostone and Metalimestone. The dolostone is dark to medium gray fine-grained dolomite (.05 to .1 mm), with bioclasts <1.0 mm in diameter. Megafossils, including rugosid corals, colonial corals (Favosites, W. Oliver, written communication, 1985), crinoids stems, ostracods, stromatoporoids, and possibly bryozoa, occur in patches several meters to tens of meters wide. These megafossils are commonly silicified, and weather black.

This unit varies from mudstone (which rarely exhibits a light and dark gray banding) to wackestone, less commonly packstone, and rarely grainstone with fossil fragments making up the grains and fine-grained dolomite probably representing original lime mud. Sparry dolomite commonly replaces fossil fragments that only rarely retain fine structures such as septa in rugosid corals. Indeterminate fossil clasts (ranging up to 1.5 mm across; possibly gastropods or foraminifera, G. Stanley, oral communication, 1986), have micritized rims from endolithic algae, and coarse, sparry dolomite and quartz cores.

Bioclastic wackestone to packstone, characterized by a mud-rich matrix (now fine-grained micritic dolomite) suggests a backreef depositional environment (James, 1983). Fine-grained alternating light and dark gray

laminated dolostone with fewer fossil remnants was probably deposited in a quieter, lagoonal facies (James, 1983). The Devonian conodont fauna are less diagnostic of depositional environments than earlier Paleozoic fauna (J. Dumoulin, oral communication, 1986). One sample (OM118, Table 1; Fig. 2), however, contains conodonts indicative of a warm, shallow, high energy environment.

Organic and other insoluble material are locally abundant in the wackestone to packstone, rendering some thin sections semi-opaque. The insolubles commonly form irregular and discontinuous concentrations that are <1cm to less commonly 1-3 cm wide. Shinn and Robbin (1983) described similar concentrations of insolubles resulting from early diagenetic pressure solution and compaction. Sutured stylolites are rare but where present crosscut earlier, more diffuse concentrations of insolubles, fossil fragments, and coated grains.

Dark to medium gray Devonian metalimestone consists of 70-95% subhedral to anhedral, fine to coarse-grained (.1 to 1.0 mm) calcite, with 5-30% anhedral dolomite. Limestone is commonly platy-weathering (5 to 20 cm partings), and contains locally abundant round to oblong patches of coarse, white calcite. Stromatoporoids are locally preserved in relatively un-recrystallized metalimestone. Stylolites are common but minor.

BCMC drill logs show intercepts (up to 150 feet (46 meters); DDH 5, Fig. 2) of "chloritic to phyllitic" metalimestone between massive coralline, probably Devonian, dolostone. Limestone apparently graded into the coralline dolostone. This "chloritic to phyllitic" lithology was not observed in contact with the dolostone at the surface, but might lie beneath rubble cover of the more resistant dolostone.

Lithologies of Unknown Age

Unit 6-Marble. Marble is massive, very coarsely crystalline, light gray to nearly white, crops out in pods and lenses and is several meters to tens of meters wide. Marble commonly occurs near the base of, and in possible fault contact with, lower Lower Ordovician metalimestone (unit 1).

Structure

Most units within the Omar area strike north and dip to the west between 50 and vertical; some beds are overturned (Fig. 2) as a result of folding into NW

trending anticlines and synclines. The lower Lower Ordovician metalimestone (unit 1) commonly preserves tight to isoclinal, centimeter to meter amplitude kink folds (Fig. 3a, 3b). Folds are variable, but generally trend northward and plunge between 40° and 20°. The more competent dolostone units rarely exhibit millimeter to meter scale folding. Microscopically, layers of insoluble material between layers of recrystallized coarse calcite within the lower Lower Ordovician metalimestone (unit 1) are commonly kinked (Fig. 3c) mimicing larger scale features.



Fig. 3a. Kink folding in Lower Ordovician metalimestone (Trail Mountain).



Fig.3b. Isoclinal folding in Lower Ordovician metalimestone (Hump Mountain).

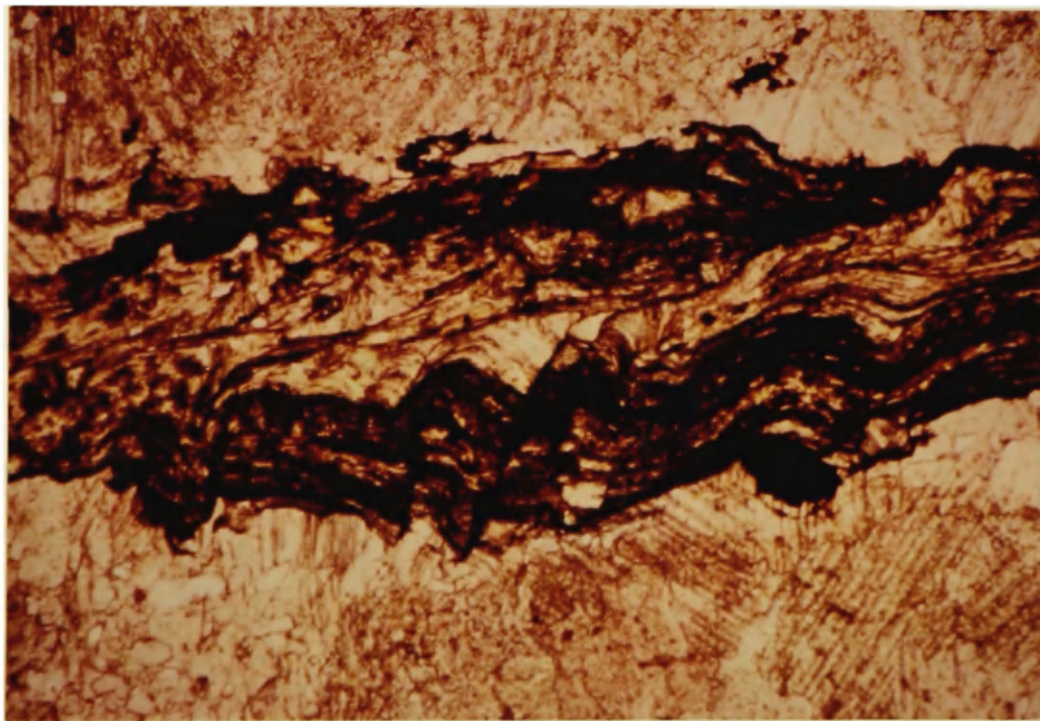


Fig. 3c. Photomicrograph (plane polarized light) of kinked bands of organic material and insoluble debris within calcite (OM123, Lower Ordovician metalimestone, magnification=40x).

Stratigraphic and structural relationships suggest both reverse and normal faults occur in the limbs of these folds (Figs. 4a, 4b), and are probably steeply dipping although fault planes are rarely exposed. Evidence for north to northwest trending faults includes fracturing, commonly accompanied by abundant quartz veining in the fractured zones. Relative displacement along these fractures or faults is uncertain because they commonly occur within one stratigraphic unit. Some of the fracture surfaces contain sulfides, but most contain only iron oxides, malachite, and rare azurite. Degenhart and others (1978) interpreted several NW trending, steeply dipping, fracture zones extending up to 9000 feet (2743 meters) over an area of up to 3500 feet (1067 meters) wide. They concluded that some, if not most of the copper mineralization occurred along these fractures. BCMC drilling logs report fractures in the subsurface below Copper Hill.

Several exposures of lower Lower Ordovician metalimestone, lying structurally above lower Lower to lower Middle Ordovician and Devonian rocks, suggest thrusting of older over younger units (Figs. 4a, 4b). Amount of displacement along thrust or reverse faults cannot be estimated because stratigraphic thicknesses are poorly known. Rare exposures of faults indicate local

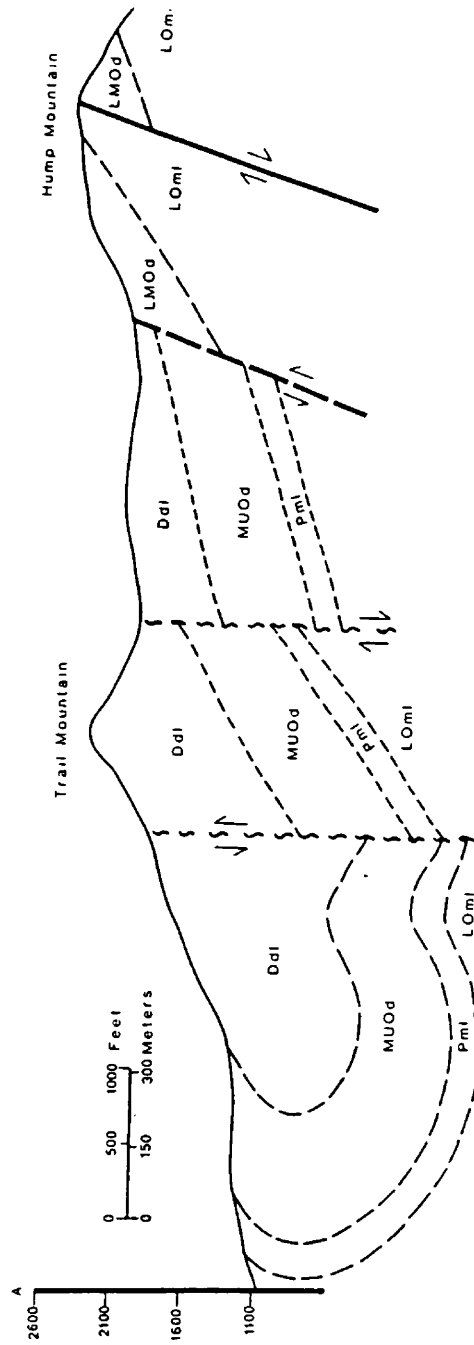


Fig. 4a. Geologic cross section from A to A'. Symbols are the same as Fig. 2.

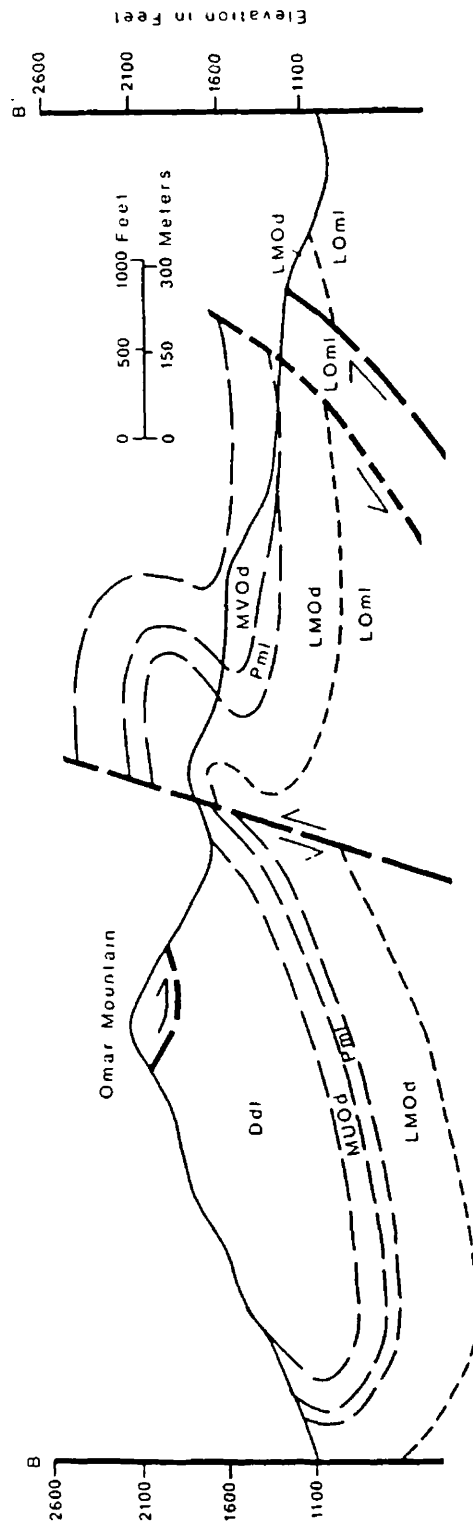


Fig. 4b. Geologic cross section from B to B'. Symbols are the same as Fig. 2.

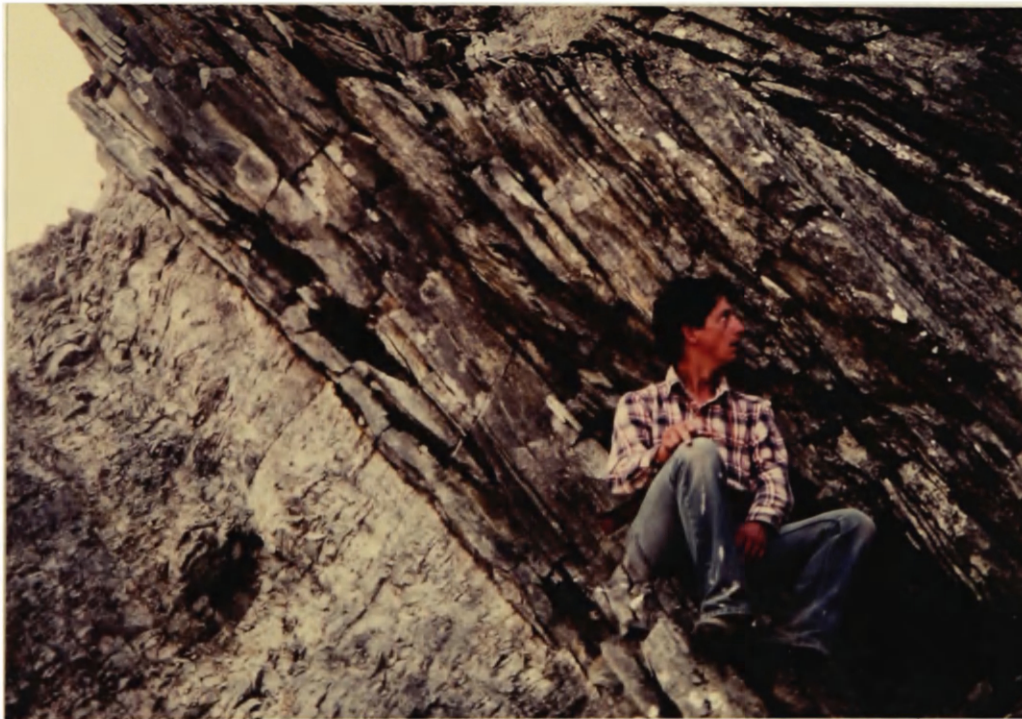


Fig. 5. Thrust/reverse fault contact placing Lower Ordovician metalimestone (right) over Lower to Middle Ordovician dolostone. Fault plane dips 72° to the west (Hump Mountain).

steep dips (72° Hump Mountain; Fig. 5), although structural relationships near Blind Spot (Fig. 2) suggest moderate (25-40°) fault plane dips.

Mineralization

Introduction

Most iron and copper sulfide mineralization at the Omar Prospect is stratabound and discordant within the Devonian dolostone (unit 5). The absolute timing of mineralization at Omar is unclear, but probably occurred prior to the mid-Jurassic(?) to Cretaceous Brooks Range orogeny. Minor amounts of copper were remobilized during or after deformation and deposited with calcite and quartz in veins (up to 6 cm thick) that cut both Devonian rocks and structurally overlying lower Lower Ordovician metalimestone (unit 1).

Earliest copper mineralization occurs as disseminations and replacement of pyrite. Pyrite, copper sulfides and sulfosalts are spatially and perhaps genetically associated with relatively concentrated bands and zones of organic and other insoluble material within the Devonian dolostone (unit 5).

Most of the copper mineralization observed on the surface at Omar occurs as bornite and chalcopyrite within dolomite veinlets (generally <2-3 cm thick) with lesser amounts of quartz and calcite. Veinlets commonly intersect each other and surround angular to subangular fragments of host dolostone, producing a "breccia" or stockwork texture. It is unclear whether veinlets were emplaced first, or followed open spaces created by dissolution of host dolostone.

Subsurface Mineralization (from BCMC Drill Logs)

BCMC drilled 10 core holes at Blind Spot and 9 at Copper Hill (Fig. 2). At Blind Spot (Fig. 2) they intersected only 1 calcite-quartz-dolomite vein containing chalcopyrite, bornite, and pyrite, within lower Lower Ordovician metalimestone (unit 1), and failed to intersect mineralization in dolostone. Drill holes 5, 6, 16, and 17 intersected significant mineralization at Copper Hill (Fig. 2, Table 3) and drill hole 8 encountered 30 feet (9 meters) of minor malachite, azurite, and chalcocite at Copper Hill. The following descriptions are summarized from BCMC drill logs.

Table 3. Summary of Mineralized Intercepts in Drill Holes 5,6,16,17
(data from BCMC drill logs)

Drill Hole	Intercept and Average Grade	Host Rock	Mineralization
5	72-75 m .743% Cu	72.5-76.8 m=massive clean dolostone	73-76.8 m=ccp, brn, py; ccp and py are intimately associated with open fractures contain sulfides oxides, and copper carbonates.
	75-76.8 m .378% Cu		
	86.6-89 m 5.25% Cu	86.9-92.7 m=fossiliferous dolostone; apparent healing and refractured	86.9-93 m=brn most abundant, ccp and py intimately associated, small runs of massive cc,
	89-92.7 m 12.12 % Cu	breccia. Breccia texture often obscured because sulfides and solid rims of cc obscure original features.	possible ten and cov; CuCO ₃ oxides replace fossils present.
6	0-36.6 m 3.16% Cu	0-36.6 m=massive coralline dolostone, py has possibly replaced some fossils. Non-oriented small blebs and blobs (of dolostone) suggest host has brecciated, healed, re-brecciated. Host graded into dark, carbonaceous dolostone.	0-12 m=massive, commonly botryoidal blebs and fragments of py. CuCO ₃ common as small crustings and blebs. Trace brn, cc. 12-20 m=trace brn as tiny discontinuous veinlets. Ten and cc up to 3%, brn rarely up to 5%. 20-32.3 m=Cu mineralization in dolo/calc stringers and open fractures, but primarily solid around clasts. Blebs of cc shot through massive and brecciated dolostone alike. 32.3-33.5 m=py occurs as clast replacement blebs. -pyrobitumen (solid hydrocarbon) and minor graphite very common.
	81-85 m .09% Cu	81-85 m=excellent "reef" limestone clastic breccia.	81-85 m=py and brn pervasively scattered through limestone clastic breccia.

Table 3 (continued)

16	32-45 m .182% Cu 51-70 m .563% Cu	-massive, fresh looking coralline, brecciated dolostone.	-py occurs as sharply defined regular to irregular to regular small blocks, often "shatter" (?) type; py surrounds and is often embayed in dull to glossy black carbonaceous material. Cu mineralization generally related to fractures, fossils, vuggy fillings, stylolites and seams.
17	17.5-59 m .315% Cu	-fine grained to massive, coralline to carbonaceous dolostone containing crinoid stems. Intensely fractured host, gets more silicified with depth. Fractures are filled with dolomite, some vuggy fractures lined with calcite. -massive dolostone commonly contains approx. 50% well laminated(muddy) dolostone fragments. Crinoid stems and anthraxolite are related to dark dolostone fragments. -below 61.6 m host is severely brecciated and silicified.	0-18 m=py occurs as discrete crystals in host and along fractures; py commonly rims breccia fragments. 18-24 m=brn and cc form discrete veinlets along vuggy fractures and occur as scattered grains. py is massive to colloform in nodular clusters. 24-33.5 m=minor cc veinlets, scattered CuCO ₃ on fractures. 33.5-62 m=massive sections (50-70%) of colloform pyrite with well developed radial and concentric structures; appears fractured locally. Massive pyrite occurs in layers of "muddy" dolostone within host coralline dolostone. -scattered veinlets of brn and cc occur along fractures. -scattered sections of coarse grained (but < 1") anthraxolite occurs in host.

Note:

py=pyrite, ccp=chalcopyrite, brn=bornite, cc=chalcocite, ten=tennantite, cov=covellite
dolo=dolomite, calc=calcite

Figure 6 displays the rock types intersected and vertical extent of mineralization for drill holes 5 and 6. Based on the previous descriptions, I have suggested probable ages for the lithologies. The contact between argillitic to phyllitic metalimestone and massive coralline dolostone (corals observed only in Devonian rocks at the surface) is gradational, suggesting the underlying metalimestone (hole 5, Fig. 6) is in stratigraphic contact with the dolostone although it was never observed in contact with Devonian rocks at the surface.

BCMC description of a "talcy" phyllitic to chloritic metalimestone most closely matches lower Lower Ordovician metalimestone (unit 1) and/or unit 3 metalimestone. In the subsurface, this unit is commonly sheared, penecontemporaneously deformed, and exhibits highly variable dips over short (vertical) distances, suggesting a possible fault contact with Devonian dolostone.

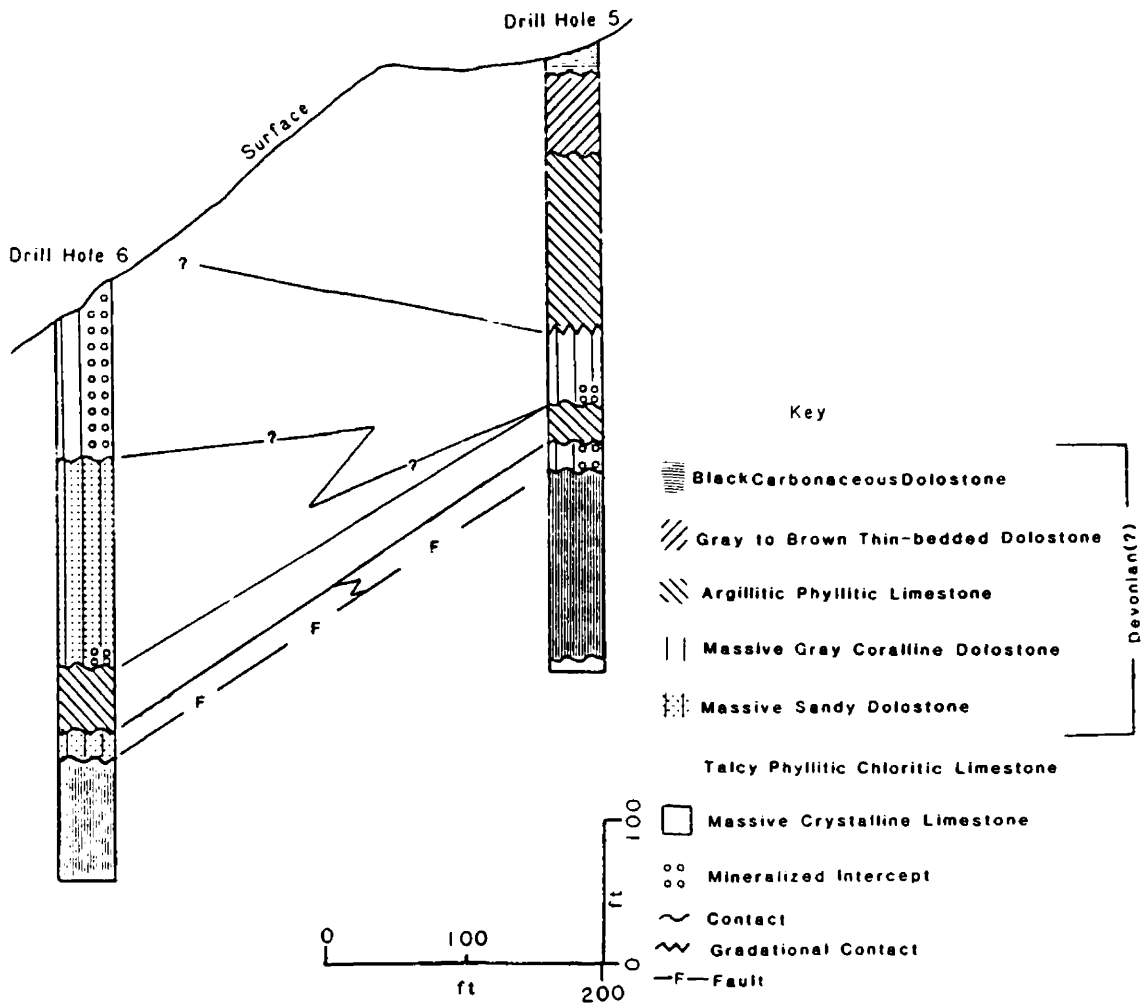


Fig. 6. Simplified geologic logs and interpretive correlation of drill holes 5 and 6 at Copper Hill (from BCMC data).

Unit thicknesses vary considerably and are difficult to correlate from hole to hole, indicating the carbonate rocks in the Copper Hill area display rapid facies changes, or have been tightly folded or faulted. BCMC favored faulting in most places. Drill hole 9 intercepted over 500' of massive, fossiliferous (probably Devonian) dolostone, but true thickness cannot be determined. Bedding and orientation are difficult to discern in the fossiliferous dolostone, so figure 6 does not show bedding. In addition, reported dips of 10° to vertical are not consistently correlatable between drill holes.

Subsurface mineralization is primarily restricted to the massive coralline dolostone (Fig 6), but is also reported within a metalimestone breccia (hole 16). Table 3 lists copper grades, and gives brief descriptions of rocks and mineralization for each mineralized intercept. Several generations of fracturing and healing of dolostone and a variety of sulfide textures (massive, disseminated and veinlets) suggest that mineralization was multistage.

BCMC described both massive and botryoidal, radiating pyrite in the subsurface. Pyrite selectively replaced dark, "muddy" clasts (probably breccia fragments), and fossils (hole 17, Table 3). BCMC reported an "intimate" spatial association of pyrite and chalcopyrite (hole 5,

table 3). Disseminated pyrite and bornite (hole 6, table 3) were noted within a metalimestone "clastic breccia", although most copper sulfides were reported to occur with dolomite and calcite in veinlets and around "clasts". From other descriptions of "clastic breccia" and similar brecciated textures I infer that BCMC meant non-tectonic, pre-deformation brecciation. Blebs and veinlets of chalcocite occur in both massive (fossiliferous, not brecciated) and brecciated dolostone.

Despite widespread brecciation, BCMC described dolostone as "fresh", commonly with preserved fossils. Zones of extreme fracturing accompanied by quartz veining (e.g. below 202' in hole 17; table 3), were probably related to tectonic deformation and fracturing.

Blebs of black organic matter (probably pyrobitumen) were noted in the subsurface within fossiliferous dolostone at Copper Hill. In hole 16 (Table 3), organic material is surrounded by or "embays" pyrite.

Surface Mineralization

Chalcopyrite, bornite, tetrahedrite-tennantite, pyrite, and minor galena and chalcocite, are preserved in outcrop at Copper Hill, whereas mainly bornite and chalcopyrite

occur in mineralized rubble at Blind Spot (Fig. 2). Rubble blocks (10-20 cm across) at Blind Spot rarely contain more than 20-25% copper sulfide by volume. Malachite, azurite, and iron oxide minerals together with copper sulfide minerals occur in other small (10-20 m²) areas along an approximately 3 km northwest trend from South Saddle to Blind Spot (Fig. 2).

I examined 40 polished thin sections of mineralized and unmineralized Devonian dolostone. Twenty thin sections contained sufficient amounts of sulfide minerals to describe textures, and to infer paragenetic relationships and some genetic processes. Most of the 20 samples contained disseminated sulfides; thirteen contained veinlets or irregular masses of copper sulfide. These surface samples apparently do not contain all the sulfide and gangue assemblages observed in the subsurface at Omar. Colloform pyrite masses from drill holes 5, 16, and 17 (table 3) were not found at the surface. Greater amounts of chalcocite were noted in the subsurface than on the surface at Copper Hill.

The following section describes the mineralized areas at Omar. Table 4 summarizes the sequence of mineralizing events.

Table 4. Mineral occurrence chart

	Diagenesis/Burial		Remobilization	Surface
	Disseminated Sulfides	Replacement	Veinlets/Brecciation	Oxidation
py	-----			
ccp	---?---	-----	-----	-----
brn		-----	-----	---
ten/tet		-----		
gal		-----		
cov				-----
dol	-----		-----	
cal			-----	-----
qtz			-----	-----
mal/az				-----
Fe-ox				-----

Note:

py=pyrite, ccp=chalcopyrite, brn=bornite, ten=tennantite, tet=tetrahedrite, gal=galena, cov=covellite, dol=dolomite, cal=calcite, qtz=quartz, mal=malachite, az=azurite, Fe-ox=iron oxides

Length of dashed lines indicates relative abundance

Disseminated and Replacement Mineralization. Grains and rare framboids of subhedral to anhedral pyrite (.005 to .01 mm across) are disseminated in Devonian dolostone (unit 5) at Copper Hill and less commonly at Blind Spot. The Devonian dolostone at Copper Hill is commonly brecciated, and most fragments are <2 cm across, but range up to 6 cm across. In contrast to coarse-grained and sparry dolomite outlining the fragments, dolomite comprising each fragment is commonly darker, finer-grained, and may contain varying amounts of organics and insoluble material. Disseminated pyrite is preferentially concentrated within the organic-rich areas (Fig. 7).

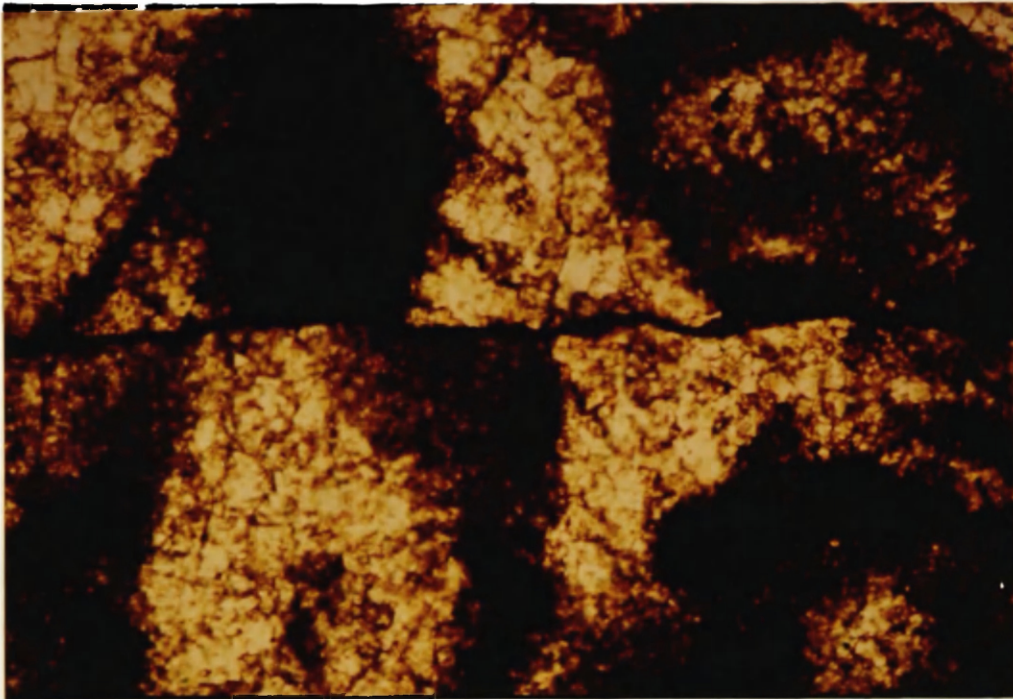


Fig. 7a. Photomicrograph (plane polarized light) of organic/insoluble-rich zones (dark) and organic/insoluble-poor zones (clear).

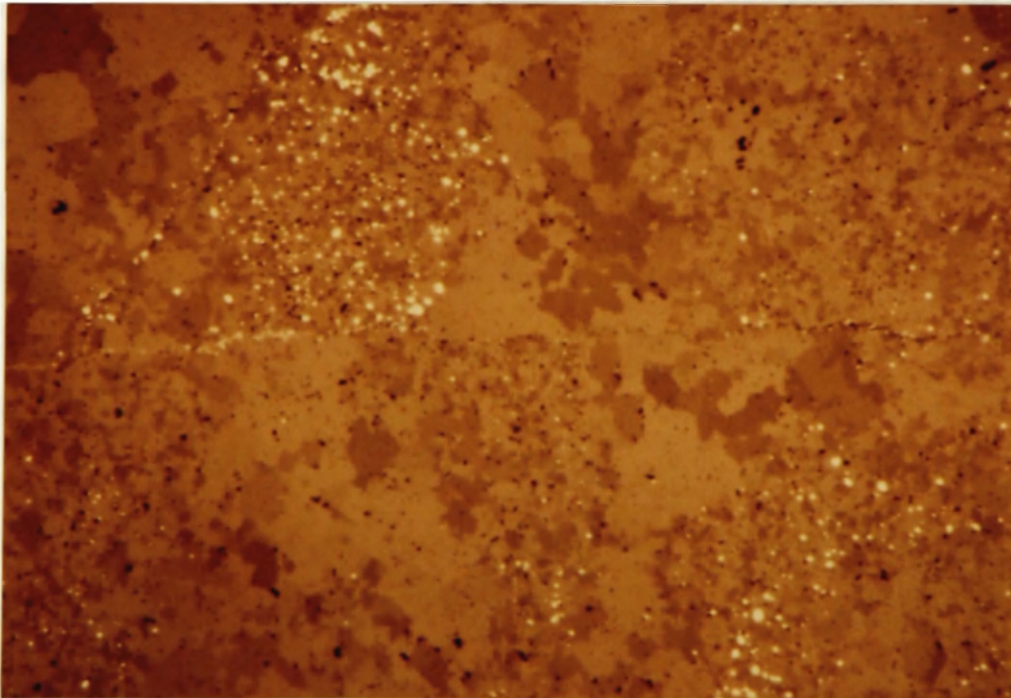


Fig. 7b. photomicrograph (reflected light) of the same area as 7a, showing the close spatial association of pyrite (white) with the organic-rich zones in dolomite (OM117, Copper Hill, magnification=100x).

Accompanying disseminated pyrite are coarser (up to 4 mm across) irregular masses of pyrite, copper sulfides and sulfosalts. In most samples, only remnants of pyrite remain surrounded by other sulfide minerals (which may have replaced earlier pyrite). Chalcopyrite grains (not in contact with pyrite) are also disseminated in the darker, organic-rich areas.

Figures 8a through 8d illustrate sulfide textures and paragenetic relationships from Copper Hill. Small "islands" of anhedral to subhedral pyrite commonly occur in a matrix of chalcopyrite. Pyrite may be rimmed and partially replaced by chalcopyrite (Fig. 8a).

Chalcopyrite either replaces or is intergrown with pyrite. Less commonly, tetrahedrite and/or tennantite surrounds pyrite (Fig. 8b). Lamellae of chalcopyrite, showing depleted zones at lamellae intersections indicative of coherent exsolution (Craig and Vaughn, 1981) commonly occur in tennantite/tetrahedrite (Fig. 8c).

Bornite replaces earlier pyrite, contains exsolved lamellae of chalcopyrite, and forms irregular masses adjacent to chalcopyrite. Exsolved chalcopyrite lamellae also coalesce into noncoherent lamellae or blebs (Brett, 1964). The timing of bornite versus sulfosalt deposition is unclear. Rare galena is intergrown with both bornite

and exsolved chalcopyrite (Fig. 8d).

Covellite coats fractures cutting across copper sulfides (Fig. 8d) and is probably an oxidation product. Goethite commonly forms rims around disseminated and coarser-grained pyrite and is also an oxidation-related alteration product.

Mineralization in Veinlets. Veinlets carrying copper sulfides cut the Devonian dolostone at Copper Hill and Blind Spot and post-date lithification of the host rock.

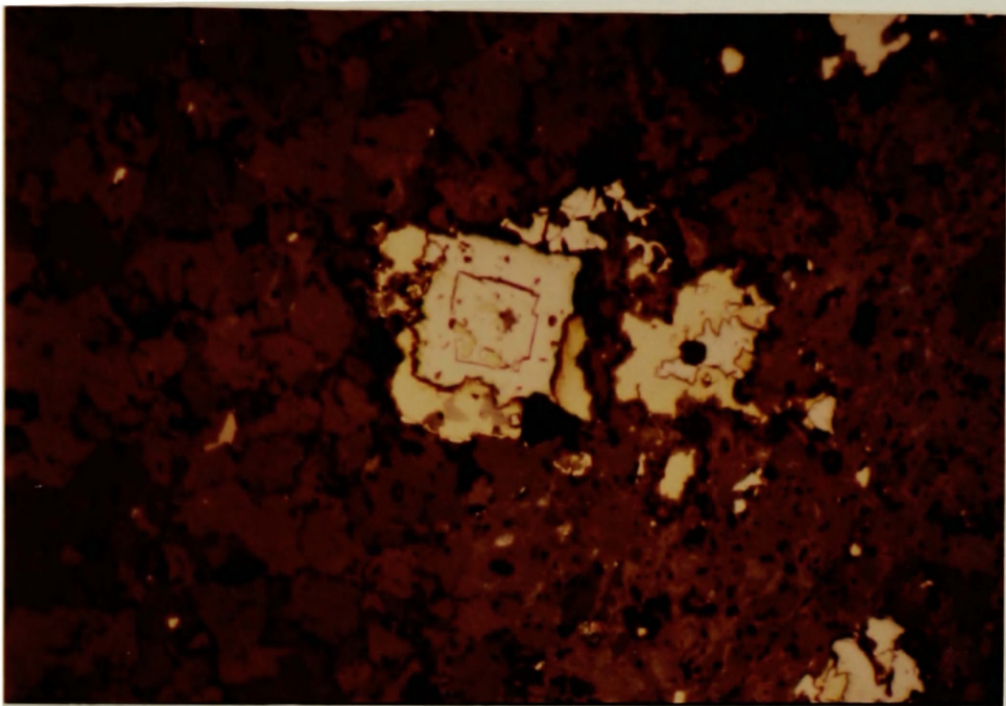


Fig. 8a. Photomicrograph of subhedral and anhedral pyrite (white) surrounded by chalcopyrite (yellow) in dolomite (brown). Pyrite may have been growth zoned prior to possible replacement by chalcopyrite (OM74e, Copper Hill, magnification=160x).

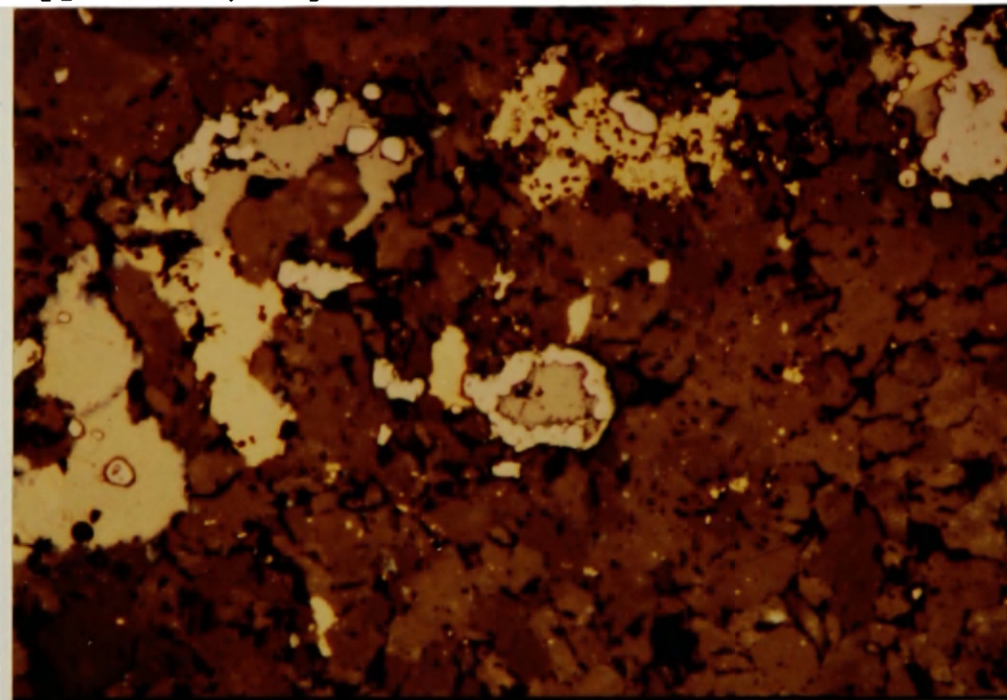


Fig. 8b. Photomicrograph (reflected light) of pyrite (white) surrounded by and/or touching tetrahedrite (light brown) and chalcopyrite (yellow) within dolomite (dark brown). Disseminated pyrite and chalcopyrite occur in the dolomite (OM74a, Copper Hill, magnification=210x).

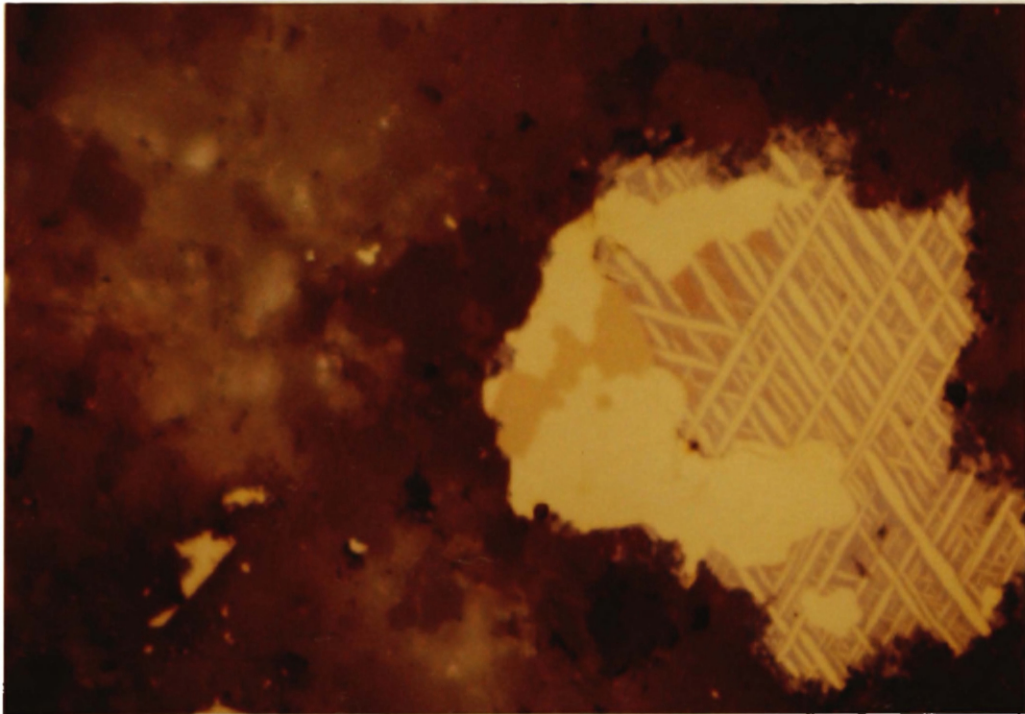


Fig. 8c. Photomicrograph (reflected light) of exsolution lamellae of chalcopyrite (yellow) within tetrahedrite (light brown) and bornite (pink) within dolomite (dark brown). Chalcopyrite lamellae show narrowing (depletion) at intersections indicative of coherent exsolution. The intergrown chalcopyrite and tetrahedrite and the right side of the large sulfide assemblage show either mutual boundaries or replacement textures with the exsolved sulfide mass, although it is unclear which assemblage is replacing which (OM74a, Copper Hill, magnification=400x).

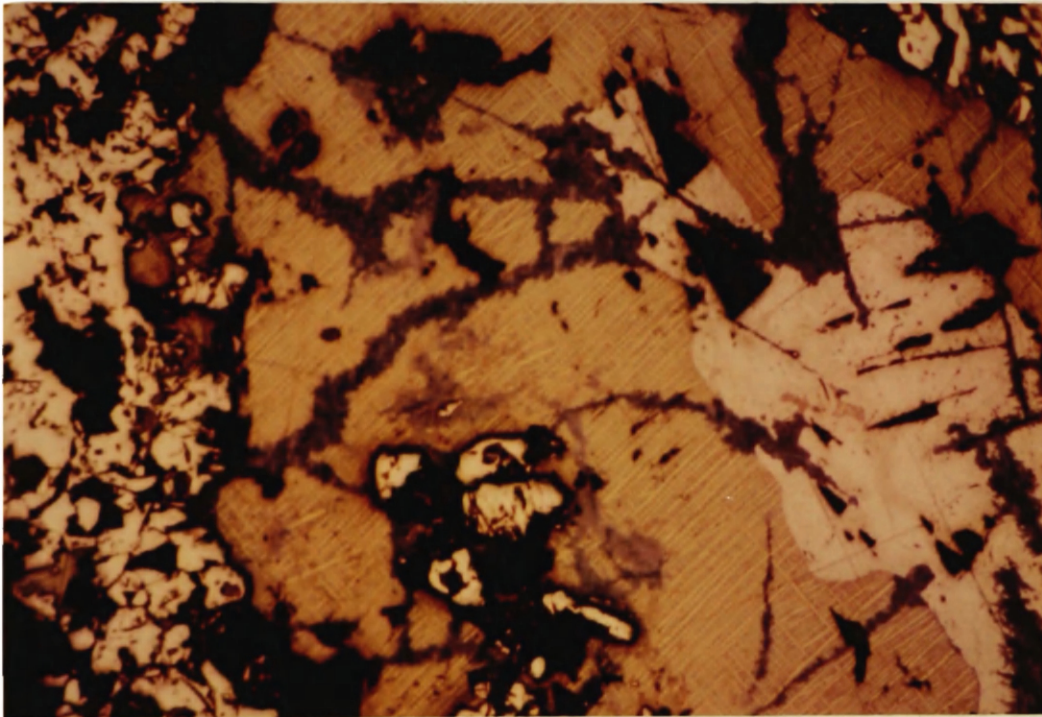


Fig. 8d. photomicrograph (reflected light) of galena (white, low relief) within tetrahedrite (light brown) containing exsolution lamellae of chalcopyrite (yellow). Pyrite (white, high relief) also occurs within tetrahedrite and chalcopyrite. Covellite (dark blue) on late fractures cuts the sulfide assemblage (OM74d, Copper Hill, magnification=80x).

At Copper Hill, the veinlets also cut zones of organics and insoluble material containing earlier copper sulfide mineralization (Fig. 9). At Blind Spot, disseminated mineralization is rare, so the relative timing of mineralization there is not clear.

Alteration in the wall rocks around the veinlets was minimal. In some places, coated grains and fossil debris are preserved even where cut by veins (Fig. 10).

Veinlets typically contain sparry, euhedral to subhedral dolomite rhombs growing outward from the veinlet walls (Fig. 11). This veinlet dolomite is coarser (up to .8 mm, average=.1 to .2 mm) than host rock dolomite (.05 to .1 mm) and is relatively free of organic material. Copper sulfides generally surround the rhombs and form the center of the veinlets.

Some rhombs display etched or corroded surfaces (Fig. 12) indicating that minor carbonate dissolution occurred after dolomite deposition. However, because many rhombs preserve euhedral crystal faces adjacent to chalcopyrite and bornite, dissolution of dolomite prior to copper sulfide deposition was probably insignificant.

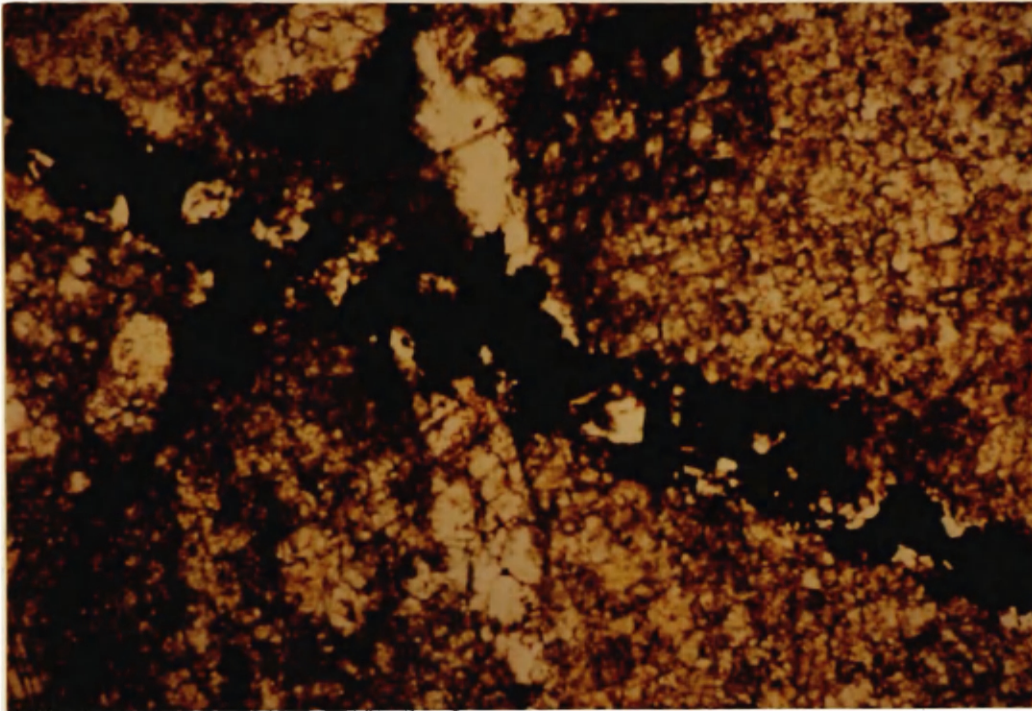


Fig. 9a. Photomicrograph (plane polarized light) of copper sulfide and dolomite vein (dark=copper sulfides, clear=dolomite) crosscutting areas of concentrated organic/insoluble material and clearer, organic/insoluble-poor dolostone.

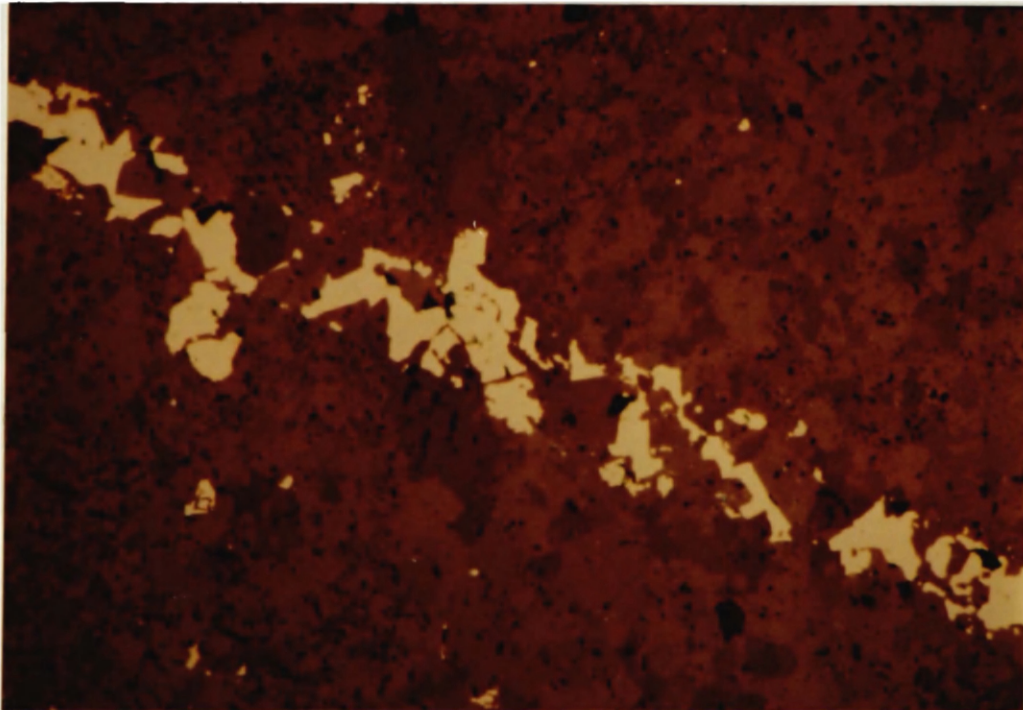


Fig 9b. Photomicrograph (reflected light) of same area as 9a, showing chalcopyrite (light yellow) in the veinlet cutting dolomite (brown) (OM74b, Copper Hill, magnification=80x).

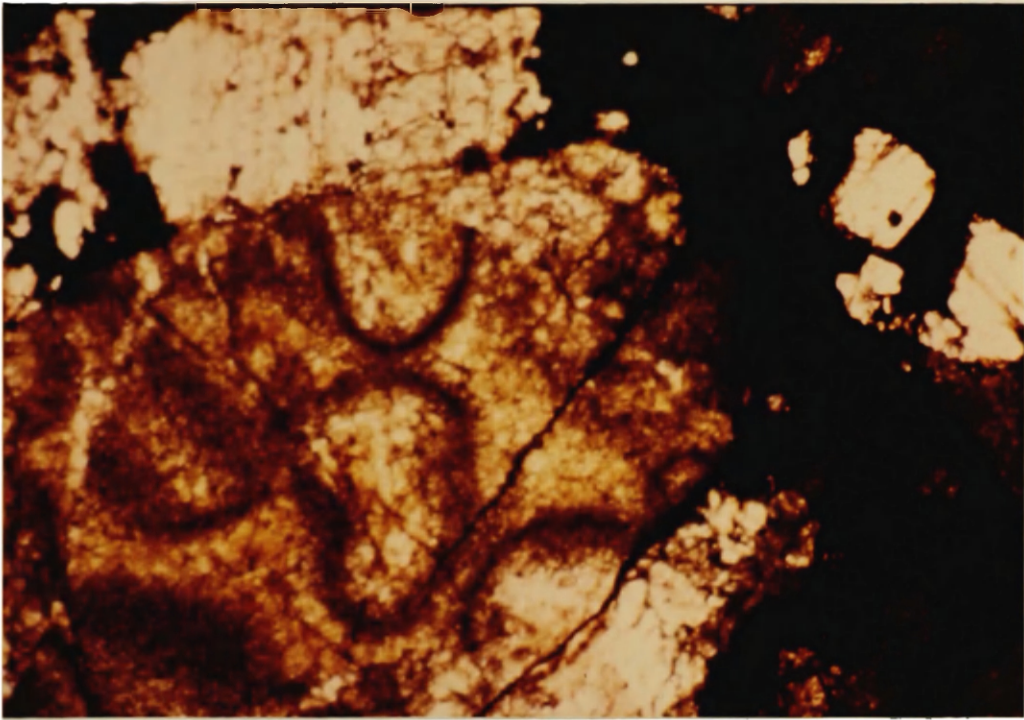


Fig. 10. Photomicrograph (plane polarized light) of a chalcopyrite, bornite (dark) and dolomite (clear) veinlet cutting coated grains (ovals) within dolostone (brown) (OM36d, Blind Spot, magnification=40x).

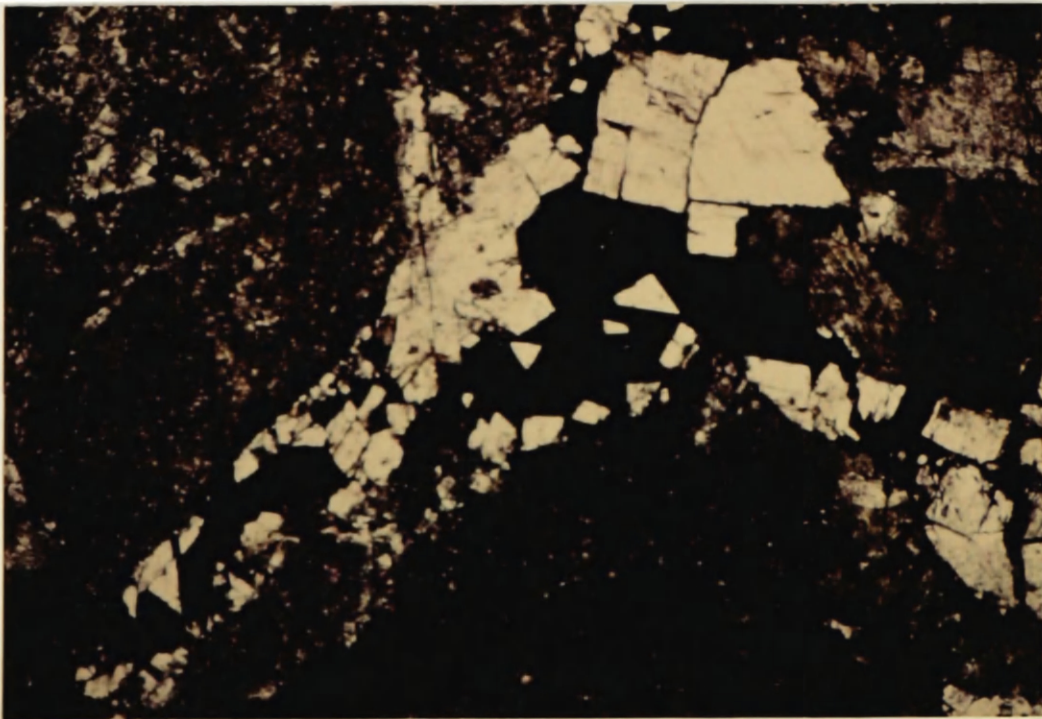


Fig. 11. Photomicrograph (plane polarized light) of a bornite and chalcopyrite (dark) and dolomite (clear) veinlet crosscutting dolostone (brown). Dolomite rhombs are growing out from veinlet walls (OM36d, Blind Spot, magnification=40x).

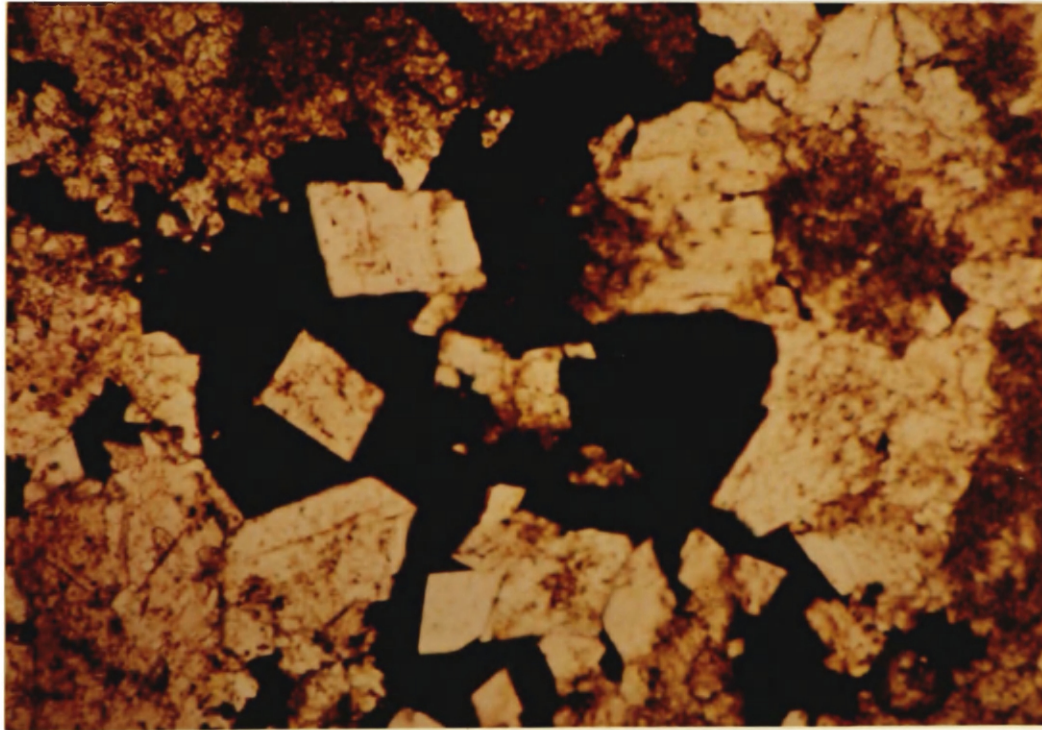


Fig. 12. Photomicrograph (plane polarized light) of euhedral to subhedral dolomite (clear) within chalcopyrite and bornite (dark) in dolostone (brown). The surface of the dolomite rhomb at the upper right of the figure (in contact with sulfide) appears etched (OM36d, Blind Spot, magnification=80x).

Sulfide minerals within the veinlets are bornite and chalcopyrite. Pyrite is rare, and late covellite +/- chalcocite occur on fractures cutting bornite or chalcopyrite. Chalcopyrite occurs within bornite as coherent lamellae, and noncoherent blebs and dots (Fig. 13). This chalcopyrite exsolved from an intermediate copper-iron-sulfur solid solution (Brett, 1964) after filling of the veinlets. Chalcopyrite also has simple mutual boundaries with bornite.

Quartz, less common than dolomite, occurs as anhedral masses within thicker (1-4 cm) copper sulfide-bearing veinlets. Euhedral dolomite rhombs commonly occur as inclusions in quartz adjacent to copper sulfides in veinlets. Calcite is rare in veinlets containing copper sulfides.

Veinlets commonly intersect and outline angular to subangular dolostone fragments to form a stockwork or breccia. Monomictic fragments of dolostone range up to approximately 10 cm in maximum dimension. Fragments have apparently not undergone extensive rotation (Fig. 14). The brecciated zones do not extend for more than 1-2 m, and are usually <1 m across.

At Copper Hill and Blind Spot more than one episode of veining is related to mineralization. Veinlets carrying bornite, chalcopyrite, dolomite, and quartz gangue cut

earlier white dolomite veinlets (Fig. 15). In thin section, however, all generations of veining are virtually indistinguishable.

Chalcopyrite and bornite only rarely surround dolomite

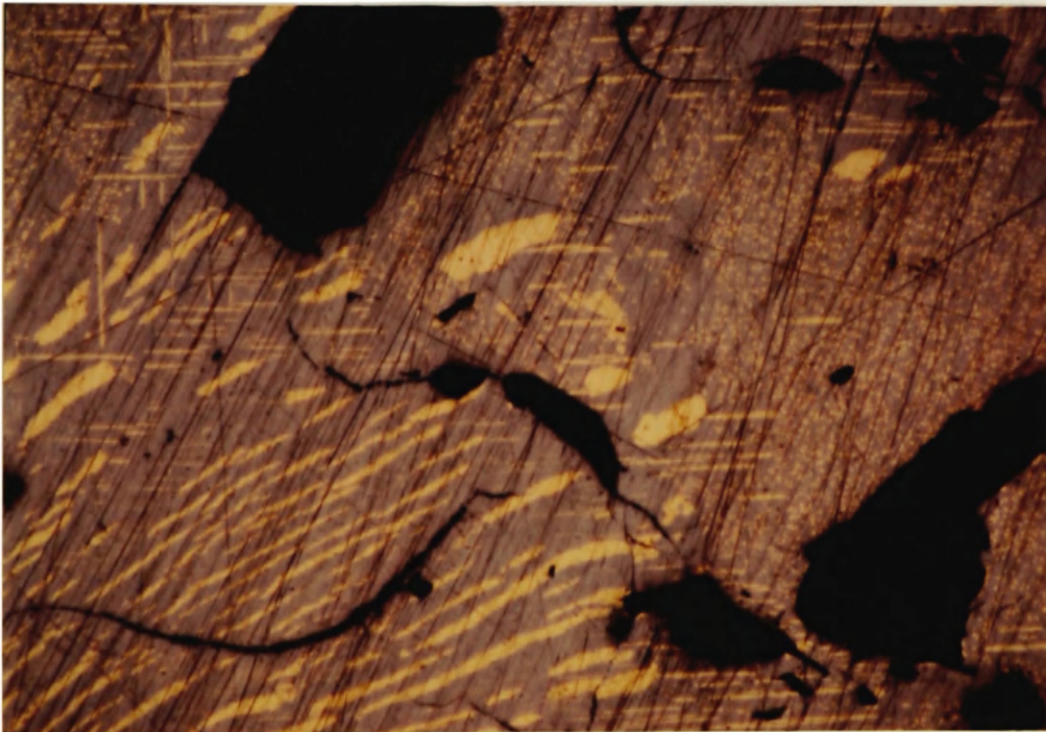


Fig. 13a. Photomicrograph (reflected light) of chalcopyrite (yellow) in bornite (purple). Horizontal and vertical lamellae of chalcopyrite may represent coherent exsolution of chalcopyrite, thicker and irregular lamellae and dots of chalcopyrite may represent noncoherent exsolution. Dark masses are dolomite with corroded edges.

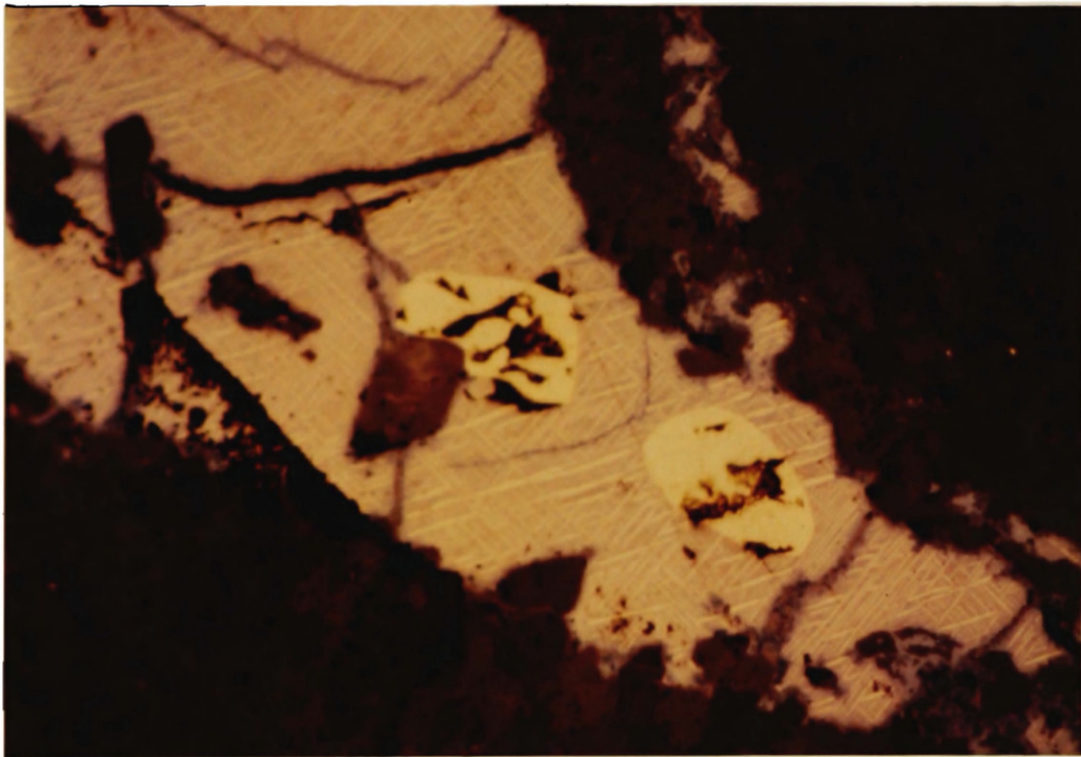


Fig. 13b. Photomicrograph (reflected light) of a chalcopyrite (yellow) and bornite (pink) veinlet crosscutting dolostone (brown). Oval grains of chalcopyrite show either mutual boundary or replacement textures with the bornite and exsolved lamellae of chalcopyrite (OM36e, Blind Spot, magnification=80x).



Fig. 14. Breccia of Devonian dolostone with dark angular fragments surrounded and cut by sparry, white dolomite (unmineralized, Copper Hill).

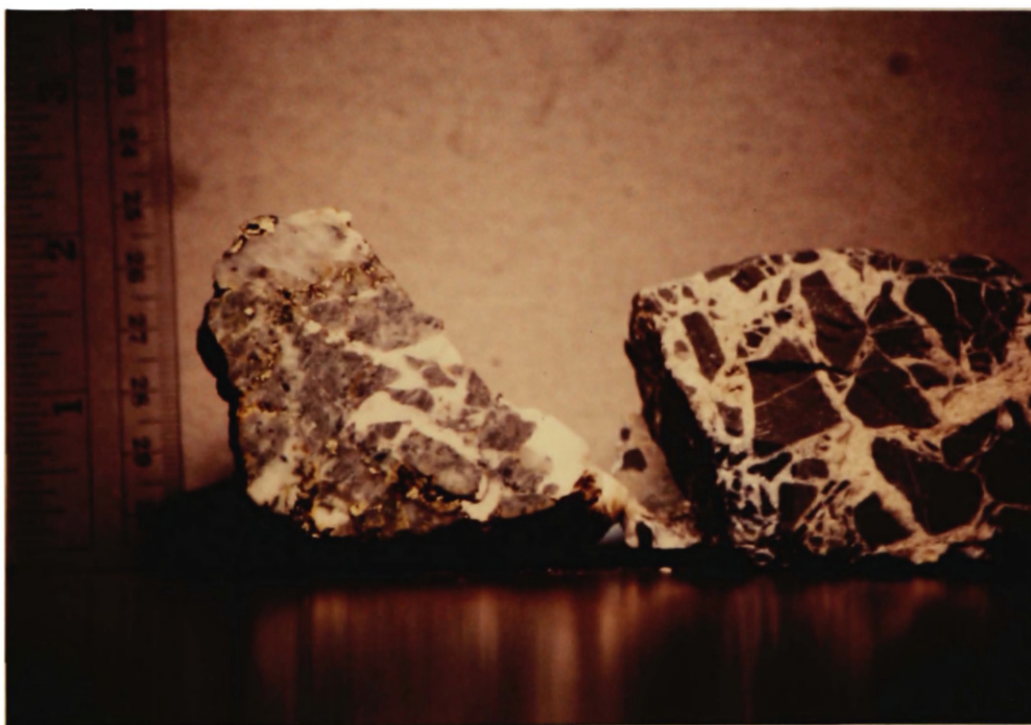


Fig. 15. Mineralized and unmineralized breccias. Sample at right is unmineralized breccia with dark fragments of Devonian dolostone surrounded and cut by white dolomite (Copper Hill). Sample at left shows a similar texture but both fragments and white dolomite are cut by dolomite-chalcopyrite-quartz veinlets (Blind Spot).

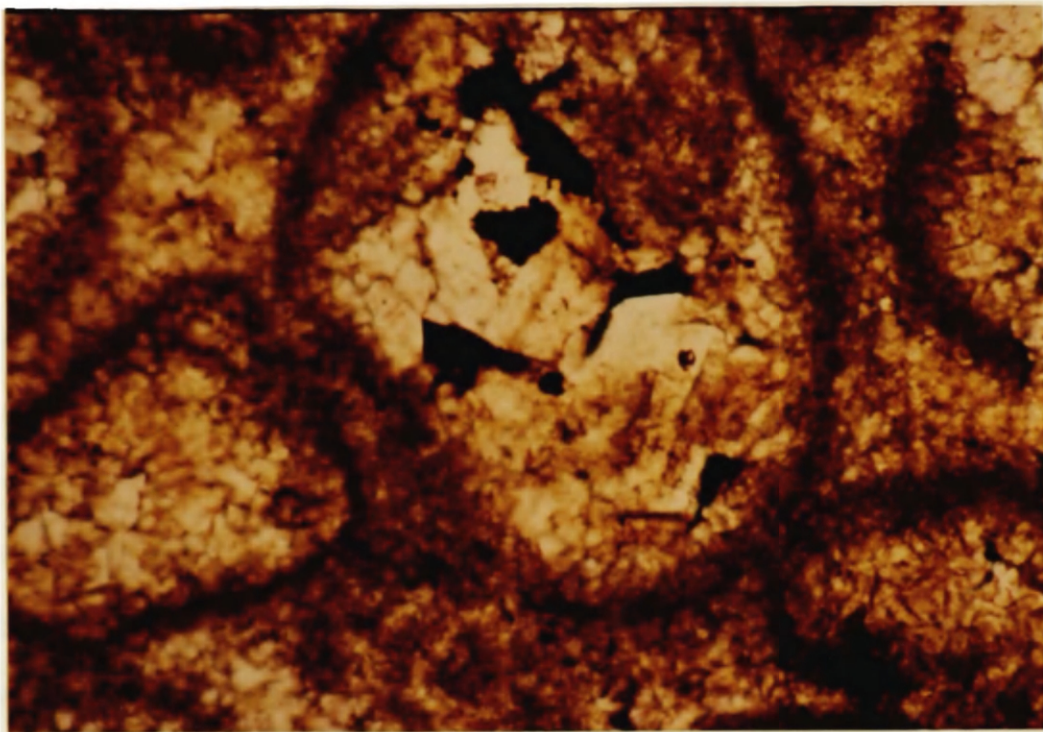


Fig. 16a. Photomicrograph (plane polarized light) of coated grain (oval) with a dark, fine-grained rim, and clear, coarser dolomite, and chalcopyrite with bornite (dark) in the core.

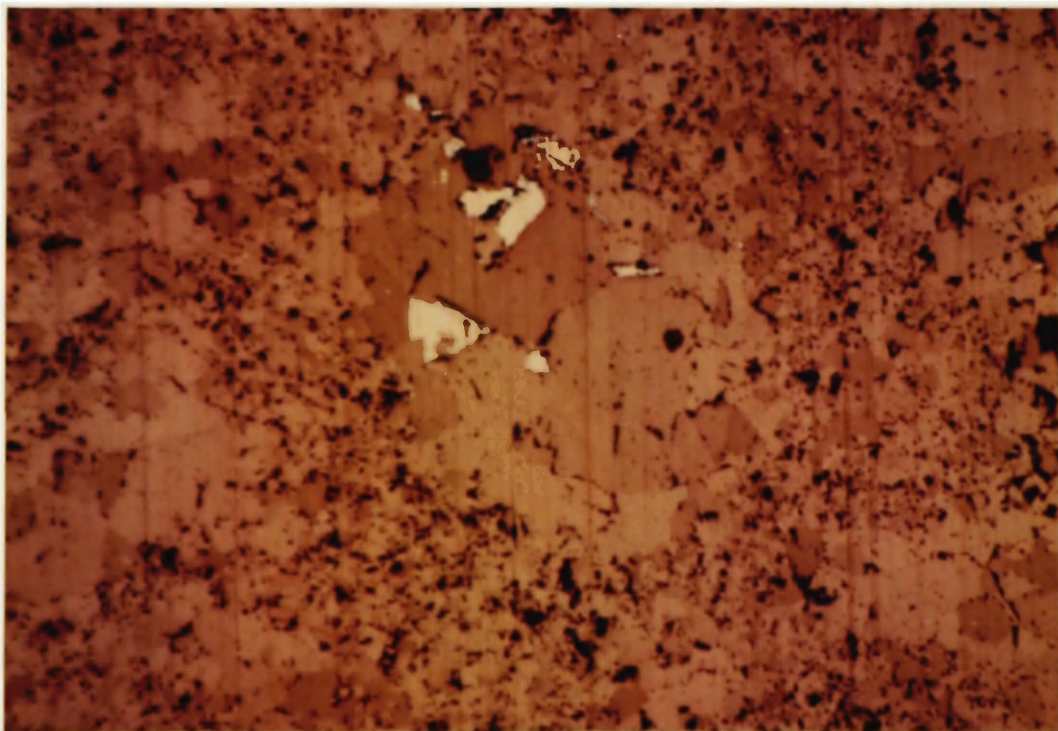


Fig. 16b. Photomicrograph (reflected light) of the same area as 16a, showing chalcopyrite and bornite (white) inside the coated grain with dolomite (OM36d, Blind Spot, magnification=80x).

rhombs not clearly associated with veinlets (Fig. 16).

Remobilization of Chalcopyrite into Late Veins and

Fractures. Late veins and veinlets crosscut all earlier textures and fill throughgoing fractures in the dolostone host. Except at Copper Hill, South Saddle, and Blind Spot (Fig. 2), copper sulfides rarely occur within these veinlets which are composed of calcite, quartz, and lesser dolomite. Up to 30% of these veinlets contain malachite and/or azurite with lesser amounts of chalcopyrite in one outcrop at Copper Hill. Veinlet orientations (both mineralized and unmineralized) from this outcrop plot closely together on a contoured Pi diagram (Fig. 17), suggesting that veins followed subparallel fractures or joints. Most calcite-bearing veinlets at Copper Hill are <1 cm thick, although some veins are up to 20 cm thick (Fig. 18).

At South Saddle (Fig. 2), quartz veins crosscutting Devonian dolostone (unit 5) are .3 to 1 cm thick, rare veins are up to .7 m thick. Most veins are unmineralized, and trend subparallel to foliation. Vein density varies within the outcrop; quartz veins rarely comprise up to 70% of the original dolostone (Fig. 19). Minor amounts of sulfide minerals (chalcopyrite, tetrahedrite, galena) occur in <5-10% of the veins at

South Saddle, but parts of some outcrops and rubble are quartz-rich gossan (Fig. 20). Atomic absorption (AA) and semi-quantitative emission spectrographic (SPEC) analyses of one gossan sample (OM66, Appendix A) show 1.1% arsenic

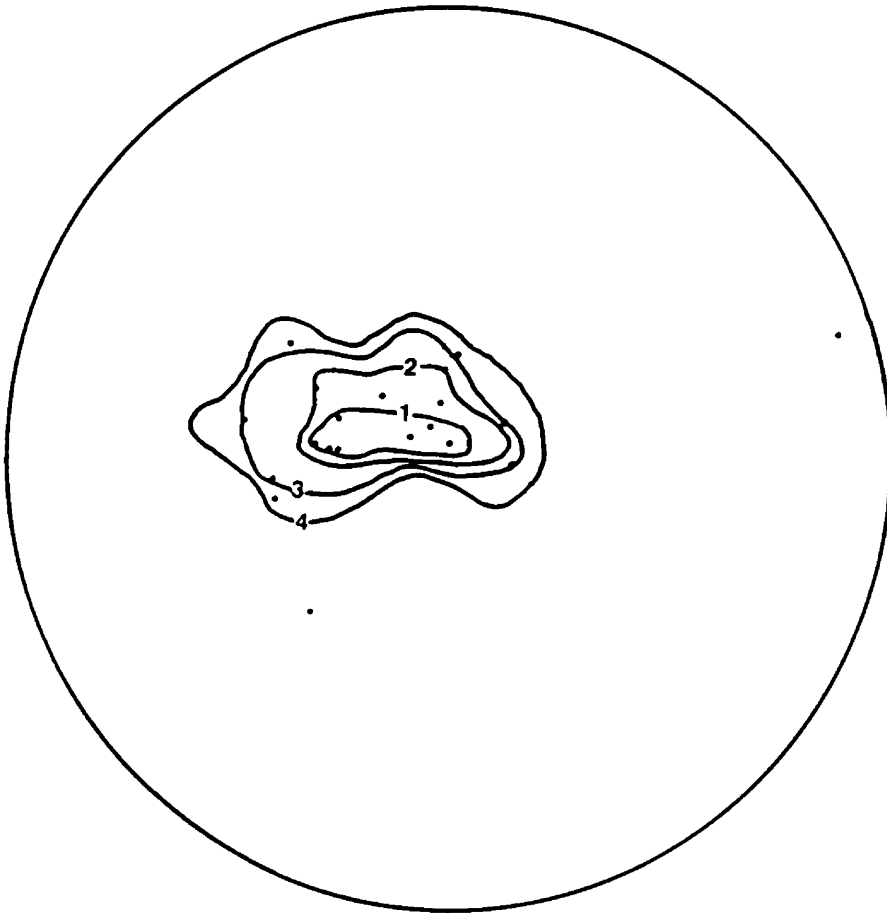


Fig. 17. Contoured Pi diagram of 20 calcite-quartz-malachite-chalcopyrite veinlets from Copper Hill. Points are poles to veinlet orientations, and show a fairly tight cluster representing shallow dipping, relatively subparallel veinlets. Contours represent 40% (1), 30%(2), 20%(3), and 10%(4) of the points.

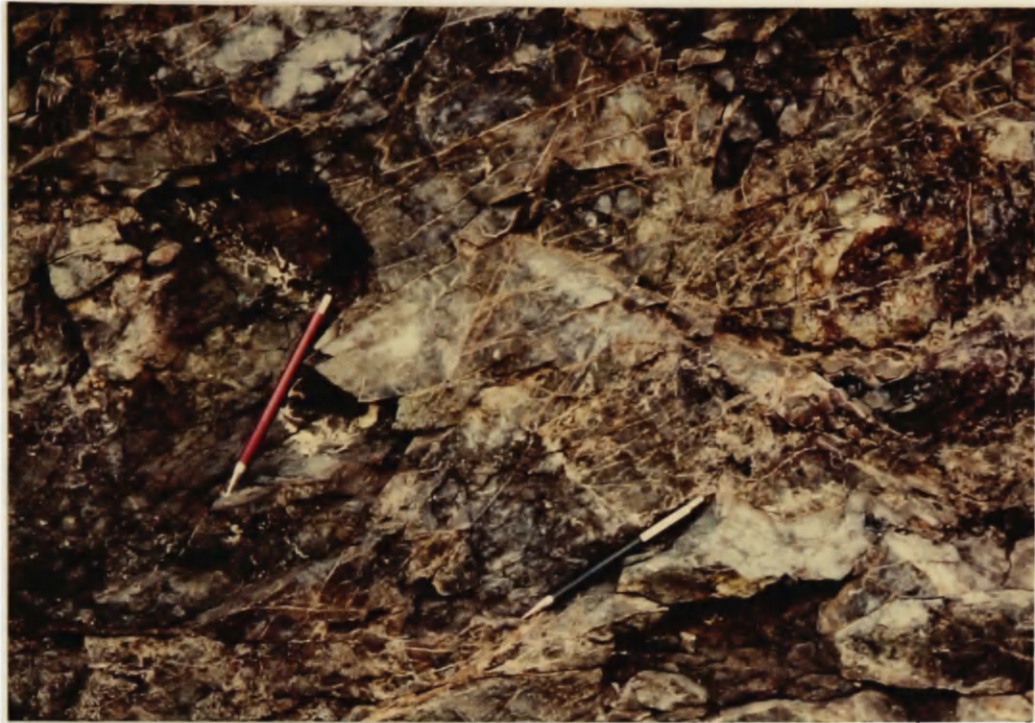


Fig. 18a. Network of thin, intersecting, calcite-filled fractures crosscutting Devonian dolostone at Copper Hill.



Fig. 18b. Calcite veinlets with minor malachite, iron oxides, and chalcopryrite crosscutting Devonian dolostone at Copper Hill.



Fig 18c. Breccia with large fragments of Devonian dolostone in a matrix of coarse, white calcite at Copper Hill.



Fig. 19. Outcrop of Devonian dolostone cut by abundant quartz veins along a fractured zone at Trail Mountain.

(AA), 3.6% copper (SPEC), 6 ppm silver (SPEC), 1500 ppm lead (SPEC), and 1000 ppm zinc (SPEC).

At Blind Spot, calcite and quartz veins up to 6 cm thick crosscut lower Lower Ordovician metalimestone (unit 1) adjacent to mineralized Devonian dolostone (unit 5) rubble. Veins trend subparallel to and also crosscut foliation within the metalimestone, and contain minor amounts of chalcopyrite and malachite (Fig. 21).

Thirty-five feet (11 meters) below the surface, BCMC drillholes 10 and 11 intercepted a 12" thick chalcopyrite, bornite, quartz, and calcite vein in platy metalimestone (probably unit 1).



Fig. 20. Gossan from fractured zone at South Saddle. Fragments of Devonian dolostone are outlined by iron oxides (OM66).



Fig. 21. Calcite-quartz vein crosscutting Lower Ordovician metalimestone at Blind Spot. Veins contain minor amounts of malachite and chalcopyrite. Calcite-quartz veins following foliation are generally thinner than crosscutting veins.

Cathodoluminescent Studies

I examined 23 polished sections and chips from mineralized and unmineralized rocks under cathodoluminescence. In most samples fine-grained host dolomite showed homogeneous moderately bright to bright orange cathodoluminescence. Less commonly, it showed slight variations or mottling in luminescence that apparently corresponded to different amounts of organic or insoluble material in the host rock.

Coarse-grained, sparry dolomite occurring in mineralized veins luminesce differently than finer-grained dolomite. These differences are probably attributable to different ratios of Mn^{+2}/Fe^{+2} in solutions that precipitated dolomite (Nickel, 1978). Manganese (Mn^{+2} , a cathodoluminescence "activator", is responsible for orange cathodoluminescence in dolomite $[(CaMg)(CO_3)_2]$, whereas iron (Fe^{+2}) "quenches" cathodoluminescence resulting in dull orange or dark dolomite (Sommer, 1972). Studies combining cathodoluminescence with microprobe analyses (Frank and others, 1982) have shown that different Mn^{+2}/Fe^{+2} ratios in fluids precipitating calcite, possibly caused by Eh and pH changes, result in distinct cathodoluminescent

zones within individual crystals. Furthermore, Voss and Hagni (1985) and Rowan (1986) documented correlatable cathodoluminescent "microstratigraphy" in dolomite gangue over 30 km in the Viburnum Trend lead-zinc district, southeast Missouri. This "microstratigraphy" may possibly extend up to 350 km to the southwest, suggesting that chemically similar solutions precipitated dolomite over great distances at the same time.

Dolomite rhombs in the crosscutting and breccia-forming veinlets are both brighter and duller orange than host rock dolomite under cathodoluminescence, and commonly display distinct dull/bright growth zonation. At Blind Spot, dolomite rhombs are generally duller than host rock dolomite, and approximately 30% of the rhombs show dull versus bright orange zonation. Some rhombs show dull cores, brighter intermediate zones, and dull rims adjacent to chalcopyrite and bornite. More commonly, rhombs exhibit bright cores, duller intermediate zones, and bright rims in contact with copper sulfides (Fig. 22).

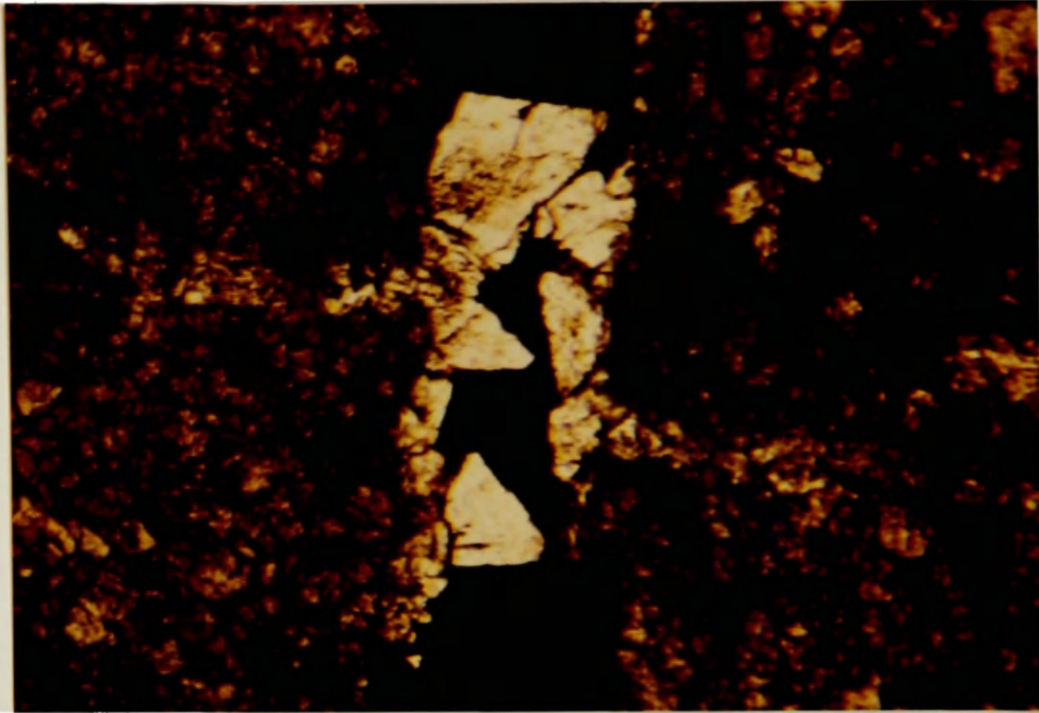


Fig. 22a. Photomicrograph (plane polarized light) of a chalcopyrite-bornite (dark) with dolomite (white) veinlet crosscutting dolostone (brown).

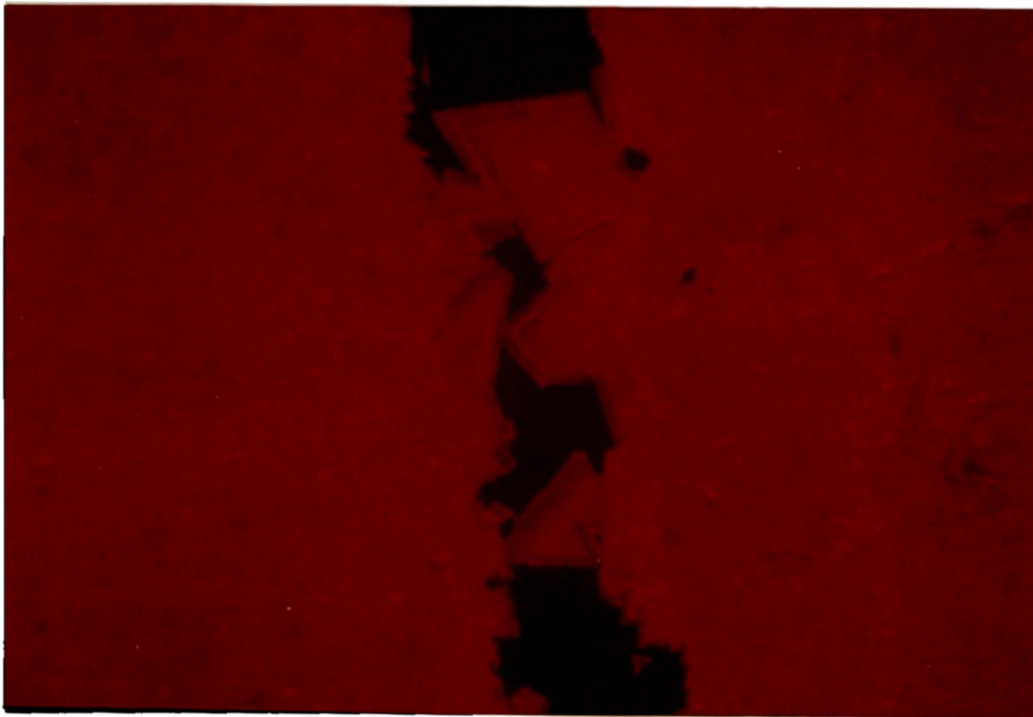


Fig 22b. Same field of view as 22a under cathodoluminescence showing relatively homogeneously bright dolostone, and zoned (bright and dull luminescing), euhedral dolomite in the veinlet.

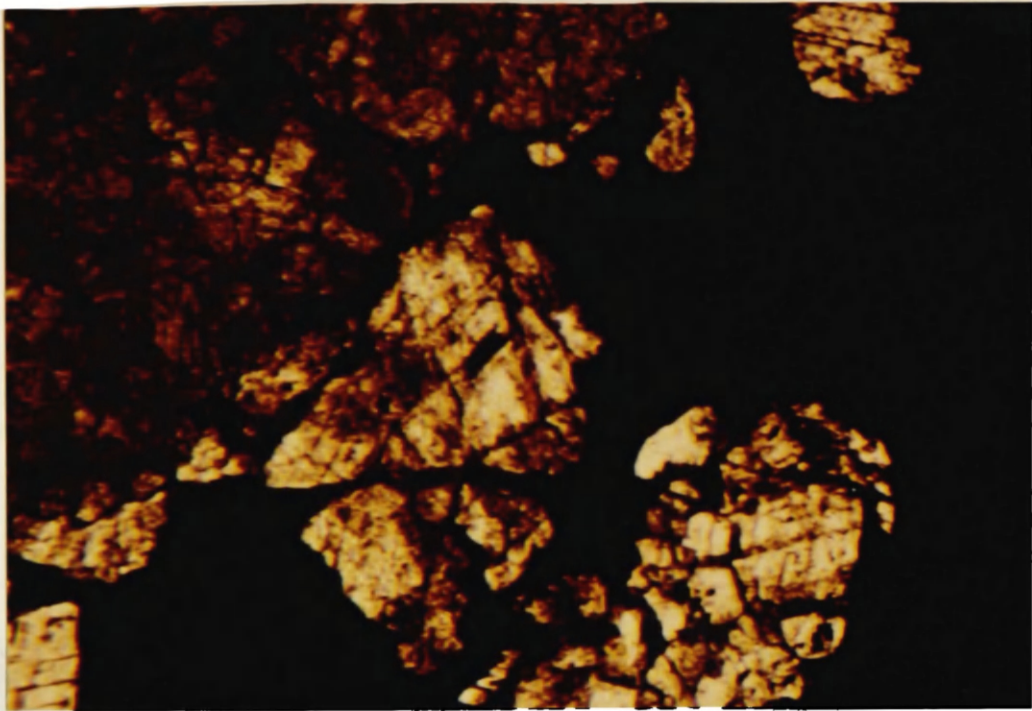


Fig. 22c. Photomicrograph (plane polarized light) of a chalcopyrite-bornite (dark) and dolomite (white) veinlet crosscutting dolostone (brown).

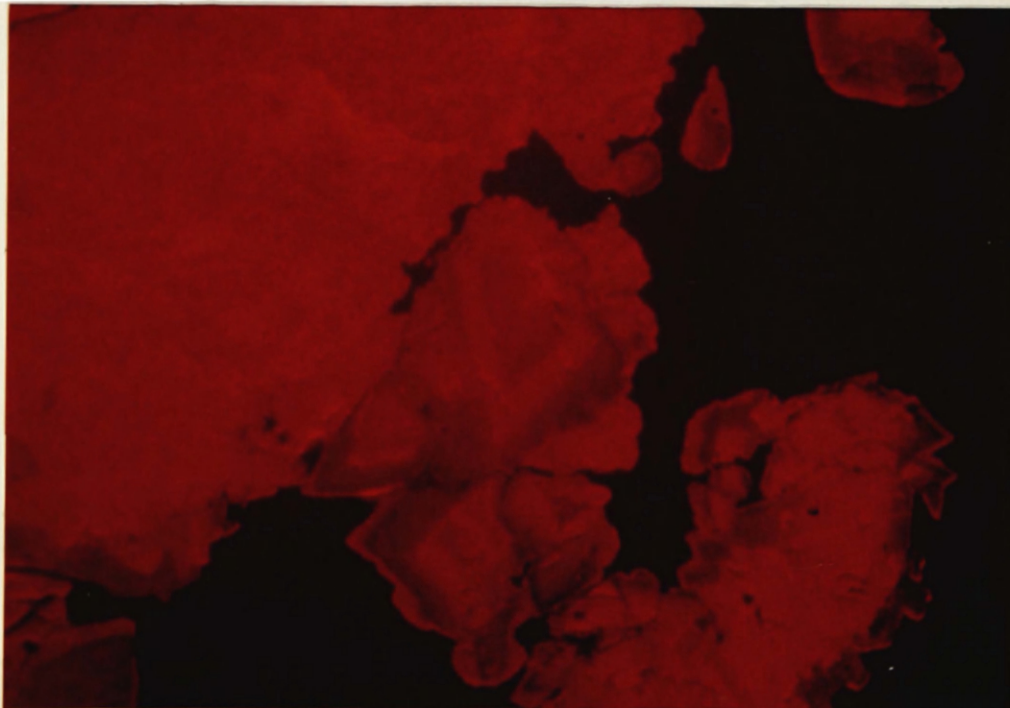


Fig 22d. Same field of view as 22c under cathodoluminescence showing zoned dolomite in the veinlet contrasted with relatively homogeneously bright dolostone surrounding the veinlet (OM36d, Blind Spot, magnification=80x).



Fig. 23a. Photomicrograph under cathodoluminescence of a chalcopyrite-bornite (nonluminescing) and dolomite veinlet crosscutting dolostone. Dolomite in the veinlet shows dull cores and bright rims adjacent to the copper sulfides. Dolostone is relatively homogeneously bright.

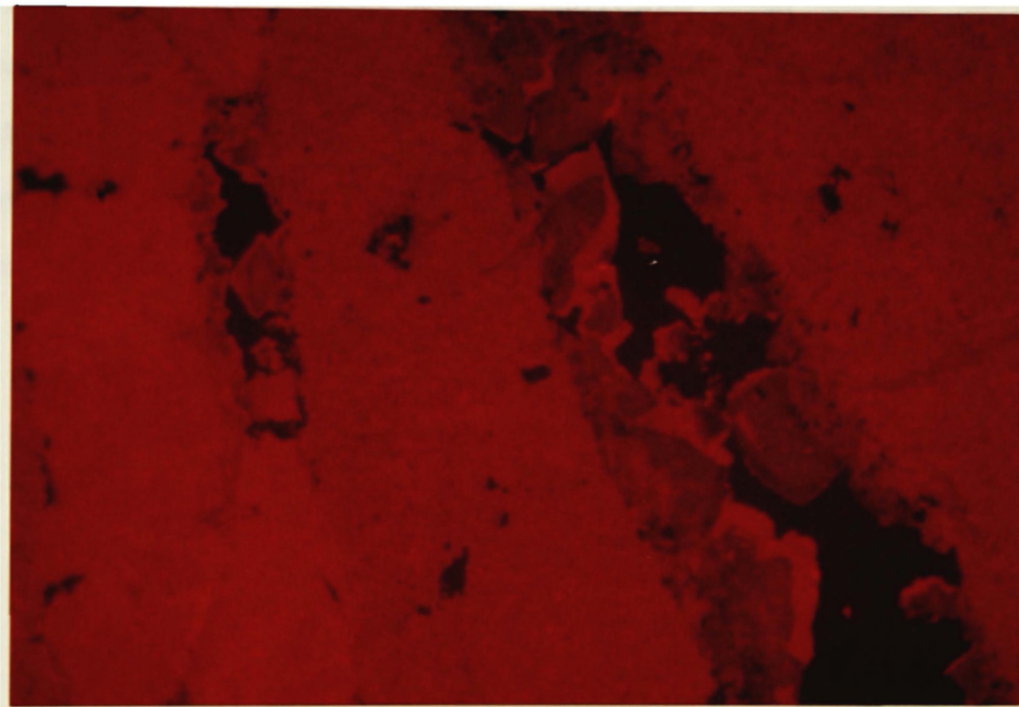


Fig 23b. Photomicrograph under cathodoluminescence of two veinlets showing dolomite with brightly luminescing outer rims and dull cores. Chalcopyrite and bornite are nonluminescing, dolostone is homogeneously bright (OM74b, Copper Hill, magnification=80x).

At Copper Hill, approximately 30% of dolomite rhombs are zoned, and late stage, bright orange cement typically occurs next to copper sulfide (Fig. 23), similar to most zoned dolomite at Blind Spot.

Cathodoluminescent zonation within individual gangue dolomite rhombs suggests changing fluid chemistry (at least different Mn^{+2}/Fe^{+2} ratios) during dolomite growth. Brightly cathodoluminescing rims adjacent to bornite and chalcopyrite for most of the zoned dolomite at both Blind Spot and Copper Hill might indicate some degree of fluid continuity (i.e. similar Mn^{+2}/Fe^{+2} ratios for fluids at the two different places, possibly at the same time) existed between the two areas (now 3 km apart) prior to copper sulfide deposition.

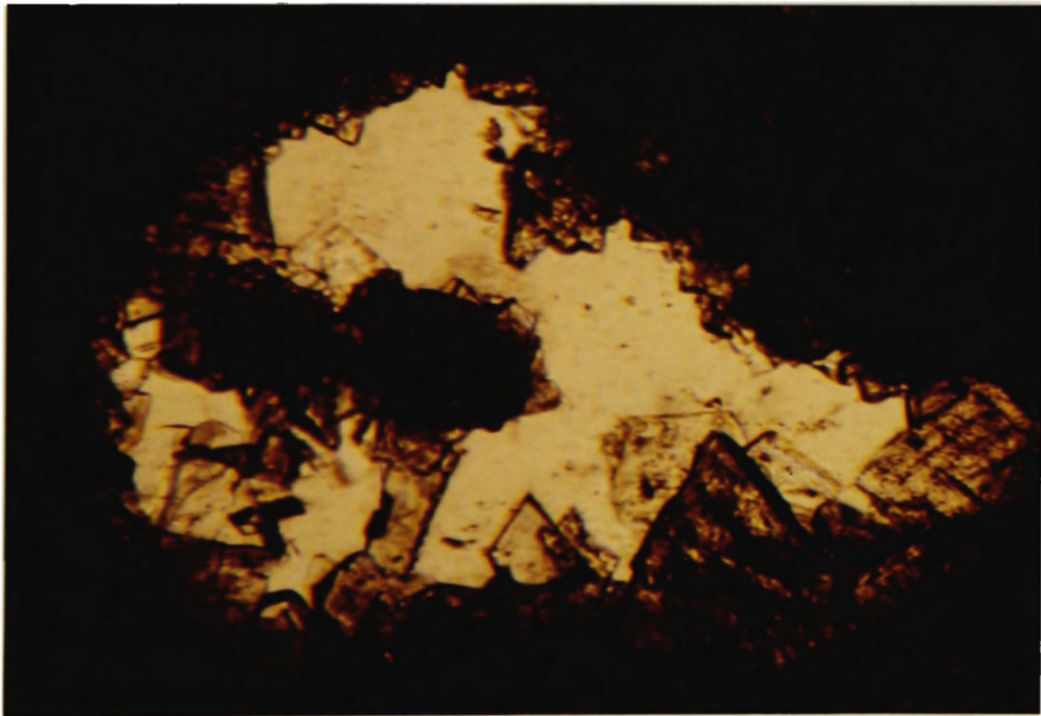


Fig. 24a. Photomicrograph (plane polarized light) of quartz (clear) and dolomite (semi-opaque rhombs) within dolostone (brown).

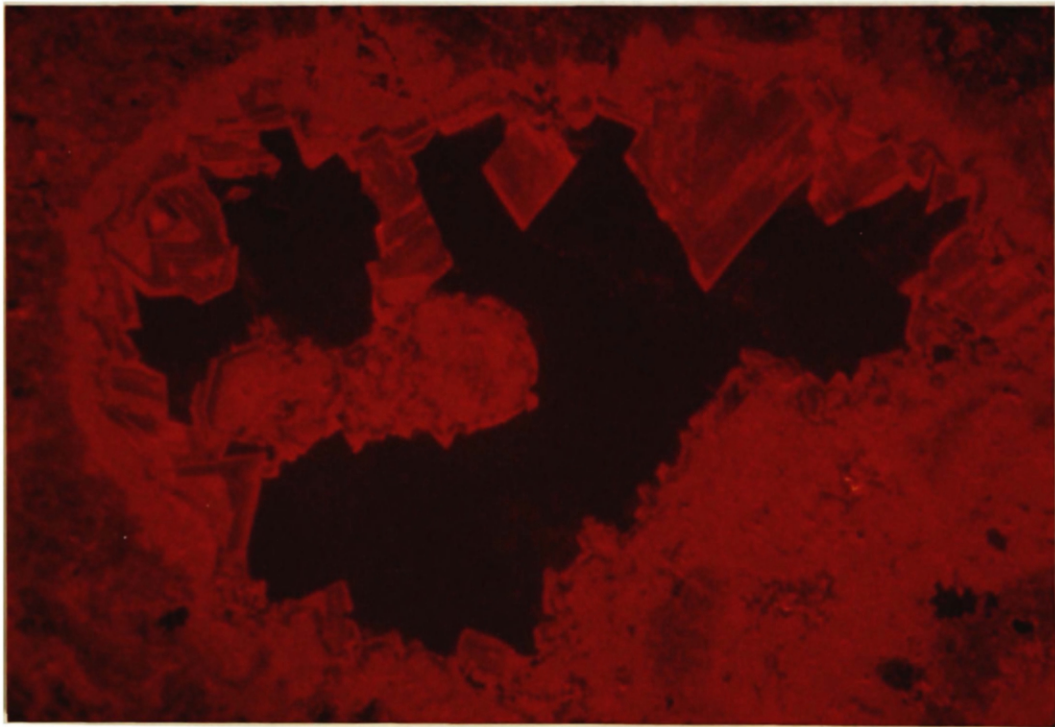


Fig. 24b. Photomicrograph under cathodoluminescence of same field of view as 24a showing nonluminescing quartz at the center, surrounded by zoned dolomite growing out from the walls of the filled vug. Dolomite cement probably grew from the walls of a former vug, and quartz later surrounded the dolomite (OM18b, Copper Hill, magnification=80x).

Well-zoned dolomite cement also occurs within Devonian (unit 5) bioclastic wackestone and packstone at Copper Hill (Fig. 24). The rhombs are commonly euhedral, apparently grew from cavity walls into the open space, and average .05 to .1 mm across. Later, non-cathodoluminescing quartz cement surrounds the dolomite. Most zoned rhombs also show bright outer rims, but only very minor amounts of pyrite and chalcopyrite occur within a few quartz and dolomite-cemented cavities, suggesting that fluids cementing the dolomite were non-mineralizing.

Maturation of Organic Material in Mineralized and Unmineralized Rocks

Spheroidal to irregularly-shaped blebs, clots, and masses of black organic material, ranging from up to 1 cm in diameter, occur only within Devonian dolostone (unit 5) and only at one mineralized outcrop at Copper Hill. The possibility of a relationship between organic blebs and mineralization at Omar warranted petrographic study and ROCK-EVAL pyrolysis of the blebs and also of the organic material within the mineralized and unmineralized country rocks. Studies by Marikos (1984) and Macqueen and

Powell (1983) revealed a relationship between similar organic material and mineralizing processes in the Viburnum Trend lead-zinc deposits and at the Pine Point lead-zinc orebody, Northwest Territories, Canada.

The organic blebs and masses at Copper Hill are brittle, crumble into a fine powder, and sometimes show conchoidal fractures. Their commonly spheroidal texture suggests that the blebs were originally immiscible in a supporting fluid. Blebs from other deposits (Marikos, 1983; Macqueen and Powell, 1983; Hitzman, 1983) were probably derived from bitumen. Thermal alteration probably associated with hydrothermal fluids have rendered these blebs relatively insoluble in organic acids, and the organic material may be termed pyrobitumen. Pyrobitumen blebs at Omar were also heated and are now overmature hydrocarbons.

Coarse-grained (>.1 mm), commonly euhedral, sparry dolomite with lesser amounts of calcite and quartz always enclose pyrobitumen in veinlets and vugs (Fig. 25).

Marikos (1983) reported a similar relationship between bitumen blebs and calcite in the Magmont West orebody, Viburnum Trend. Furthermore, pyrobitumen at Pine Point is always associated with white, coarsely crystalline, hydrothermal dolomite (Macqueen and Powell, 1983).

Dolomite occurring with pyrobitumen at Omar is commonly

zoned under cathodoluminescence, and shows a brightly cathodoluminescent rim adjacent to pyrobitumen, similar to dolomite gangue associated with copper sulfides at Blind Spot and Copper Hill (Fig. 26).



Fig. 25a. Black pyrobitumen enclosed within white dolomite and calcite veinlets crosscutting Devonian dolostone at Copper Hill.

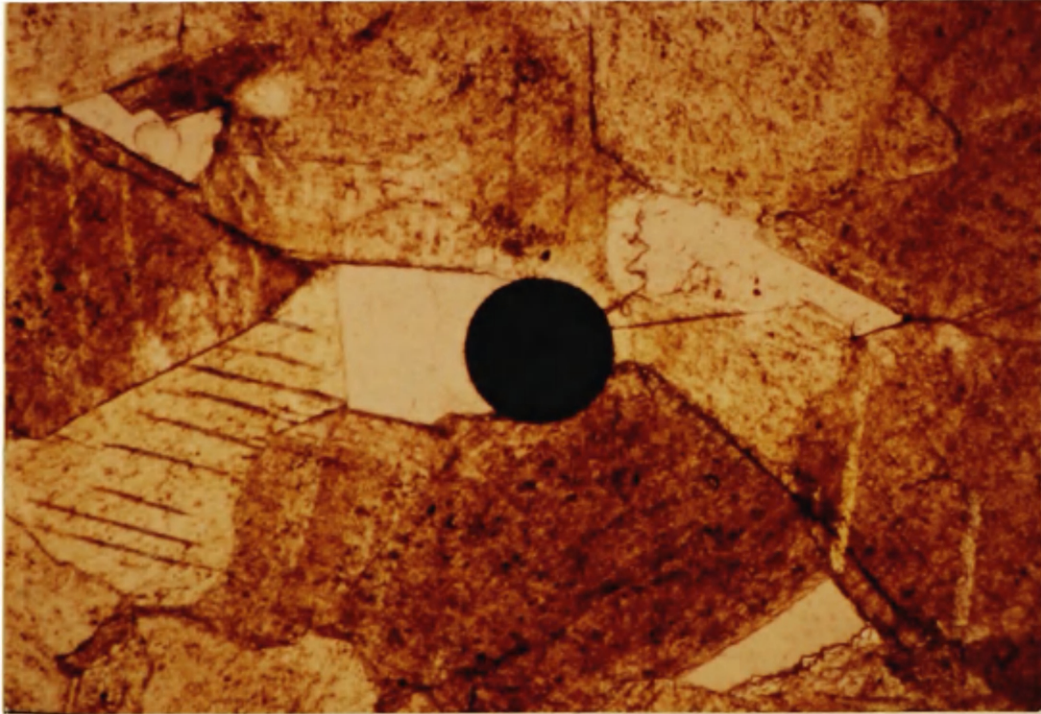


Fig 25b. Photomicrograph (plane polarized light) of spherical pyrobitumen bleb within dolomite (brown) and quartz (clear) (OM159, Copper Hill, magnification=40x).

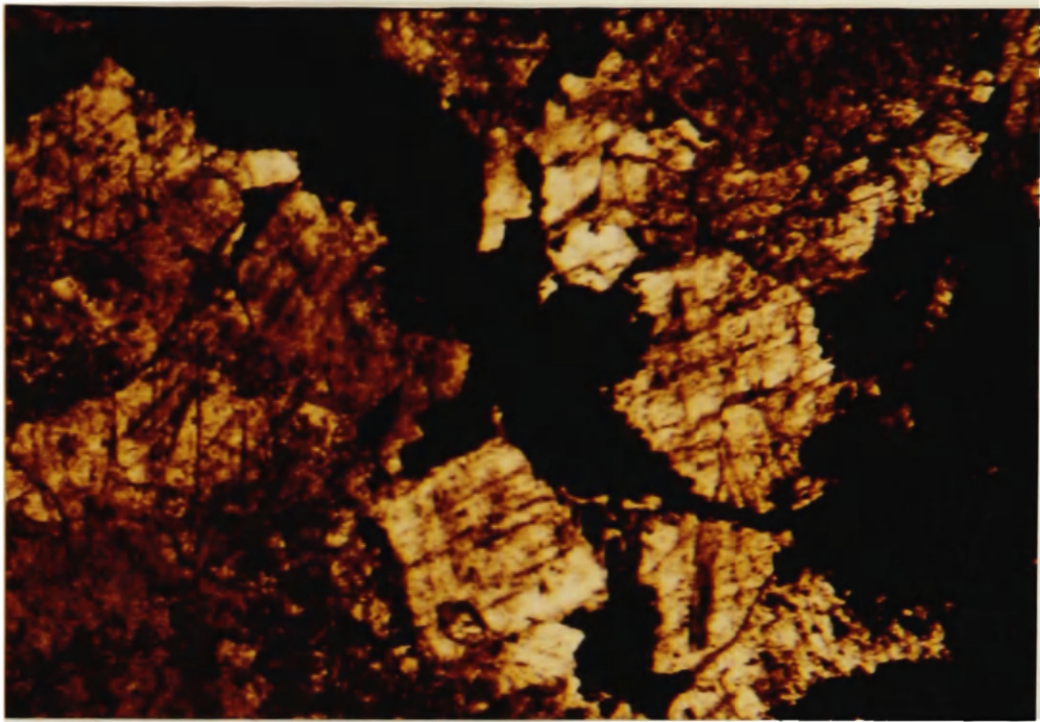


Fig. 26a. Photomicrograph (plane polarized light) of a pyrobitumen (black)-dolomite (white) veinlet crosscutting dolostone (brown).

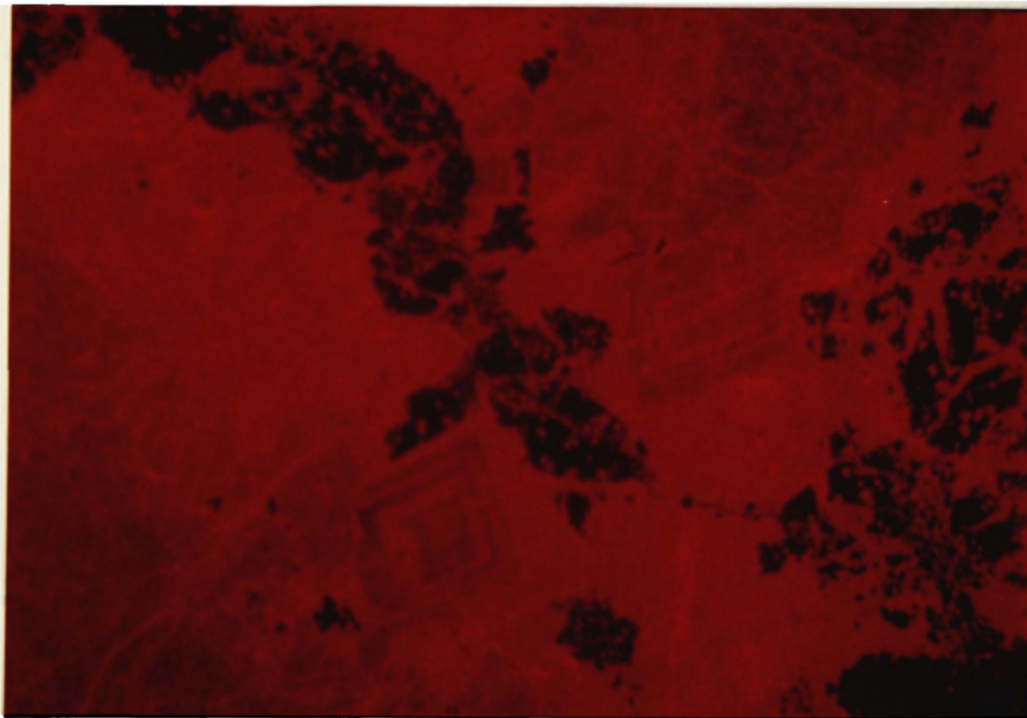


Fig. 26b. Photomicrograph of the same field of view as 26a under cathodoluminescence showing zoned dolomite in the veinlet contrasted with homogeneously bright dolostone.

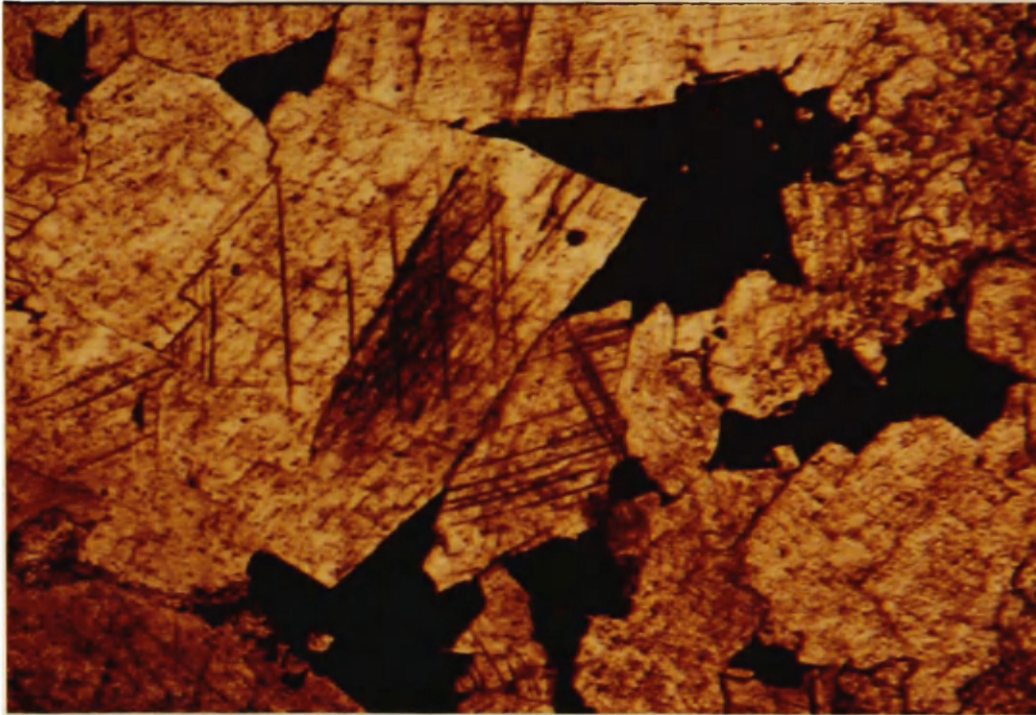


Fig 26c. Photomicrograph of euhedral dolomite (white) and pyrobitumen (black) within a veinlet.

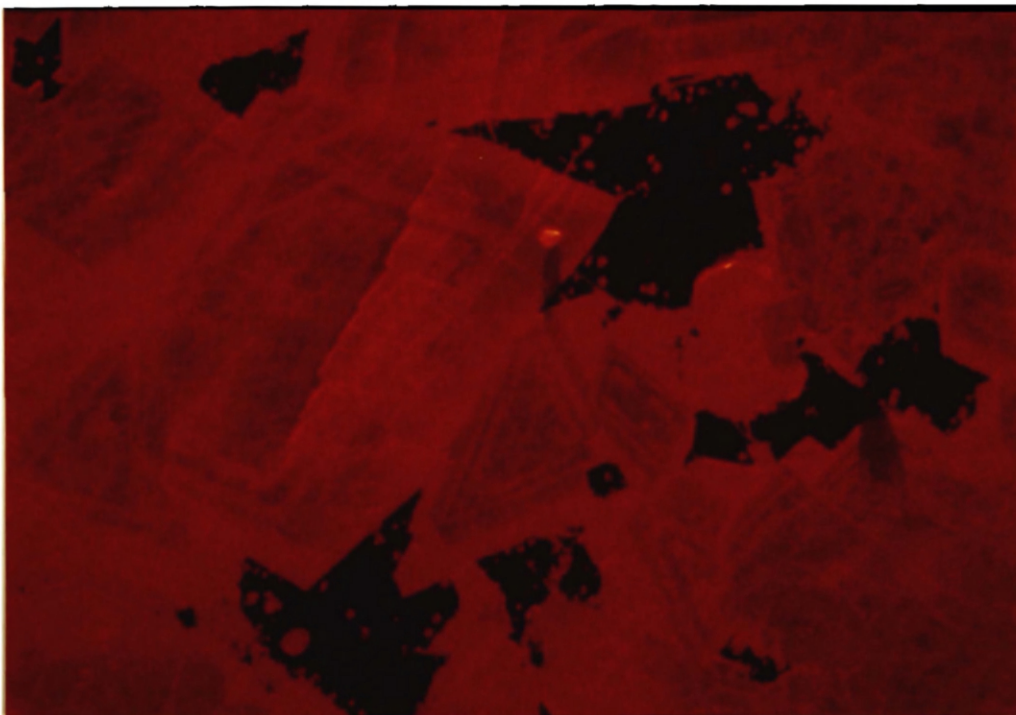


Fig 26d. Photomicrograph of the same field of view as 26c under cathodoluminescence showing zoned dolomite in the veinlet. 26b and 26d both show dolomite rhombs with brightly luminescent rims adjacent to pyrobitumen.

Very minor amounts of fine-grained (<.01 mm) pyrite and chalcopyrite occur within dolomite and quartz-cemented cavities at Copper Hill. Minor amounts of pyrobitumen (recognizable as spherical, opaque, and with similar reflectance as other pyrobitumen) also occur in some voids, surrounded by quartz. Rarely, chalcopyrite and/or pyrite are in contact with a pyrobitumen bleb (Fig. 27).

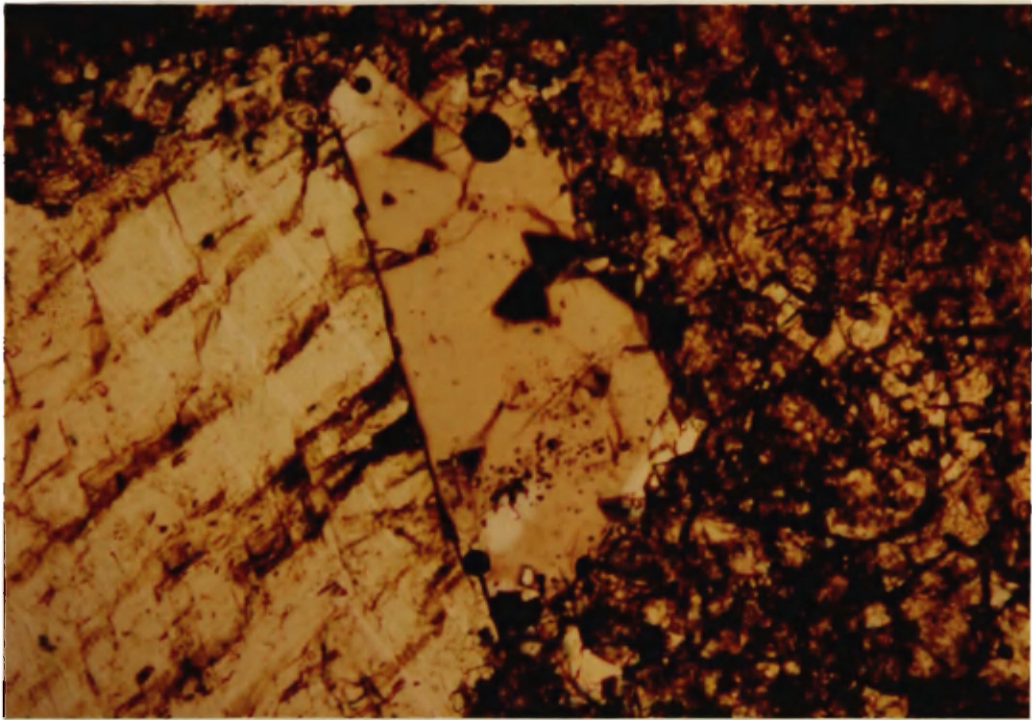


Fig. 27a. Photomicrograph (plane polarized light) of vug in dolostone with quartz (clear) and dolomite (white) within dolostone (brown). Spherical blebs of pyrobitumen are at the top and bottom of the quartz.

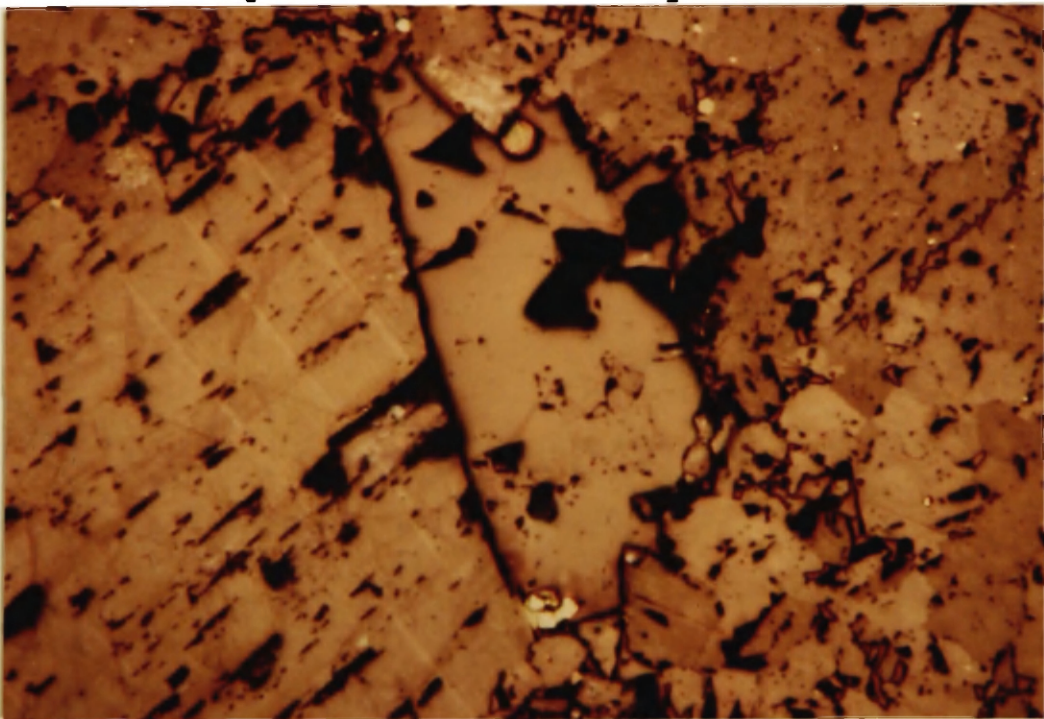


Fig 27b. Photomicrograph (reflected light) of the same field of view as 27a showing partial replacement of the top bleb by chalcopyrite (yellow) and partial replacement of a bottom bleb by pyrite (white, high relief).

ROCK-EVAL Pyrolysis Study

ROCK-EVAL pyrolysis is a useful tool for estimating amount, maturation history, and possible type and evolution path of kerogen within sedimentary rocks (Bustin and others, 1985). It is most commonly used in petroleum exploration; for ore deposit studies, the often higher temperatures and more complicated histories restricts the interpretations that can be derived from ROCK-EVAL pyrolysis (J. Leventhal, oral communication, 1986). Furthermore, surface oxidation of outcrop samples may result in misinterpretation of kerogen type and evolution paths for the organic material (Leventhal, 1982). Consequently, I discuss only the organic carbon contents and relative maturation of organic material from 12 outcrop samples across the Omar Prospect, and 2 pyrobitumen bleb samples from Copper Hill.

All analyses were performed by EXLOG Laboratories, Anchorage, Alaska. Details of analytical equipment and procedure are given in Appendix B. Results of the analyses are summarized in Table 5.

Table 5. Results of ROCK-EVAL pyrolysis (data from EXLOG Laboratories, Anchorage, Alaska)

No.	Description	TOC wt%	TMAX (° C)	S1	S2	S3	HI	OI	S1/S1+S2
OM9	Mineralized dolostone, Unit 5	.05	---	.19	.01	6.32	---	---	---
OM74a	Mineralized dolostone, Unit 5	.05	---	.46	.01	2.49	---	---	---
OM74b	Mineralized dolostone, Unit 5	.69	---	2.89	.01	2.89	---	---	---
OM77	Mineralized dolostone, Unit 5	.73	---	.09	.01	.37	---	---	---
OM83	Unmineralized dolostone, Unit 5	.19	---	.02	.01	.16	---	---	---
OM55	Unmineralized dolostone, Unit 5	.22	416	.49	.05	.17	23	77	.91
OM52	Unmineralized dolostone Unit 4	.09	---	.59	.04	.10	44	111	.94
OM112	Unmineralized dolostone Unit 2	.15	---	.24	.15	.34	---	---	---
OM57	Unmineralized dolostone Unit 2	.07	390	.33	.03	.08	43	114	.92
OM86	Unmineralized dolostone Unit 2	.08	410	.28	.06	.73	100	912	.78
OM8	Unmineralized meta- limestone, unit 1	.11	334	.97	.08	.10	73	91	.92
OM11	Unmineralized meta- limestone, unit 1	.10	337	.64	.11	.19	110	190	.85
OM159a	Pyrobitumen bleb, Unit 5	---	360	.5	.60	12.33	---	---	.45
OM159b	Pyrobitumen bleb, Unit 5	---	342	1.52	.54	10.4	---	---	.74

Note:

S1: Free low temperature hydrocarbon yield (mg hydrocarbon / g of rock).
S2: High temperature kerogen hydrocarbon yield (mg hydrocarbon / g of rock)
S3: Organic CO₂- kerogen derived (mg CO₂ / g rock).
TMAX: Temperature at which maximum emission of S2 occurs.
S1/(S1+S2): Transformation or Productivity Ratio.
HI: Hydrogen Index (kerogen type) [S2/(TOC x 100)].
OI: Oxygen Index (kerogen type) [S3/(TOC x 100)].
When S2 > .20 TMAX error is approximately +/- 4°C.
When S2 < .20 TMAX error is approximately +/- 8-10° C.
S2 = .01 is default value (below detection limit).
TMAX not reported when S2 is below instrument lower detection limit.

Total Organic Carbon (TOC). TOC contents for the 12 rocks are low (<1 wt%) but fairly distinctive for each lithology. For unmineralized rocks: Ordovician dolostone and metalimestone (OM8,11,52,57,86,112, units 1, 2, and 4) contain the lowest TOC, ranging from .07 wt% to .15 wt% (Table 5). Three of four Ordovician dolostones contained lesser amounts of organic material than the metalimestones (<.10 wt% TOC), suggesting that the dolostone contained the least amount of organic matter. Unmineralized Devonian dolostone (OM83,55, unit 5) contained greater TOC (.19 wt % and .22 wt%) than the Ordovician lithologies. One sample of Ordovician metalimestone, and two samples of Ordovician dolostone from approximately 8 km southeast of the Omar Prospect yielded TOC contents similar to Ordovician lithologies at Omar (.06 and .12 wt% for the dolostones, .14 wt% for the limestones; J. Dumoulin, U.S.G.S., written communication, 1986), indicating that TOC may be correlatable for some carbonate rocks types near Omar.

Mineralized dolostones (OM9-Blind Spot, OM74a,74b,77-Copper Hill) contain the lowest TOC (.05 wt%-OM9,74a) and the highest TOC (.69 wt%-OM74b, .73 wt%-OM77) for all rock types sampled (Table 5). High TOC content of OM77 may be explained by small blebs of pyrobitumen that occur with malachite and azurite. OM74b

contains early disseminated pyrite and chalcopyrite replacing pyrite within relatively dark and organic/insoluble-rich zones. However, OM9 contains only veinlet mineralization, neither disseminated sulfides nor visible pyrobitumen blebs were observed. OM74a also contains mostly veinlet mineralization, which may account for the large TOC difference among the mineralized samples.

Maturity of Organic Material. Organic material at Omar is overmature, heated far beyond oil (T=70-130o C) and gas (T=90-200o C) generation windows (Tissot and Welte, 1978). High Productivity Ratios (S1/S1+S2, see Table 5) for samples OM159a,159b,112,and 11(?) indicate that kerogen has been thermally degraded. All other samples, mineralized and unmineralized, contain insignificant or undetectable amounts of unevolved kerogen (S2), also suggesting that the organic material has been thermally degraded. There is no significant difference in kerogen maturity between mineralized and unmineralized samples. Any thermal imprint on organic material by hydrothermal fluids accompanying mineralization was masked by heating during burial and metamorphism, at minimum temperatures of 300-350o C suggested by CAIs (Tables 1 and 2).

Ultraviolet fluorescence of pyrobitumen blebs also

indicated that the material was overmature.

Carbonate Staining

I stained thin sections, chips, and slabs with Aliziran Red-s/potassium ferricyanide solution (Dickson, 1966) to identify calcite versus dolomite and estimate relative differences in iron content within the two minerals. Of 105 samples, 16 mineralized samples (either copper sulfide-bearing or containing anomalous amounts of copper) from the Copper Hill, Blind Spot, South Saddle, and one small area on Trail Mountain (Fig. 2) stained strongly blue, indicating relatively ferroan dolomite. Only 5 unmineralized samples displayed a similar color. Of the 50 samples that showed no blue color, 43 were unmineralized, whereas only 7 were mineralized. Thirty-four samples stained weakly blue, of which 19 samples were mineralized, 15 were unmineralized. The results are tabulated in Table 6).

Table 6. Results of Staining Mineralized and Unmineralized Thin Sections, Chips, and Slabs with Alizarin Red-S/Potassium Ferricyanide Solution.

Sample Type	Strong Blue (Ferroan)	Weak Blue (Slightly Ferroan)	Unstained (non-ferroan)	Totals
Mineralized	16	19	7	42
Unmineralized	5	15	43	63
Totals	21	34	50	105

The mineralizing/alteration fluids were apparently iron-rich relative to unmineralized rocks. Of 42 mineralized samples, 83% were stained blue (38% strongly blue, 45% weakly blue). In contrast, only 32% of unmineralized samples were stained blue (8% strongly blue, 24% weakly blue). A few samples of a breccia from Copper Hill contain fragments that are slightly bluer, hence more ferroan, than veinlets outlining the fragments. Although this is not a consistent relationship in all rocks, it suggests that crosscutting veinlets are iron-poor relative to fine-grained dolostone at Copper Hill.

At the Ruby Creek copper-cobalt deposit 180 km to the east of Omar, both a strong spatial zoning and the different stages of hydrothermal alteration are characterized by distinctive iron contents within dolostone host rocks (hydrothermal dolostone of Hitzman, 1983). At Omar, hydrothermal alteration as revealed by staining is less pervasive and less well-developed within dolostone host rocks than at Ruby Creek.

Trace Element Geochemistry of Rocks, Soils, and
Stream Sediments

A total of 77 mineralized and unmineralized rock samples, 81 soil samples, and 44 stream sediment samples were collected around the Omar Prospect. Poor exposure and extensive talus cover precluded systematic sampling of rock and soil over a uniform grid pattern. Yet, the data were valuable for characterizing the lithochemical signature of the prospect and identifying the most significant pathfinder elements in the weathering environment. All samples were analyzed by Elizabeth Bailey and Steve Sutley (U.S. Geological Survey, Golden, CO) for 31 elements by semi-quantitative emission spectrography, and by Rich O'Leary (U.S. Geological Survey, Golden, CO) for arsenic, zinc, cadmium, bismuth, and antimony by atomic absorption (AA). Analytical results are shown in Appendix A.

Statistical Methods

Univariate statistics for rock, stream sediment, and soil data are reported in tables 7, 10, and 13. Some values for particular elements are typically above or below the detection limits of semi-quantitative emission spectrography, resulting in a censored data base.

Detection ratios shown in the statistical tables (uncensored values divided by total number of analyses) show the degree to which data are censored for individual elements. Geometric means and deviations were not calculated for highly censored elements (detection ratios less than .20).

Trace element geochemical values are typically positively skewed, therefore all data was logarithmically transformed prior to statistical analysis. Geometric means and standard deviations reported in tables 7, 10, and 13 were calculated using Cohen's (1959) maximum likelihood method, which is a better approximation for censored data. Additionally, the expected range for 95% of all values in the lognormal distribution (Miesch, 1976) is included for each element.

The 95th percentile values are also reported for each element. These values reflect mineralized rocks, soil samples overlying mineralized zones, and stream sediment samples from creeks draining mineralized zones.

I used R-mode factor analysis with varimax rotation to examine the relationship among elements in the rock, soil, and stream sediment data. Factor analysis is commonly used by geologists to place similarly behaving experimental variables (elements) into groups termed factors (Johnston, 1978). These factors can help explain

geochemical associations within the studied data base that are related to lithology or mineralization.

Rocks

Copper, iron, arsenic, and antimony, are anomalous in most mineralized rocks. High values for cobalt, zinc, lead, and silver also occur in some mineralized samples. Gold, beryllium, lanthanum, niobium, scandium, tin, tungsten, and thorium were also analyzed for but were below detection limits in all samples. Univariate statistics for rock data are shown in table 7. High cobalt contents for rocks, soils, and stream sediments at

Table 7. Univariate Statistics for Mineralized and Unmineralized Rocks

Element	Detection Ratio	Minimum	Maximum	Median	Geometric Mean	Geometric Deviation	Expected Range	95th Percentile
Fe	0.91	0.05	20.00	0.30	0.40	5.90	.01-14	15.00
Mg	1.00	0.03	12.00	5.00	3.20	4.00	.21-50	10.00
Ca	0.99	0.05	20.00	15.00	8.80	3.80	.61-127	20.00
Ti	0.78	0.002	0.50	0.005	0.01	6.50	.0002-.29	0.30
Mn	0.97	10.00	1500.00	200.00	189.00	3.50	16-2250	1500.00
Ag	0.16	0.50	20.00	0.50	-----	-----	-----	7.00
B	0.27	10.00	300.00	10.00	2.80	8.00	.04-178	100.00
Ba	0.25	20.00	5000.00	20.00	1.50	45.00	.60-3078	1000.00
Co	0.56	5.00	2000.00	7.00	6.90	8.90	.09-540	700.00
Cr	0.26	10.00	300.00	10.00	2.30	10.00	.02-228	150.00
Cu	0.82	5.00	20000.00	50.00	65.00	23.00	.12-35023	10000.00
Mo	0.13	5.00	20.00	5.00	-----	-----	-----	10.00
Ni	0.61	5.00	300.00	7.00	7.60	5.10	.29-199	150.00
Pb	0.56	10.00	1500.00	10.00	11.00	6.40	.27-467	700.00
Sr	0.45	100.00	5000.00	100.00	80.00	4.20	4.5-1408	1000.00
V	0.75	10.00	200.00	10.00	14.00	2.80	1.8-111	150.00
Y	0.44	10.00	50.00	10.00	8.50	2.20	1.8-40	30.00
Zr	0.52	10.00	150.00	10.00	17.00	2.40	2.9-106	100.00
As	0.38	10.00	11000.00	10.00	3.70	16.00	.01-995	450.00
Zn	0.87	5.00	19900.00	30.00	37.00	8.10	4.6-2461	1200.00
Cd	0.53	0.10	100.00	0.10	0.10	13.00	.001-20.6	5.00
Bi	0.09	1.00	16.00	1.00	-----	-----	-----	2.00
Sb	0.38	2.00	550.00	2.00	0.94	6.80	.02-43.2	20.00

Note:

As, Zn, Cd, Bi, and Sb were analyzed by atomic absorption, all other elements were analyzed by semi-quantitative emission spectroscopy
 Fe, Ca, Mg, and Ti are reported in percent, all other elements are reported in parts per million

Omar were also reported by Jansons (1982). Samples from mineralized areas collected during this study contain up to and greater than 2000 ppm cobalt. However, cobalt content may vary considerably within the same rock. For example, four analyses of the same rock (OM9) from Blind Spot revealed a broad range of values: 36 ppm and 207 ppm (AA, Bondar-Clegg, Inc., J. Foley, written communication, 1986), versus 700 ppm and >2000 ppm (SPEC, this study). Analytical error and variance between laboratories may account for some of the discrepancy, but the wide range between low and high values suggests that a cobalt or cobalt-bearing phase is present but not abundant or evenly distributed within the rock. Scanning electron microscopy of one sample from Blind Spot (OM9) and one sample from Copper Hill (OM74) did not detect cobalt minerals (J. Foley, written communication, 1986); cobalt is probably contained within the copper or iron sulfide crystal structures.

Table 8 shows factor loadings for the 4 factors determined to be significant (eigenvalues > 1). Factor loadings are a measure of the influence of each factor on a variable, and may be interpreted similarly to correlation coefficients (Johnston, 1978). These 4 factors explain 78% of the total variance within the rock dataset. Factors 2 and 4 define element suites associated

with mineralization. Copper, lead, and zinc show relatively high loadings onto both factors. Factor 2 also includes strong loadings for iron, manganese, cobalt, and nickel, whereas factor 4 includes high arsenic, antimony, and yttrium loadings.

Table 8. Factor loadings for 77 rock samples.

Element	Factor 1	Factor 2	Factor 3	Factor 4
Fe	--	.79	--	--
Mg	--	--	.73	--
Ca	--	--	.87	--
Ti	.87	--	--	--
Mn	--	.69	.52	--
B	.89	--	--	--
Ba	.70	--	--	--
Co	--	.94	--	--
Cr	.84	--	--	--
Cu	--	.68	--	.61
Ni	.41	.79	--	--
Pb	--	.78	--	.43
Sr	.62	--	--	--
V	.79	--	--	--
Y	.63	--	--	.44
Zr	.93	--	--	--
As	--	--	--	.89
Zn	--	.73	--	.46
Sb	--	--	--	.89
Proportion of the total variance:	28%	24%	12%	15%

Note:

Loadings <.4 are omitted

Samples with high factor scores (corresponding to the 90th percentile cutoff for each factor) for both factors 2 and 4 plot at Copper Hill, and do not reveal a clear spatial zonation there (Fig. 28). Samples from Blind Spot have high factor scores onto factor 2, possibly reflecting greater amounts of cobalt within copper sulfides at Blind Spot, contrasted with the more common occurrence of tennantite/tetrahedrite (high loadings for arsenic and antimony onto factor 4) at Copper Hill. Alternatively, the two factors may reflect different degrees of weathering; certain elements (arsenic, antimony) becoming residually concentrated more than others. Some samples from Copper Hill and South Saddle were gossan with no visible sulfides, whereas Blind Spot samples were weathered and oxidized but most contained visible copper sulfides. Table 9 gives some trace element values for samples with the highest factor scores onto factors 2 and 4.

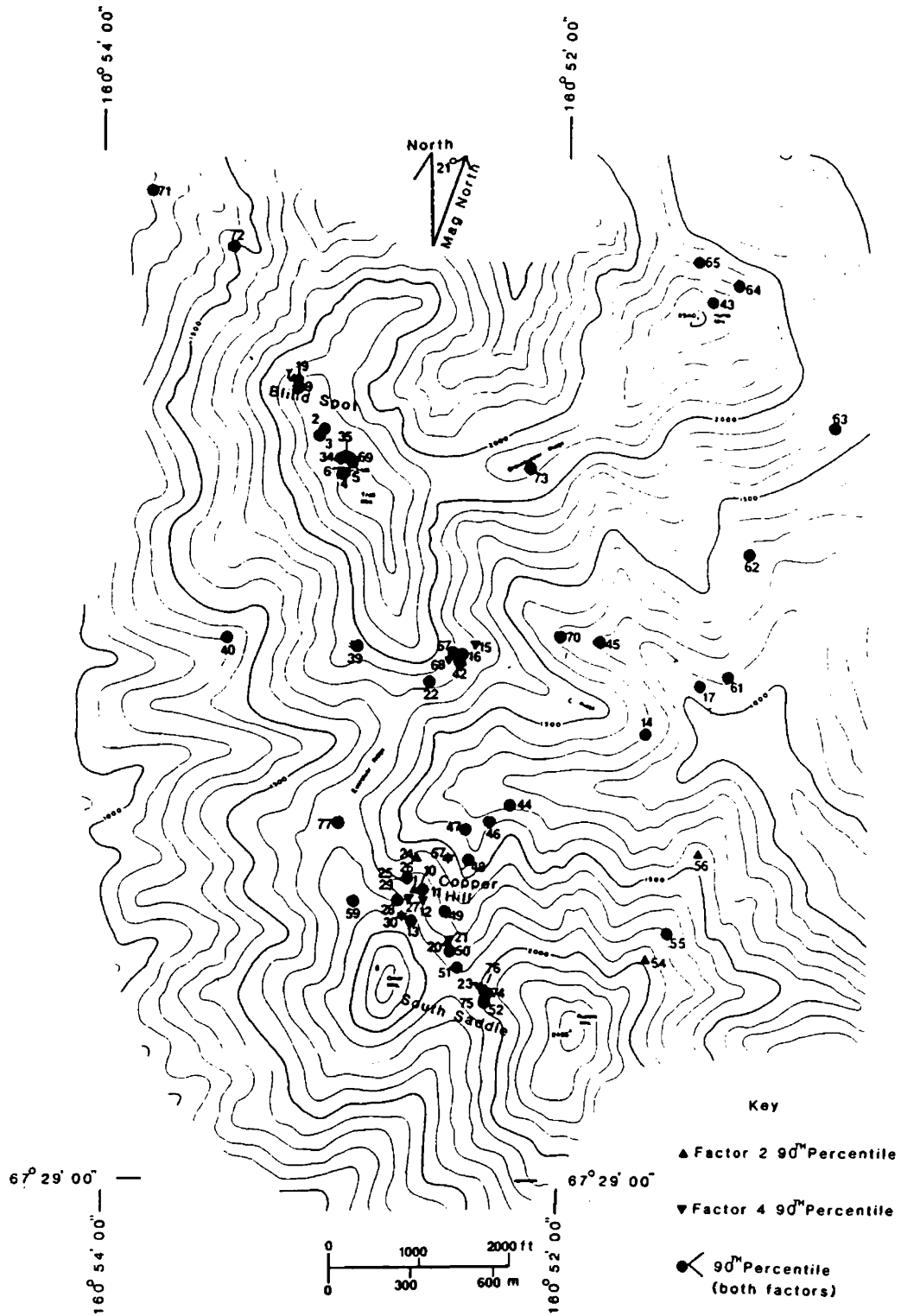


Fig. 28. Geochemical factor map of rock samples showing samples with factor scores above the 90th percentile for factors 2 and 4; and sample sites for samples less than the 90th percentile for both factors.

I interpret factors 1 and 3 to reflect lithologic distinctions. Factor 3 shows high loadings for calcium, magnesium, and manganese, probably indicating relatively clean carbonates. Factor 1 apparently groups together the argillaceous carbonates, including the platy-weathering brown to gray metalimestone (units 1 and 3).

Table 9. Geochemical values for rock samples with high factor scores onto factors 2 and 4.

No.	Factor	Fe	Mn	Ag	Co	Ni	Pb	Y	As	Zn	Cd	Sb	Cu
15b	2	1.5	1000	10.0	100	20	200	15	60	1000	20.0	5	>20000
9	2	20.0	200	20.0	700	100	300	N	N	15	1.0	N	>20000
36	2	5.0	1000	1.5	2000	200	100	N	20	100	2.6	4	>20000
42	2	2.0	1000	L	70	20	30	50	20	400	1.0	2	1500
72	2	15.0	500	7.0	700	150	1500	L	30	16000	70.0	8	1000
114	2	20.0	200	N	100	150	30	N	30	160	0.2	2	300
116	2	20.0	150	L	150	300	100	N	N	70	0.4	N	200
117	2,4	.5	700	2.0	100	30	200	10	1100	19900	15.0	20	10000
17	4	.15	700	1.5	10	L	30	10	30	40	0.3	12	7700
25	4	10.0	30	1.0	150	50	150	N	300	400	1.0	4	3000
41	4	.05	150	L	L	L	10	50	1000	230	3.6	26	1500
66	4	.15	200	2.0	7	L	1500	L	11000	1300	15.0	550	20000
75	4	5.0	200	10.0	150	20	100	50	180	110	1.0	130	>20000
79	4,2	20.0	500	7.0	200	70	700	L	480	400	2.9	5	5000
139b	4	.05	150	.5	N	N	L	20	210	20	0.1	6	1000
158a	4	.2	500	N	7	L	10	L	450	150	1.7	28	1000

Note:

Fe reported as %, all other in parts per million.

As, Zn, Cd, and Sb analyzed by atomic absorption, all other elements by emission spectrography.

L=detected, but below detection limits.

N=undetected.

Soil and Stream Sediments

Identification of pathfinder elements from primary mineralization in the secondary weathering environment is important in exploration for particular deposit types. BCMC originally located mineralization at Omar following copper anomalies in stream sediment. Folger and others (1985) showed above background copper and arsenic concentrations 3 km downstream of the mineralized source. Degenhart and others (1977) reported copper values of >20000 ppm in soils, and up to 2600 ppm in stream sediments at Omar.

I collected 81 soil samples and 44 stream sediments at Omar for geochemical analysis. Soil at Omar is generally less than 30 cm thick, and is located only on broad ridge tops and gentler slopes. Attempts were made to sample only the more stable soils. Table 10 gives univariate statistics for the soil sample data. Gold, beryllium, bismuth, niobium, tin, tungsten, and thorium were analyzed for but were below detection limits in all samples. Values of soil samples distant from known mineralization at Omar are similar to background values from unmineralized rock samples.

Table 10. Univariate Statistics for Soil Samples

Element	Detection Ratio	Minimum	Maximum	Median	Geometric Mean	Geometric Deviation	Expected Range	95th Percentile
Fe	1.0	0.15	20.00	1.00	1.10	2.40	.18-6.6	7.00
Mg	1.0	0.30	15.00	5.00	3.60	2.40	.62-21	15.00
Ca	1.0	0.10	15.00	5.00	3.40	2.90	.40-29	15.00
Ti	1.0	0.01	0.70	0.10	0.10	2.40	.01-46	0.50
Mn	1.0	20.00	1000.00	200.00	183.00	2.30	35-970	700.00
B	0.75	10.00	300.00	30.00	24.00	3.40	2-275	200.00
Ba	0.72	20.00	1000.00	50.00	44.00	4.10	2.6-743	500.00
Co	0.72	5.00	300.00	10.00	9.50	3.40	.82-110	70.00
Cr	0.96	10.00	200.00	50.00	46.00	2.50	7.3-287	200.00
Mo	0.43	5.00	200.00	5.00	3.80	5.30	.13-105	100.00
Ni	0.96	5.00	300.00	30.00	32.00	3.10	3.4-312	200.00
Pb	0.90	10.00	300.00	30.00	32.00	2.70	4.4-236	200.00
Sc	0.73	5.00	30.00	5.00	6.20	1.70	2.1-18	20.00
V	0.98	10.00	2000.00	50.00	69.00	4.50	3.5-1380	1500.00
Y	0.70	10.00	100.00	15.00	14.00	2.40	2.4-81	70.00
Zr	0.90	10.00	150.00	30.00	28.00	2.40	4.5-176	100.00
La	0.17	20.00	100.00	20.00	-----	-----	-----	70.00
Sr	0.12	100.00	700.00	100.00	-----	-----	-----	200.00
As	0.84	10.00	220.00	20.00	17.00	2.30	3.1-88	90.00
Zn	1.0	10.00	3000.00	80.00	104.00	3.80	7.2-1498	1100.00
Ag	0.48	0.10	4.10	0.10	0.10	4.40	.01-1.9	0.90
Cd	0.89	0.10	7.20	0.40	0.50	4.30	.03-8.7	5.90
Sb	0.41	2.00	23.00	2.00	1.50	2.30	.28-12	10.00
Cu	1.00	5.00	16000.00	60.00	62.00	5.20	2.3-1674	2000.00

Note:

As, Zn, Ag, Cd, Sb, and Cu were analyzed by atomic absorption, all other elements were analyzed by semi-quantitative emission spectrography
 Fe, Mg, Ca, and Ti are reported in percent, all other elements are reported in parts per million

Trace element associations from soil data are similar to the associations noted in rocks. However, the two factors (Table 11) containing element suites indicating mineralization plot in different locations (Copper Hill/South Saddle--factor 3; Everclear Ridge--factor 2; Fig. 29). Copper, lead, arsenic, zinc, and silver have high loadings onto both factors, but iron, cobalt, and manganese have high loadings only onto factor 3, whereas antimony, nickel, vanadium, yttrium, and molybdenum have high loadings onto factor 2 (Table 11). Mineralization is not exposed along Everclear Ridge, and outcrops are rare, but rubble chips in soil suggest that the underlying rock is Devonian dolostone and metalimestone (unit 5). Factor 2 may reflect an extension of Copper Hill mineralization at Everclear Ridge, with either a different sulfide assemblage or different amounts of trace elements (silver, antimony, cadmium, nickel, vanadium, yttrium, and molybdenum) within chalcopyrite, bornite, and tetrahedrite/tennantite.

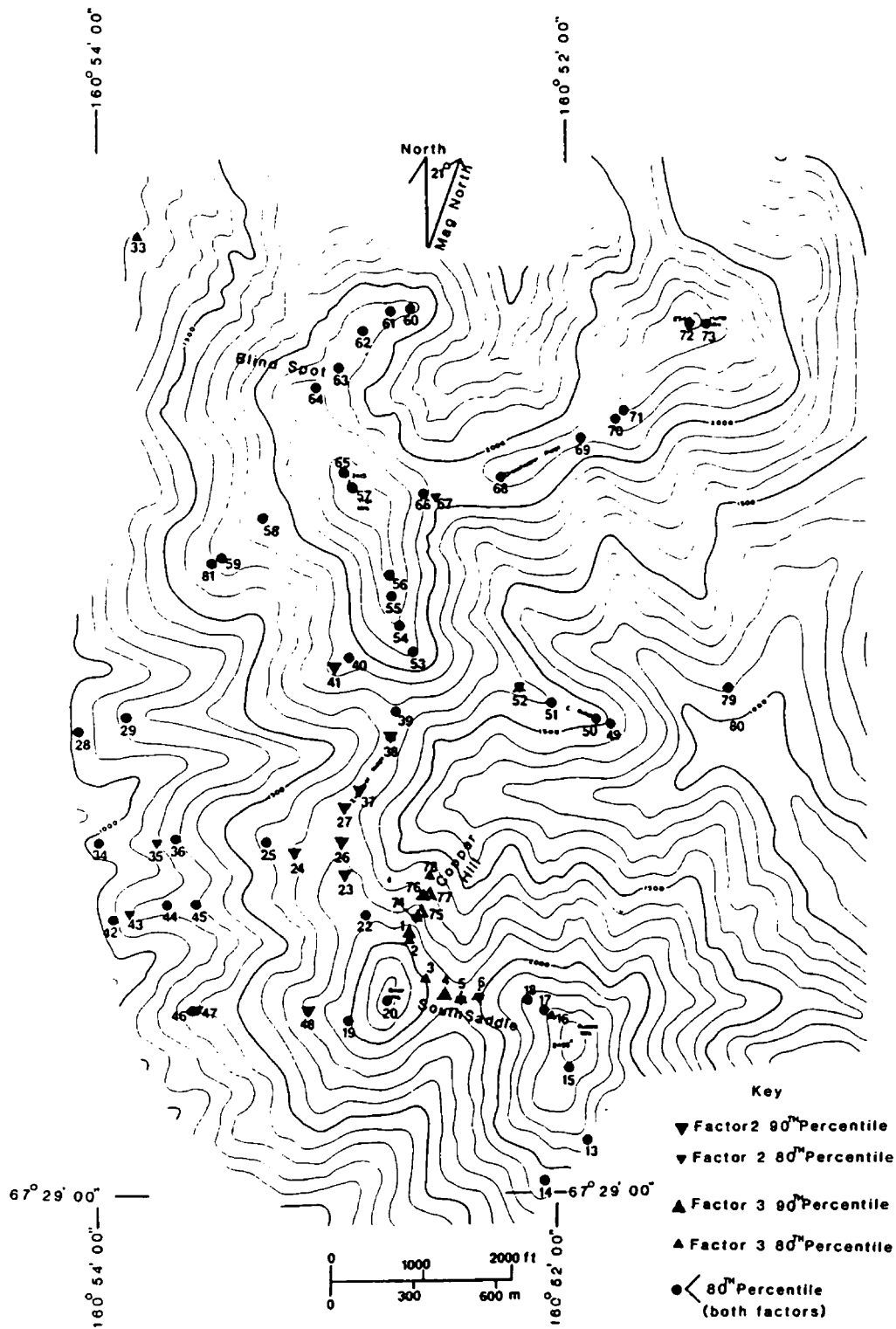


Fig. 29. Geochemical factor map of soil samples with factor scores above the 90th and 80th percentile for factors 2 and 3, and samples sites below the 80th percentile for both factors. Samples with high factor 2 scores plot along Everclear Ridge and the west side of the prospect, whereas samples with high factor 3 scores plot at Copper Hill.

Table 11. Factor loadings for 81 soil samples.

Element	Factor 1	Factor 2	Factor 3	Factor 4
Fe	.55	--	.65	--
Mg	--	--	--	.85
Ca	--	--	--	.92
Ti	.92	--	--	--
Mn	--	--	.72	--
B	.81	--	--	--
Ba	.67	--	--	--
Co	--	--	.85	--
Cr	.87	--	--	--
Mo	--	.91	--	--
Ni	.59	.65	--	--
Pb	--	.50	.69	--
Sc	.85	--	--	--
V	.55	.68	--	--
Y	.52	.67	--	--
Zr	.78	--	--	--
As	--	.53	.72	--
Zn	--	.66	.59	--
Ag	--	.75	.46	--
Sb	--	.88	--	--
Cu	--	.43	.84	--
Proportion of the total variance:	26%	24%	20%	10%

Note:

Loadings <.4 are omitted

Stream sediment data reveal that copper, lead, zinc, arsenic, cobalt, and manganese in the sediments are good pathfinders for Omar-type mineralization (Table 12, factor 2). Table 13 gives univariate statistics for the stream sediment data. Gold, beryllium, bismuth, lanthanum, molybdenum, niobium, antimony, tin, tungsten, and thorium were analyzed for but were below detection limits in all samples. The samples with highest scores onto factor 2 drain mineralized outcrops in the Copper Hill area and south of Trail Mountain, but fail to identify mineralization upstream at Blind Spot (Fig. 30). The stream draining Blind Spot is poorly developed, and only relatively minor amounts of copper sulfide are exposed there.

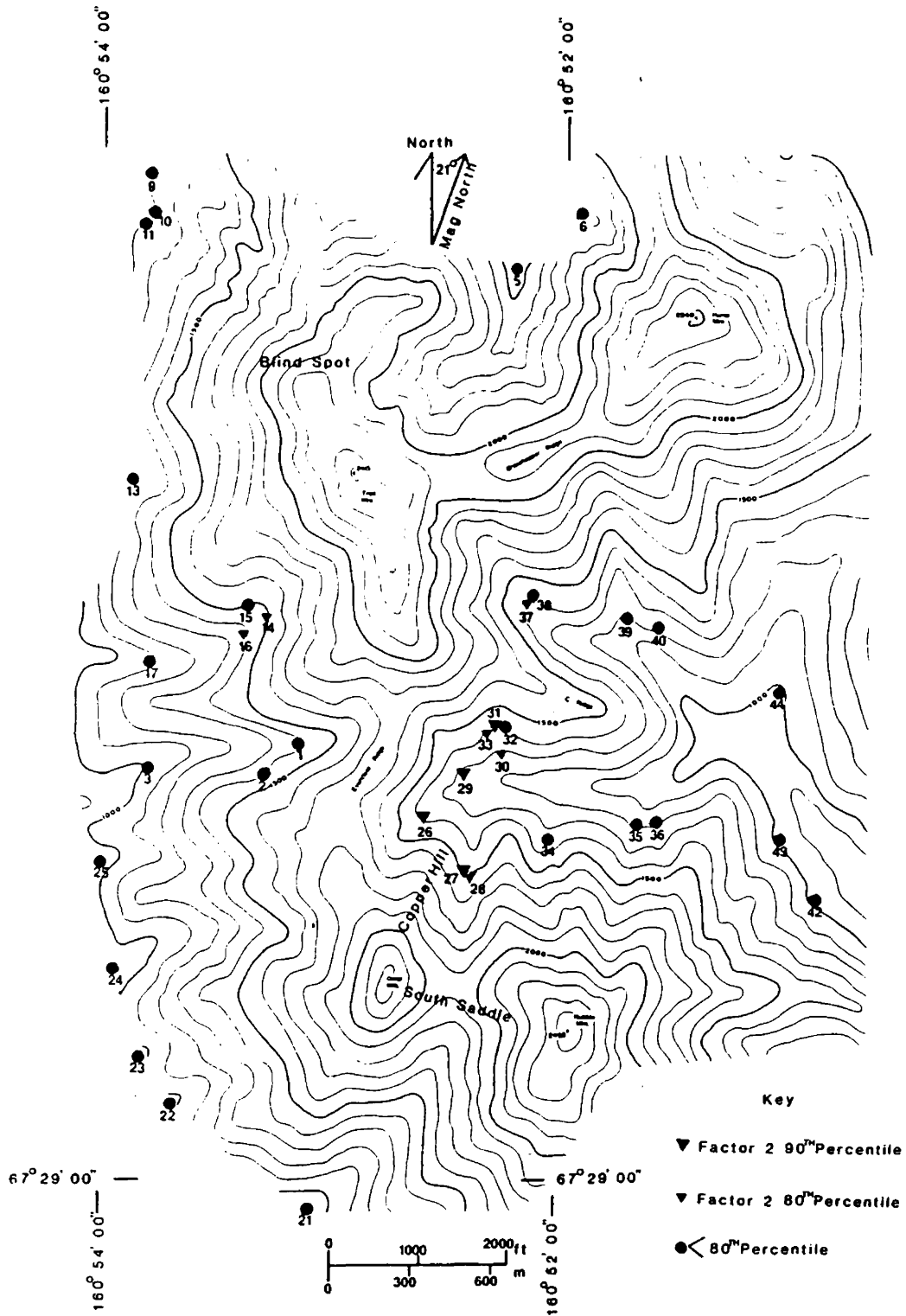


Fig. 30. Geochemical factor map of stream sediment samples showing samples with factor scores above the 90th percentile for factor 2, and sample sites below the 80th percentile. Samples with high factor scores clearly reflect mineralization in the Copper Hill/South Saddle area.

Table 12. Factor loadings for 44 stream sediment samples

Element	Factor 1	Factor 2	Factor 3	Factor 4
Fe	.75	.43	--	--
Mg	--	--	-.58	.72
Ca	--	--	--	.91
Ti	.80	--	--	--
Mn	.62	.60	--	--
B	.90	--	--	--
Ba	.51	--	.68	--
Co	--	.77	.43	--
Cr	.87	--	--	--
Cu	--	.89	--	--
Ni	.81	.40	--	--
Pb	--	.83	--	--
Sc	.52	--	.70	--
Sr	--	--	.83	--
V	.86	--	--	--
Y	.51	.44	--	--
Zr	.78	--	--	--
As	--	.92	--	--
Zn	.46	.68	--	--
Ag	--	.89	--	--
Proportion of the total variance:	32%	28%	16%	8%

Note:

Loadings <.4 are omitted

Table 13. Univariate Statistics for Stream Sediment Samples

Element	Detection Ratio	Minimum	Maximum	Median	Geometric Mean	Geometric Deviation	Expected Range	95th Percentile
Fe	1.00	0.20	5.00	0.70	0.80	2.10	.19-3.6	3.00
Mg	1.00	2.00	15.00	7.00	7.70	1.70	2.7-22	15.00
Ca	1.00	2.00	25.00	7.00	7.30	1.60	2.8-19	15.00
Ti	1.00	0.01	0.30	0.07	0.10	2.20	.02-.34	0.20
Mn	1.00	30.00	700.00	150.00	160.00	2.10	36-704	500.00
B	0.70	10.00	150.00	15.00	17.00	3.00	1.9-153	100.00
Ba	0.61	20.00	500.00	20.00	29.00	3.90	2.1-406	300.00
Co	0.68	5.00	100.00	7.00	8.70	3.40	.75-101	70.00
Cr	0.98	10.00	150.00	50.00	39.00	2.20	8-187	100.00
Cu	0.95	5.00	1500.00	20.00	32.00	4.90	1.3-768	700.00
Ni	0.98	5.00	100.00	20.00	23.00	2.40	4-133	70.00
Pb	0.91	10.00	150.00	20.00	23.00	2.20	4.8-110	100.00
Sc	0.45	5.00	15.00	5.00	4.60	1.70	1.6-13.3	10.00
Sr	0.36	100.00	300.00	100.00	83.00	1.70	29-241	200.00
V	0.93	10.00	700.00	70.00	61.00	3.20	6-622	300.00
Y	0.61	10.00	30.00	10.00	12.00	1.70	4.1-35	30.00
Zr	0.82	10.00	100.00	20.00	18.00	2.10	4.1-79	70.00
As	0.68	10.00	100.00	10.00	11.00	2.30	2.2-61	60.00
Zn	1.00	10.00	800.00	65.00	61.00	3.00	6.8-549	370.00
Ag	0.25	0.10	0.40	0.10	0.05	3.20	.005-.51	0.35
Cd	0.80	0.10	2.70	0.30	0.30	3.60	.03-4.4	1.80

Note:

As, Zn, Ag, and Cd were analyzed by atomic absorption, all other elements were analyzed by semi-quantitative emission spectrography

Fe, Ca, Mg, and Ti are reported in percent, all other elements are reported in parts per million

Lead Isotopes

Two chalcopyrite samples from Copper Hill were analyzed for lead isotopes and contained radiogenic lead (Table 14). Lead isotope data from the western Brooks Range ore deposits are insufficient to establish a growth curve and calculate a reasonable mineralization age for Omar. However, the radiogenic nature of lead in the chalcopyrite suggests that lead has been derived from upper crustal sediments, and represents preferential enrichment of uranogenic lead versus common lead by processes in upper crust (Doe and Stacy, 1973). An igneous source for lead, therefore, is unlikely, and also would not be expected to yield two very different $^{206}/^{204}$ ratios for samples from the same deposit. Rather, heterogeneous (and radiogenic) values are common in some Mississippi Valley-type deposits (Sverjensky and others, 1979). The Pb-isotope heterogeneity may reflect the interaction of mineralizing fluids with variably radiogenic rocks and/or sediments somewhere along the fluid path prior to mineralization at Omar.

Table 14. Lead isotope results from two Copper Hill chalcopyrite samples.

Sample no.	Pb ²⁰⁶ /Pb ²⁰⁴	Pb ²⁰⁷ /Pb ²⁰⁴	Pb ²⁰⁸ /Pb ²⁰⁴
OM74	20.46	15.71	38.19
OM125	18.79	15.62	38.23

Note:

Data provided by M. Delevaux, written communication, 1986

Fluid Inclusions

I measured melting and homogenation temperatures from fluid inclusions in quartz in mineralized veinlets from Blind Spot. The results are summarized in Table 15. Inclusions in dolomite from the same veinlets were too small for study. Homogenation temperatures for 13 inclusions vary widely, one sample (OM142d4) contained three inclusions ranging from 113 ± 4 C to 243 ± 3 C, suggesting that inclusions have necked (Roedder, 1962) down from originally larger inclusions. Some fluid inclusions within the same sample show different vapor/liquid ratios, also suggesting necking occurred.

Melting temperatures from 15 inclusions clustered together, ranging from -3.5 ± 0.2 to -4.7 ± 0.2 C, indicating fairly low salinities of 5.7 to 7.4 equivalent wt% NaCl (two inclusions melted at -0.8 ± 0.2 C, corresponding to 1.39 equivalent wt% NaCl). Although salinities are consistent between different inclusions, the relationship between the measured inclusions and the actual ore-forming event is uncertain. Further work is needed to identify mineralizing versus other fluids.

Table 15a. Melting point temperatures and corresponding gross salinities in weight percent NaCl equivalent for 15 fluid inclusion measurements in quartz.

Sample no.	T _m equivalent	Weight % NaCl
OM142D4	-3.9+/- .2	6.29+/- .028
"	-3.9+/- .1	"
"	-.8+/- .2	1.39+/- .028
OM142D8	-.8+/- .2	"
"	-3.6+/- .2	5.84+/- .028
"	-4.4+/- .2	7.01+/- .028
"	-3.8+/- .2	6.14+/- .028
OM142D	-3.5+/- .2	5.69+/- .028
"	-4.4+/- .2	7.01+/- .028
"	-4.0+/- .2	6.43+/- .028
"	-4.4+/- .2	7.01+/- .028
OM142D6	-3.8+/- .2	6.14+/- .028
"	-3.8+/- .2	6.14+/- .028
"	-4.7+/- .2	7.4+/- .028
"	-3.9+/- .2	6.29+/- .028

Table 15b. Homogenization temperatures for 13 fluid inclusion measurements in quartz.

Sample no.	T _h
OM142D4	155+ -1
"	243+ -3
"	113+ -4
OM142D8	222+ -2
OM142D	294+ -1
"	314+ -2
"	333+ -2
"	210+ -5
"	233+ -3
OM142D6	103+ -2
"	114+ -2
"	114+ -2
"	128+ -2

Note:

T_m = melting temperature in degrees C.

T_h = homogenization temperature in degrees C.

Discussion

Omar does not fit neatly into one deposit type. The spatial relationship between disseminated/replacement mineralization and organic material, and the stratabound vein/breccia-hosted mineralization, bear similarities to other deposits including the Ruby Creek copper-cobalt deposit, Mississippi Valley-type deposits, and carbonate-hosted stratabound copper deposits in Australia. I suggest that mineralization occurred prior to deep burial, metamorphism, and deformation associated with the Brooks Range orogeny, and that copper was remobilized from earlier mineralization during or after the deformational event. Accordingly, diagenetic changes within the host dolostone were important to localize mineralization.

The Relationship Between Organic Material and Mineralization

In-Situ Organic Material. The presence of organic material, either disseminated or locally concentrated in zones with other insoluble material, suggests that the Devonian carbonate sediment was buried before oxidation

and destruction of organics could occur. These zones may have resulted from pressure solution and stylolitization of organics and insoluble material (Wanless, 1979).

Alternatively, they may also represent original and possibly algal material. However, the organic/insoluble zones are commonly adjacent to clearer and coarser-grained areas, may contain solitary dolomite rhombs, and look similar to features produced from early compaction of limey sediment (Shinn and Robbin, 1983). In fact, early compaction and subsequent dissolution along grain to grain contacts or along organic layers would release carbonate ions to provide cement for lithification (Shinn and Robbin, 1983). It is probable that early cementation and/or dolomitization was necessary to preserve fossil clasts and primary sedimentary features in the Devonian unit.

The local close spatial association between sulfides and zones of organics/insolubles within dolostone (unit 5) is compatible with anaerobic bacterial reduction of seawater sulfate to sulfide (Trudinger and others, 1972). Most hydrogen sulfide in modern environments is derived from bacterial reduction of sulfate, and the amount produced is often but not always directly proportional to the amount of organic matter present (Rickard, 1973; Williams, 1978). It seems reasonable to believe that

ferrous iron within the sediment reacted with readily available reduced sulfur in the presence of organic material and formed pyrite. Hagni (1986) reports examples from Mississippi Valley-type deposits in the Viburnum Trend where early pyrite formed around crinoid stems and also within organic-rich carbonates prior to replacement of pyrite by copper sulfides. The early pyrite he described also occurs as partially replaced inclusions within later copper sulfide ore minerals.

Copper-bearing solutions may have reacted with earlier-formed pyrite or bacterially-produced sulfide during early diagenesis at Omar and formed chalcopyrite. Precipitation of copper sulfides in the diagenetic environment has been proposed for Kupferschiefer and Zambian Copper Belt deposits (Trudinger and others, 1972).

Transported Pyrobitumen Blebs. Marikos (1984) determined that bitumen blebs at the Magmont West orebody, Viburnum Trend, southeast Missouri, were not genetically associated with mineralization, but were transported to ore depositional sites by hydrothermal fluids and precipitated later than, sometimes directly on top of, main-stage galena crystals. The blebs he examined are spheroidal to ellipsoidal, were polymerized, range from

brittle to soft (indented with a fingernail) depending on low temperature biodegradational or water washing effects, and rarely entrain pyrite on their surfaces. Although blebs at the Magmont West Mine were not thermally degraded like blebs at Omar, they are also consistently associated with carbonate gangue minerals. In some cases blebs at the Magmont Mine were completely enclosed in calcite.

Based on textural evidence, Marikos (1984) concluded that the hydrocarbons at the Magmont Mine were derived locally from the organic-rich host dolostone, and that calculated burial depths were insufficient to obtain temperatures required to generate petroleum. Hence, heat provided by the mineralizing fluids was necessary for catagenesis and migration. The textural similarities between blebs at Omar and blebs at the Magmont Mine, together with the unique occurrence of blebs at Copper Hill, suggest that hydrothermal fluids may have generated and transported hydrocarbons at Omar. If, for example, simple burial at normal geothermal gradients was responsible for hydrocarbon generation at Omar, then hydrocarbons would probably not be restricted to the rocks hosting copper sulfides only at Copper Hill, but would be expected occur throughout the Devonian dolostone.

The very minor pyrite and chalcopyrite that occurs within veinlets carrying pyrobitumen blebs indicates that the fluids were not concomitantly depositing copper sulfides when hydrocarbon droplets were enclosed within dolomite or calcite. Because blebs occur within crosscutting veinlets, they are paragenetically, later than early replacement mineralization, but are not clearly before or after veinlet mineralization.

Coarse-grained pyrobitumen and small spherical blebs of pyrobitumen also occur within the hydrothermal dolostone at Ruby Creek (Hitzman, 1983). These grains are opaque, black, have a conchoidal fracture, and are commonly surrounded by organic-free, recrystallized dolomite with minor calcite (Hitzman, 1983). Hitzman also suggested that the blebs were originally liquid hydrocarbon.

The pyrobitumen in Ruby Creek rocks has been heated beyond oil generation temperatures. CAIs from rocks in the Cosmos Hills hosting Ruby Creek mineralization east of Omar indicate minimum temperatures of 300-350°C. (A. Harris, written communication, 1986), similar to host rocks at Omar. Yet, because mineralization at Ruby Creek lacks extensive metamorphic recrystallization of sulfides, and because different pyrobitumen populations within the hydrothermal dolostone retain distinct chemical and reflectance differences, Hitzman concluded

that hydrothermal fluids were responsible for hydrocarbon maturation. I suggest that pyrobitumen at Ruby Creek must have been thermally degraded by minimum burial temperatures of 300-350o C like Omar, after prior thermal degradation by hydrothermal fluids.

More detailed study of pyrobitumen blebs from Omar is needed to determine whether their organic chemistry is distinguishable from in-situ organic material.

Stratabound Mineralization

Early Versus Remobilized. Minimum temperatures of 300-350o C were reached by both Ordovician and Devonian lithologies at Omar, suggesting that synkinematic metamorphism affected all rocks. If mineralization was related to metamorphism, then both Ordovician and Devonian rocks should be mineralized. Minor amounts of copper occur in calcite-quartz veins cutting Devonian and Ordovician rocks, but the veins are not similar to the dolomite/copper sulfide veinlets, and are interpreted to be remobilized from earlier mineralization.

Ordovician and Devonian dolostones, although differing in fossil assemblages, are both relatively shallow water, platform, carbonate rocks. Ordovician dolostone is

commonly veined and brecciated but unmineralized. Ordovician dolostone also commonly contains disseminated pyrite, but no copper sulfides associated with earlier pyrite. Because mineralization at Omar is clearly Early Devonian or later, processes responsible for veining and brecciation in Devonian dolostone must have occurred at least 30 million years after Ordovician carbonate was deposited. Porosity and permeability were probably quite different in Ordovician versus Devonian carbonate at the time of mineralization, and other lithologic differences probably distinguished the two rock types. Therefore, either lithologic differences between the Devonian and Ordovician dolostones during mineralization favored the Devonian over the Ordovician as a host rock, or perhaps mineralizing fluids never came in contact with Ordovician rocks.

Dissolution(?) Features. Intersecting veinlets and breccias are common within the Devonian dolostone, and most are unmineralized. Angular fragments, lack of evidence for significant rotation of the fragments, and common white, sparry dolomite surrounding the fragments are similar to "crackle breccias" common to Mississippi Valley type deposits, and possibly result from dissolution of carbonate. Most of the copper sulfides

exposed at Omar are contained within veinlets surrounding angular fragments. Carbonate dissolution accompanying sulfide deposition (Anderson, 1983) may have occurred locally, but many other processes may have been responsible for more widespread dissolution, including interaction with meteoric water (Estaban and Klappa, 1983), dissolution of evaporite minerals (Gerdemann and Myers, 1972), or even acid generation accompanying hydrocarbon maturation (Surdham and Crossey, 1985). Presently, there is no evidence to suggest which process(es) were most important at Omar.

Sources of Metals and Fluids

The source of fluids, metals, and sulfur at Omar is enigmatic. For many stratabound base metal deposits, Pine Point, midcontinent Mississippi Valley-type deposits, Cooley and Ridge deposits, Australia, and Ruby Creek, a nearby sedimentary basin may have provided both fluids and metals (Beales and Jackson, 1966; Cathles and Smith, 1983; Williams, 1978; Hitzman, 1983). However, regional stratigraphic relationships are not known well enough around Omar to suggest a similar relationship.

The source of metals and fluids at Omar was probably

not magmatic. Igneous rocks are rare near Omar, and lead isotope values from Copper Hill suggest an upper crustal, probably sedimentary source. Adequate amounts of metals for mineralization could be leached from many different sources, none of which need to contain anomalous amounts of metals (Ohle, 1980). The intriguing predominance of copper over lead and zinc may have resulted from either the original chemistry of the fluid, Eh and pH conditions, and/or interactions along the fluid path. For example, zinc-dominated deposits may form from fluids travelling through a carbonate aquifer, lead-rich deposits from a sandstone aquifer, and copper-rich deposits from a red-bed aquifer (Sverjensky, 1981). The fluid path at Omar is unknown.

Comparison to other deposits

Omar shares many characteristics with other stratabound base-metal deposits including the Cooley and Ridge deposits at McArthur River, and the Lady Annie deposit in Australia, the southeast Missouri (Old Lead Belt, Viburnum Trend) lead-zinc(copper) district, and the Ruby Creek copper deposit in Alaska. The similarities and differences of host rocks, mineralogy, geochemistry,

mineralizing style, and timing between these deposits and Omar is worth examining.

The discordant Cooley and Ridge deposits at McArthur River, Australia contain disseminated (though also massive) and vein mineralization in brecciated dolostone bodies similar to Omar (Williams, 1978). Like early replacement mineralization at Omar, chalcopyrite replaced earlier-deposited pyrite; bornite formed later as a reaction product between pyrite and chalcopyrite (Williams, 1978). Also, sulfides comprising main-stage mineralization at the Cooley and Ridge deposits are both fine- and coarse-grained (10ths of μm to 1 cm) and display classic open-space filling textures. Unlike Omar, the mineralogy is dominated by pyrite, sphalerite, and galena, with lesser chalcopyrite, bornite, marcasite, and tetrahedrite. Later replacement of both disseminated and vein-hosted copper sulfides by sphalerite and galena characterizes McArthur River, whereas Omar displays less common clearcut replacement textures.

Copper mineralization at the Lady Annie copper deposit, Paradise Valley, Australia, is similar to Omar and consists of disseminated clots of chalcopyrite, pyrite, and bornite, with replacement and lining of pyrite by chalcopyrite within dolostones (Hitzman, 1983).

Mineralized samples from both Lady Annie and Omar are

anomalously high in cobalt. Organic material is spatially associated with mineralization at Lady Annie like mineralization at Copper Hill; chalcopyrite and pyrite occur within coarse-grained white dolomite veins containing quartz and anthracitic organic material (Lewis, 1975). However, Lewis also noted that carbonaceous material in the veins is replaced by chalcopyrite. Hydrothermal fluids at both Lady Annie and Omar may have remobilized the organic material into veinlets, but organic material in veins served as loci for sulfide mineralization at Lady Annie and not at Omar.

Mississippi Valley-type deposits are stratabound, epigenetic, base metal occurrences hosted in Paleozoic carbonates. Except for the southeast Missouri lead-zinc-copper district, most Mississippi Valley-type deposits are zinc/lead-rich, and contain only small amounts of copper. Copper mineralization in the Viburnum Trend displays some textures similar to those at Omar. Early, disseminated pyrite is common to many deposits and, like Omar, pyrite may be closely associated with concentrations of organic material (Hagni, 1986). In some Viburnum Trend mines, framboidal and crystalline pyrite was partially replaced and commonly occurs as inclusions within pods and lenses of later massive bornite and chalcopyrite (Hagni, 1986). Main-stage

mineralization in the Viburnum Trend, however, consists of galena, sphalerite, and only minor copper sulfides.

The Ruby Creek copper-cobalt deposit is hosted within Devonian dolostone 180 km east of Omar. Most copper mineralization at Ruby Creek, like Omar, was fracture-controlled, occurring as vein, stockwork, and massive mineralization. Veins at Ruby Creek also commonly contain planar, white dolomite crystals with euhedral terminations towards the vein core (Hitzman, 1983). Chalcopyrite replaces pyrite at both Omar and Ruby Creek, and bornite intergrew with chalcopyrite in the copper-rich assemblages. Both deposits are anomalous in cobalt. Organic material is also spatially associated with mineralization at Ruby Creek; chalcopyrite rims and forms veinlets within pyrobitumen grains near the fringe of the stockwork zones.

Unlike Omar, hydrothermal alteration produced several generations of dolomite, reflected by a well-developed iron zonation at Ruby Creek (Hitzman, 1983). The hydrothermal dolostone body at Ruby Creek contains only rare depositional features, whereas hydrothermal alteration at Omar is less pervasive. Also, earlier chalcopyrite/bornite intergrowths are replaced by bornite and chalcocite-digenite at Ruby Creek.

Omar is not a Mississippi Valley-type deposit, nor is

it rich enough in lead and zinc to be grouped with the Cooley and Ridge deposits. Although Omar is similar to many stratabound, carbonate-hosted deposits, more work is needed on the genetic aspects of mineralization before Omar can be classified with a larger group of deposits. Similarities in age of the host rocks, mineralization style, and mineralogy, however, suggest that Omar is most like the Ruby Creek deposit.

Suggestions for Exploration

Known base metal mineralization at Omar is too low in tonnage and grade for commercial exploitation at present. BCMC determined that, despite some high-grade intercepts, mineralization was discontinuous at depth due to either extensive faulting, rapid facies changes, or irregular distribution of veinlets. Cobalt minerals were not detected at Omar despite more than 2000 ppm cobalt in some rock samples.

The trace element suite in stream sediments and soils that is useful as a pathfinder for Omar-type mineralization includes copper, lead, zinc, cobalt, arsenic, silver, and +/-manganese. Exploration for Omar-type mineralization should utilize soil and stream sediment sampling to detect mineralization, although anomaly contrast is generally poor in drainage basins

underlain by carbonate rocks (Degenhart and others, 1978). Soil sampling is effective but hampered by poor soil development and solifluction common to permafrost areas.

A favorable geologic environment for Omar-type deposits includes fossiliferous, reef-facies, relatively organic-rich dolostone, with evidence for brecciation and open-space development. Other common features might include proximity to a sedimentary basin (possible metal/fluid source), relatively ferroan hydrothermal dolomite accompanying mineralized rocks (easily determined by staining), and evidence for hydrocarbon migration possibly driven by hydrothermal fluids.

Summary

Fig. 31 schematically illustrates the hydrothermal mineralization of the Devonian dolostone and later remobilization. The main features of mineralization at Omar are listed below.

1. Omar is stratabound and discordant within Devonian dolostone host rocks.

2. Syngenetic or early diagenetic pyrite is concentrated along organic-rich zones within the host rocks, and may have utilized bacterially-reduced sulfate.

3. Copper-sulfides and sulfosalts locally replaced the coarser-grained pyrite. Chalcopyrite replaced pyrite blebs and masses, and occurs as exsolution lamellae within tetrahedrite and bornite.

4. Copper sulfide-bearing sharp-walled veinlets cut the dolostone, indicating veining occurred after lithification.

5. Clear, euhedral to subhedral dolomite rhombs grew into open spaces within veins that were later filled by sulfide.

6. Dolomite rhombs abutting sulfides in veinlets commonly show bright/dull growth zoning under cathode luminescence, indicating Mn^{+2}/Fe^{+2} ratios changed within the fluid during dolomite growth. Brightly luminescent rims adjacent to copper sulfides at both Blind Spot and Copper Hill suggests fluid composition may have been similar at both sites prior to copper mineralization.

Bright/dull zoning also occurs within sparry, euhedral dolomite cement that grew into small dissolution cavities in the host dolostone, and within dolomite rhombs adjacent to pyrobitumen within sharp-walled veinlets.

7. Pyrobitumen occurs as grains and spheroidal blebs, and is most abundant near mineralization at Copper Hill. Blebs may represent migrated hydrocarbons. Rarely, blebs entrain copper and iron sulfides.

8. Conodont alteration indexes indicate that the rocks reached minimum temperatures of 300-350°C during regional metamorphism. Temperatures were not anomalously high at Copper Hill, suggesting that mineralization temperatures were no higher than 300-350°C.

9. Late calcite, quartz, and dolomite-bearing veins carry minor amounts of remobilized chalcopyrite and follow fractures and joints that formed during or after mid-Jurassic to Cretaceous deformation and metamorphism.

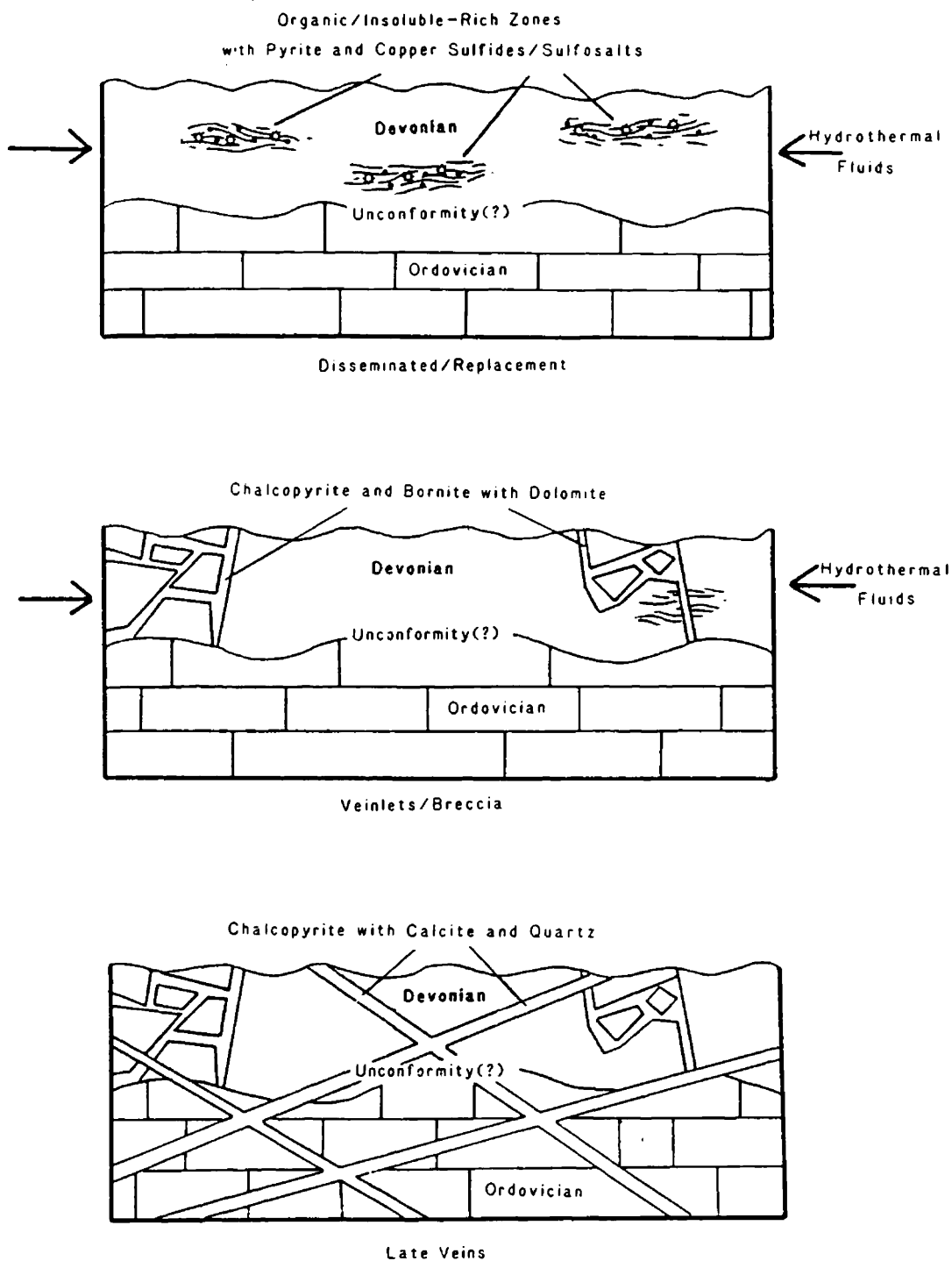


Fig. 31. Schematic diagram showing the interaction of the Devonian dolostone with hydrothermal fluids to form disseminated and replacement mineralization (top), and veinlet/breccia mineralization (middle). Late veins with minor amounts of remobilized chalcopyrite are shown crosscutting all earlier textures (bottom).

Conclusions

Copper sulfide mineralization at Omar was epigenetic, and was accompanied by minor hydrothermal alteration limited to dolomite formation, with minor quartz and calcite. Mineralizing fluids preferred the Devonian dolostone over Ordovician lithologies, or possibly never encountered Ordovician rocks. Organic material in the Devonian host rocks served as loci for disseminated and local replacement mineralization. Hydrocarbons may have been mobilized by hydrothermal fluids, but were not directly involved with most copper sulfide mineralization. Hydrothermal fluids were relatively iron-rich, and Mn^{+2}/Fe^{+2} ratios changed within the fluid during growth of gangue dolomite in veinlets. Temperature of mineralization did not exceed 300-350° C. The source of the mineralizing fluids is unknown, but metals may have been derived from an upper crustal sediment source.

References

- Anderson, G.M., 1983, Some geochemical aspects of sulfide precipitation in carbonate rocks, in Kisvarsanyi, G., Grant, S., Pratt, W.P., and Koenig, J.W., eds., International Conference on Mississippi Valley Type lead-zinc deposits, Proceedings Volume, University of Missouri, Rolla, Missouri, pp. 61-76.
- Beales, F.W., and Jackson, S.A., 1966, Precipitation of lead-zinc ores in carbonate reservoirs as illustrated by Pine Point ore field, Canada, Trans. Inst. Mining Metall., Sec. B, vol. 75, pp. B278-B285.
- Beikman, H.M., 1980, Geologic map of Alaska, U.S. Geological Survey, 2 sheets, 1:250,000.
- Brett, R., 1964, Experimental data from the system copper-iron-sulfur and their bearing on exsolution textures in ores, Economic Geology, vol. 59, pp. 1241-1269.
- Bustin, R.M., Barnes, M.A., and Barnes, W.C., 1985, Diagenesis 10. Quantification and modelling of organic diagenesis, Geoscience Canada, vol. 12, no.1, pp 1-21.

Cathles, L.M., and Smith, A.T., 1983, Thermal constraints on the formation of Mississippi Valley-type lead-zinc deposits and their implications for episodic basin dewatering and deposit genesis, *Economic Geology*, vol. 78, pp. 983-1002.

Cohen, C.C. Jr., 1959, Simplified estimators for the normal distribution when samples are singly censored or truncated, *Technometrics*, vol. 1, no. 3, pp. 217-237.

Craig, J.R., and Vaughan, D.J., 1981, *Ore microscopy and ore petrography*, John Wiley and Sons, New York, 406 p.

Degenhart, C.E., Griffis, R.J., McQuat, J.F., and Bigelow, C.G., 1978, Mineral studies of certain ANCSA 17(d)(2) lands in Alaska, performed under contract J0155089; U.S. Bureau of Mines Open File Report 103-78, pp. 250-279.

Detterman, R.L., 1970, Sedimentary history of the Sadlerochit and Shublik Formations in northeastern Alaska, in Adkison, W.L., and Brosge, M.M., eds., *Geological seminar on the North Slope of Alaska*, Palo Alto, Calif., 1970, American Association of Petroleum

Geologists, Pacific Section meeting, Proceedings.

Dickson, J.A.D., 1966, Carbonate identification and genesis as revealed by staining, *Journal of Sedimentary Petrology*, vol. 36, no. 2, pp. 491-505.

Doe, B.R., and Stacy, J.S., 1974, The application of lead isotopes to the problems of Ore genesis and ore prospect evaluation: a review, *Economic Geology*, vol. 69, pp. 757-776.

Dumoulin, J.D., and Harris, A., 1985, Lower Paleozoic rocks of the Baird Mountains quadrangle, Alaska, Abstracts with Programs, AAPG Pacific Section Meeting, May 1985, p. 55.

Dumoulin, J.D., and Harris, A., 1986, Lower Paleozoic rocks of the Baird Mountains quadrangle, western Brooks Range, Alaska, *SEPM Special Volume*, in prep.

Epstein, A.G., Epstein, J.B., and Harris, L.D., 1977, Conodont color alteration--an index to organic metamorphism, *U.S. Geological Survey Professional Paper* 995, 27 p.

Estaban, M., and Klappa, C.F., 1983, Subaerial exposure, in Carbonate Depositional Environments, Scholle, P.A., Bebout, D.G., and Moore, C.H., eds., AAPG Memoir 33, pp. 1-55.

Folger, P.F., Goldfarb, R.J., Bailey, E.A., O'Leary, R.M., and Sutley, S.J., 1985, Use of stream sediment insoluble residues in geochemical exploration for carbonate-hosted mineral deposits in the Baird Mountains, the United States Geological Survey in Alaska: accomplishments during 1984, U.S. Geological Survey Circular 967, p. 5-8.

Frank, J.R., Carpenter, A.B., and Oglesby, T.W., 1982, Cathodoluminescence and composition of calcite cement in the Taum Sauk limestone (Upper Cambrian), southeast Missouri, Journal of Sedimentary Petrology, vol. 52, pp 631-638.

Gerdemann, P.E., and Meyers, H.E., 1972, Relationships of carbonate facies patterns to ore distribution and to ore genesis in the southeast Missouri lead district, Economic Geology, vol. 67, pp. 426-433.

Hagni, R.D., 1986, Mineral paragenetic sequence of the lead-zinc-copper-cobalt-nickel ores of the Southeast Missouri Lead District, U.S.A., in Mineral Parageneses, Theophrastus Publications S.A., Athens, 696 p.

Hitzman, M., 1983, The geology of the Cosmos Hills and its relationship to the Ruby Creek copper-cobalt deposit, unpublished PhD thesis, Stanford University, 266 p.

-----, 1986, Copper deposits in stratiform zinc-lead districts--a possible example: the Ruby Creek copper deposit, southwestern Brooks Range, Alaska, in Turner, R.J.W., and Einaudi, M.T., eds., The genesis of stratiform sediment-hosted lead and zinc deposit: conference proceedings, Stanford University Press, pp. 65-72.

James, N.P., 1983, Reef, in Carbonate Depositional Environments, Scholle, P.A., Bebout, D.G., and Moore, C.H., eds., AAPG Memoir 33, pp. 345-441.

Jansons, U., 1982, Cobalt content in samples from the Omar copper prospect, Baird Mountains, Alaska, U.S. Geological Survey Open File Report 83-779, 14 p.

Johnston, R.J., 1980, Multivariate statistical analysis in geography, Longman, London, 280 p.

Leventhal, J.S., Limitations of Rock-Eval pyrolysis to characterize kerogen (abs.), American Association of Petroleum Geologists Bulletin, p. 593.

Lewis, R.W., 1975, Lady Annie secondary copper deposit, Queensland, Australasian Institute of Mining and Metallurgy, Monograph 5, pp. 1023-1032.

Macqueen, R.W., and Powell, T.G., 1983, Organic chemistry of the Pine Point lead-zinc ore field and region, Northwest Territories, Canada, Economic Geology, vol. 78, no. 1, pp. 1-25.

Marikos, M.A., 1984, Relation of bitumen to ore in the Magmont West orebody, Southeast Missouri, unpublished Master's thesis, University of Missouri-Rolla, 122 p.

Martin, A.J., 1970, Structure and tectonic history of the western Brooks Range, De Long Mountains and Lisburne Hills, northern Alaska, Geological Society of America Bulletin, vol. 81, pp. 3605-3622.

Mayfield, C.F., Tailleux, I.L., and Ellersieck, I., 1983, Stratigraphy, structure, and palinspastic synthesis of the western Brooks Range, northwestern Alaska, U.S. Geological Survey Open File Report 83-779, 53 p.

Miesch, A.T., 1976, Geochemical survey of Missouri-methods of sampling, laboratory analysis, and statistical reduction of data, U.S. Geological Survey Professional Paper 954-A, 39 pages.

Mull, C.G., 1982, Tectonic evolution and structural style of the Brooks Range, Alaska: an illustrated summary, in Powers, R.B., ed., Geologic studies of the Cordilleran thrust belt, Rocky Mountain Association of Geologists, vol. 1, pp. 1-47.

Nickel, E., 1978, The present status of cathode luminescence as a tool in sedimentology, Mineral Science Engineering, vol. 10, no. 2, pp. 73-100.

Rickard, D.T., 1973, Limiting conditions for synsedimentary ore formation, Economic Geology, vol. 68, no. 5, pp. 605-617.

Roedder, E., 1962, Ancient fluids in crystals, Scientific American, vol. 207, pp. 38-47.

Rowan, L., 1986, The contribution of cathodoluminescence to an understanding of Mississippi Valley-type lead-zinc mineralization in southern Missouri and northern Arkansas, American Institute of Mining and Engineering, Process Mineralogy VI, in press.

Shinn, E.A., and Robbin, D.M., 1983, Mechanical and chemical compaction in fine-grained shallow-water metalimestones, Journal of Sedimentary Petrology, vol. 53, no. 2, pp. 595-618.

Snelson, S., and Tailleur, I.L., 1968, Large scale thrusting and migrating Cretaceous foredeeps in the western Brooks Range and adjacent regions of northwest Alaska (abs), American Association of Petroleum Geologists Bulletin, vol. 52, no. 3, p. 567.

Sommer, S.E., 1972, Cathodoluminescence of carbonates, 1. characterization of cathodoluminescence from carbonate solid solutions, Chemical Geology, vol. 9, pp. 257-273.

Surdham, R.C., and Crossey, L.J., 1985, Organic-inorganic

reactions during progressive burial: key to porosity and permeability enhancement and preservation, Phil. Trans. R. Soc. Lond., A 315, pp. 135-156.

Sverjensky, D.A., 1981, Genesis of Mississippi Valley-type lead-zinc deposits, Annual Review of Earth Planetary Science, vol. 14, pp. 177-199.

Sverjensky, D.A., Rye, D.A., and Doe, B.R., 1979, The lead and sulfur isotopic composition of galena from a Mississippi Valley-type deposit in the New Lead Belt, southeast Missouri, Economic Geology, vol. 74, pp. 149-153.

Tailleur, I.L., and Snelson, S., 1969, Large scale thrusting in northwest Alaska probably related to rifting of the Arctic Ocean, Geological Society of America Special Paper 121, p. 569.

Tailleur, I.L., Mayfield, C.F., Ellersieck, I., 1977, Late Paleozoic sedimentary sequence, southwest Brooks Range, U.S. Geological Survey Accomplishments in Alaska, 1976, U.S. Geological Survey Circular 751-B, p. 25.

Tissot, B.P., and Welte, D.H., 1978, Petroleum formation and occurrence, Springer-Verlag, Berlin, 538 p.

Trudinger, P.A., Lambert, I.B., and Skyring, G.W., 1972, Biogenic sulfide ores: a feasibility study, Economic Geology, vol. 67, pp. 1114-1127.

Voss, R.L., and Hagni, R.D., 1985, The application of cathodoluminescent microscopy to the study of sparry dolomite from the Viburnum Trend, southeastern Missouri, in Hausen, D.W., and Kopp, O., eds., Proceedings, Paul F. Kerr Memorial Symposium, Process Mineralogy V. New York, AIME.

Wanless, H.R., 1979, Limestone response to stress: pressure solution and dolomitization, Journal of Sedimentary Petrology, vol. 49, no. 2, pp. 0437-0462.

Williams, N., 1978, Studies of the base metal sulfide deposits at McArthur River, Northern Territory, Australia: I. the Cooley and Ridge deposits, Economic Geology, vol. 73, no. 6, pp. 1005-1035.

APPENDIX A. OMAR ROCK SAMPLES
 (N, not detected; (-, detected but below the limit of determination shown); (+, determined to be greater than the value shown).)

Sample	Latitude	Longitude	Fe	Mg	Ca	Ti	Mn	Ag	B	Ba	Co	Cr	Cu
1	67 29 32	160 52 35	1.50	5.00	10.00	.005	1,000	10.0	N	200	100	N	20,000
2	67 30 21	160 53 3	.70	1.50	5.00	N	300	N	N	N	10	N	1,000
3	67 30 21	160 53 4	.50	7.00	5.00	.020	700	N	10	500	15	15	20
4	67 30 15	160 52 56	.70	7.00	10.00	.010	150	N	N	N	15	(10	5,000
5	67 30 19	160 52 56	.30	10.00	7.00	.010	150	N	N	N	N	(10	5,000
6	67 30 15	160 52 59	1.00	12.00	20.00	.050	100	N	20	20	10	50	10
7	67 30 25	160 53 13	20.00	2.00	1.50	N	200	20.0	N	N	700	N	20,000
8	67 30 25	160 53 12	.20	.70	20.00	.002	150	N	10	N	N	N	70
9	67 30 25	160 53 12	.50	2.00	20.00	.050	100	N	20	30	N	150	70
10	67 29 32	160 52 35	.20	10.00	15.00	N	700	(.5	N	(20	50	N	1,500
11	67 29 31	160 52 35	.15	10.00	15.00	N	700	N	N	20	20	N	700
12	67 29 30	160 52 34	.15	10.00	15.00	N	700	1.5	N	(20	10	N	3,000
13	67 29 28	160 52 37	.20	10.00	15.00	N	1,000	(.5	N	(20	70	N	1,000
14	67 29 48	160 51 30	3.00	10.00	10.00	.200	150	(.5	70	100	30	300	100
15	67 29 36	160 52 20	10.00	.03	.30	.003	30	1.0	20	N	150	N	3,000
16	67 30 56	160 52 23	.50	10.00	15.00	N	1,500	N	N	N	20	N	1,500
17	67 30 16	160 52 57	1.50	3.00	7.00	.300	500	N	300	1,500	20	50	50
18	67 30 16	160 52 57	1.00	5.00	10.00	.200	700	(.3	200	1,500	20	50	100
19	67 30 26	160 53 10	5.00	5.00	7.00	.003	1,000	1.5	(10	(20	2,000	N	20,000
20	67 29 29	160 52 25	.05	.30	20.00	N	150	(.5	N	N	(5	N	1,500
21	67 29 26	160 52 26	2.00	7.00	10.00	N	1,000	(.5	N	(20	70	N	1,500
22	67 29 53	160 52 35	.50	10.00	15.00	.005	1,000	N	(10	(20	30	N	1,000
23	67 29 21	160 52 18	.15	3.00	7.00	N	200	2.0	10	(20	7	N	20,000
24	67 29 34	160 52 36	15.00	3.00	5.00	.003	500	7.0	(10	(70	700	(10	1,000
25	67 29 32	160 52 27	.30	10.00	10.00	N	700	(.5	N	N	50	N	2,000
26	67 29 30	160 52 38	3.00	2.00	20.00	N	200	10.0	N	(20	150	N	2,000
27	67 29 30	160 52 39	.15	10.00	10.00	N	1,000	(.5	(10	N	15	N	20,000
28	67 29 30	160 52 39	.50	1.50	15.00	.150	150	(.5	50	5,000	10	20	700
29	67 29 29	160 52 40	20.00	.20	.30	N	500	7.0	N	1,000	200	N	5,000
30	67 31 4	160 53 55	(.05	10.00	10.00	.003	20	N	N	N	N	N	15
31	67 31 3	160 53 33	.10	10.00	15.00	.005	30	N	N	N	N	N	N
32	67 31 2	160 53 27	(.05	10.00	20.00	.003	30	N	N	N	N	N	(5
33	67 31 2	160 53 27	(.05	2.00	2.00	N	(10	N	N	N	N	N	N
34	67 30 40	160 52 11	.30	5.00	15.00	.002	100	N	N	N	N	N	7
35	67 30 43	160 52 14	(.05	7.00	7.00	N	30	N	N	N	N	15	(5
36	67 31 0	160 53 17	.10	10.00	20.00	.003	50	N	N	N	N	N	(5
37	67 29 57	160 52 23	.50	.20	20.00	.020	200	N	10	N	N	15	20
38	67 29 58	160 53 34	3.00	3.00	10.00	.200	200	N	15	100	20	150	30
39	67 29 45	160 52 52	.15	10.00	20.00	.005	100	N	N	N	N	N	(5
40	67 29 56	160 52 21	.70	5.00	20.00	.003	500	N	N	N	15	N	20
41	67 29 33	160 51 12	.10	10.00	20.00	.003	50	N	N	N	N	N	(5
42	67 29 40	160 52 11	.20	10.00	7.00	.015	30	N	N	N	N	N	(5
43	67 29 57	160 51 41	(.05	10.00	7.00	N	(10	N	N	N	N	N	(5
44	67 29 38	160 52 18	.10	7.00	20.00	.010	100	N	N	20	N	N	7
45	67 29 37	160 52 19	.15	10.00	15.00	.005	300	N	N	(20	5	(10	10
46	67 29 39	160 52 25	.70	3.00	20.00	.050	200	N	50	(20	(5	15	7
47	67 29 28	160 52 2	.10	7.00	20.00	.010	300	N	(10	(20	N	(10	5
48	67 29 25	160 52 28	.20	7.00	20.00	.003	500	N	N	N	5	(10	100

APPENDIX A. OMAR ROCK SAMPLES--Continued

Sample	Mo	Ni	Pb	Sr	V	Y	Zr	As	Zn	Cd	Bi	Sb
1	7	20	200	N	30	15	N	60	1,000	5.0	N	5
2	N	15	10	300	N	N	N	N	10	N	N	N
3	N	7	<10	N	30	10	10	N	110	.7	N	N
4	20	10	15	N	30	<10	10	N	70	.3	N	N
5	N	5	N	N	20	10	10	60	20	.1	N	8
6	N	30	20	700	20	10	20	N	10	N	N	N
7	N	100	300	N	N	N	N	N	15	1.0	N	N
8	N	N	<10	700	N	20	<10	N	N	N	N	N
9	N	15	10	1,000	15	10	30	N	15	N	N	N
10	N	10	70	100	20	15	N	10	1,300	4.0	N	<2
11	N	5	30	100	20	15	N	10	300	1.0	N	<2
12	N	N	30	100	<10	10	N	30	40	.3	N	12
13	N	10	30	<100	<10	10	N	10	120	.3	N	<2
14	N	100	100	<100	100	15	15	20	85	.3	N	<2
15	(5	50	150	N	20	N	N	300	400	1.0	8	4
16	N	(5	30	100	<10	<10	10	250	55	.4	N	<2
17	N	50	20	300	150	50	150	N	120	.2	N	<2
18	(5	30	50	150	100	50	150	10	180	.8	N	2
19	(5	200	100	200	<10	10	N	20	100	2.6	N	4
20	N	(5	10	300	<10	50	<10	1,000	230	3.6	N	26
21	N	20	30	N	<10	15	N	20	400	1.0	N	2
22	N	5	30	150	15	15	<10	30	220	1.4	N	<2
23	N	(5	1,500	N	10	<10	N	11,000	1,300	15.0	N	550
24	15	150	1,500	N	N	<10	N	30	16,000	70.0	1	3
25	(5	15	50	100	15	10	N	40	430	100.0	2	10
26	N	10	70	<100	<10	10	<10	20	410	1.8	1	<2
27	(5	20	100	200	<10	30	<10	180	110	1.0	6	130
28	(5	15	10	<100	10	<10	N	N	20	N	N	2
29	N	15	30	5,000	50	30	100	N	45	.2	N	N
30	5	70	700	N	<10	<10	N	480	400	2.9	16	5
31	N	N	N	N	10	N	10	N	5	N	N	N
32	N	N	N	<100	10	N	10	<10	5	N	N	N
33	N	N	N	N	10	N	<10	N	10	N	N	N
34	N	N	N	N	10	N	10	<10	5	N	N	N
35	N	N	N	200	10	20	<10	N	5	N	N	N
36	N	N	N	N	15	N	10	N	5	N	N	N
37	N	N	N	N	10	N	10	N	5	N	N	N
38	N	N	N	200	15	<10	<10	<10	5	N	N	N
39	N	15	10	100	20	10	15	10	180	.2	N	N
40	N	70	<10	150	70	20	50	N	35	N	N	N
41	N	N	<10	N	10	N	<10	N	10	N	N	N
42	N	5	10	100	10	N	<10	10	20	N	N	N
43	N	N	N	N	<10	N	<10	10	5	N	N	N
44	N	N	N	N	10	N	10	N	5	N	N	N
45	N	N	N	N	10	N	10	N	5	N	N	N
46	(5	(5	<10	100	<10	N	10	N	15	N	N	N
47	(5	5	<10	<100	10	N	10	N	20	N	N	N
48	N	10	<10	500	20	<10	20	N	15	N	N	2
49	N	N	<10	N	10	N	10	N	20	N	N	N
50	N	(5	<10	N	10	N	10	N	30	N	N	2

-143-

APPENDIX A. OMAR ROCK SAMPLES--Continued

Sample	Latitude	Longitude	Fe	Mg	Ca	Ti	Mn	Ag	B	Ba	Co	Cr	Cu
51	67 29 22	160 52 27	.10	2.00	20.00	.005	200	N	(10	N	N	N	200
52	67 29 19	160 52 20	.10	5.00	20.00	.005	200	N	(10	N	N	N	7
53	67 29 19	160 52 20	.10	.05	1.00	.020	10	N	50	(20	N	N	15
54	67 29 23	160 51 37	20.00	.15	.05	.100	200	N	15	30	100	100	300
55	67 29 27	160 51 33	15.00	.30	(.05	.500	70	.5	20	(20	20	200	200
56	67 29 35	160 51 22	20.00	.10	.10	.005	150	(.5	N	(20	150	N	200
57	67 29 35	160 52 28	.50	7.00	20.00	.007	700	2.0	(10	(20	100	(10	10,000
58	67 29 32	160 52 37	.30	7.00	20.00	.005	1,000	N	N	N	50	(10	500
59	67 29 33	160 52 47	.20	5.00	15.00	.003	300	N	N	N	N	N	100
60	67 29 33	160 52 47	3.00	1.50	3.00	.300	300	N	200	300	20	70	50
61	67 29 54	160 51 15	.20	1.00	20.00	.020	200	N	N	N	N	N	7
62	67 30 9	160 51 7	1.50	1.00	20.00	.150	300	N	150	200	15	100	20
63	67 30 26	160 50 50	.20	.70	20.00	.020	150	N	N	N	N	N	15
64	67 30 37	160 51 14	1.00	2.00	10.00	.150	500	N	30	300	5	50	10
65	67 30 37	160 51 23	.70	10.00	15.00	.005	200	N	N	N	N	N	10
66	67 29 53	160 51 22	.50	1.00	20.00	.020	150	N	(10	N	N	10	5
67	67 29 56	160 52 26	.70	1.00	2.00	.010	100	N	(10	20	10	(10	50
68	67 29 56	160 52 28	.05	.50	20.00	.007	150	.5	N	N	N	N	1,000
69	67 30 17	160 52 53	1.50	1.00	10.00	.100	500	N	100	200	15	50	7
70	67 29 58	160 51 53	.20	5.00	15.00	.030	70	N	15	N	N	10	10
71	67 30 47	160 53 45	.10	7.00	10.00	.007	70	N	(10	N	N	N	(5
72	67 30 42	160 53 22	(.05	3.00	20.00	.007	50	N	N	5,000	N	N	N
73	67 30 15	160 52 18	(.05	10.00	20.00	.005	150	N	N	N	N	(10	5
74	67 29 21	160 52 18	.30	3.00	15.00	.010	200	N	(10	N	10	N	70
75	67 29 21	160 52 18	2.00	5.00	10.00	.007	500	N	(10	N	30	N	100
76	67 29 21	160 52 18	.20	5.00	10.00	.005	500	N	(10	(20	7	N	1,000
77	67 29 45	160 53 0	.30	10.00	20.00	.020	150	N	(10	(20	(5	10	10

APPENDIX A. OMAR ROCK SAMPLES--Continued

Sample	Mo	Ni	Pb	Sr	V	Y	Zr	As	Zn	Cd	Bi
51	N	N	(10	100	10	20	10	20	30	.4	N
52	N	N	(10	N	15	N	(10	N	45	.3	N
53	N	N	(10	N	10	N	10	N	20	N	N
54	10	150	30	N	150	N	20	30	160	.2	N
55	7	170	50	N	200	10	50	20	110	N	N
56	7	300	100	N	70	N	N	N	70	.4	N
57	5	30	200	N	(10	10	(10	1,100	19,900	15.0	10
58	15	15	20	N	(10	10	(10	N	150	.2	N
59	10	70	(10	N	(10	(10	100	N	35	.1	N
60	10	10	10	300	100	30	100	N	90	.1	N
61	5	50	50	1,000	100	20	70	N	30	(.1	N
62	15	(10	(10	1,000	10	(10	10	N	15	.5	N
63	2	30	(10	500	70	20	100	N	10	.2	N
64	15	15	(10	100	10	N	(10	N	20	N	N
65	15	15	(10	500	15	N	10	N	20	N	N
66	15	15	(10	300	10	20	(10	10	20	.1	N
67	50	(10	(10	500	70	20	50	210	20	.2	N
68	7	(10	(10	200	10	N	10	N	5	N	N
69	2	N	N	N	(10	N	10	N	3	N	N
70	2	N	N	1,000	(10	N	(10	N	N	N	N
71	5	7	15	(100	50	N	(10	N	10	N	N
72	15	20	15	(100	15	(10	10	N	150	.5	N
73	15	15	15	(100	10	10	N	N	1,200	.6	N
74	15	15	10	(100	10	10	N	450	150	1.7	N
75	15	10	10	N	10	(10	10	N	15	N	N
76	10	10	10	N	10	(10	10	N	15	N	N

APPENDIX A. OMAR SOIL SAMPLES

(N, not detected; (, detected but below the limit of determination shown;), determined to be greater than the value shown.)

Sample	Latitude	Longitude	Fe	Mg	Ca	Ti	Mn	B	Be	Co	Cr	Mo	Ni	Pb
1	67 29 29	160 52 37	2.00	7.0	5.0	.01	1,000	(10	(20	150	(10	7	30	150
2	67 29 28	160 52 38	1.50	.7	1.0	.10	150	(10	100	30	N	10	30	50
3	67 29 23	150 52 32	3.00	7.0	7.0	.20	700	100	500	20	100	20	100	150
4	67 29 22	160 52 25	1.50	7.0	10.0	.01	1,000	(10	20	150	10	5	30	70
5	67 29 21	160 52 22	3.00	7.0	5.0	.07	1,000	(10	1,000	100	30	20	100	200
6	67 29 21	160 52 18	20.00	1.5	1.5	.10	300	20	100	50	50	50	70	300
7	67 28 48	160 50 52	1.50	7.0	10.0	.15	200	10	100	50	50	7	70	30
8	67 28 49	160 51 8	.50	5.0	5.0	.03	150	(10	(20	N	20	N	5	(10
9	67 28 53	160 50 54	.70	5.0	7.0	.15	100	50	70	10	70	(0	10	30
10	67 28 55	160 51 21	7.00	3.0	1.0	.30	100	100	50	30	200	N	50	150
11	67 28 57	160 51 30	.30	7.0	7.0	.02	100	(10	(20	5	15	N	10	10
12	67 29 2	160 51 36	5.00	5.0	3.0	.15	150	50	(20	30	150	N	70	70
13	67 29 6	160 51 45	.70	7.0	10.0	.10	300	(10	50	15	30	(0	15	20
14	67 29 2	160 51 59	.70	3.0	7.0	.10	200	30	70	N	50	N	15	30
15	67 29 14	160 51 52	.50	10.0	15.0	.05	500	N	(20	7	15	(0	10	30
16	67 29 19	160 51 57	3.00	3.0	2.0	.20	100	70	(20	15	100	N	50	100
17	67 29 20	160 51 53	2.00	15.0	5.0	.10	300	30	50	15	70	N	30	30
18	67 29 21	160 52 4	1.00	7.0	7.0	.15	300	10	30	15	50	5	20	50
19	67 29 19	160 52 54	1.50	2.0	2.0	.20	300	50	200	20	100	N	30	15
20	67 29 21	160 52 43	3.00	3.0	1.5	.30	300	200	500	30	100	N	70	30
21	67 29 31	160 52 34	3.00	2.0	2.0	.30	500	100	500	15	100	5	70	10
22	67 29 29	160 52 48	7.00	3.0	.7	.70	200	300	500	30	200	20	100	50
23	67 29 35	160 52 57	1.50	2.0	10.0	.10	150	30	50	N	100	100	150	70
24	67 29 36	160 53 10	.70	1.0	.7	.20	20	100	100	10	150	50	200	100
25	67 29 36	160 53 12	.70	5.0	7.0	.05	150	15	20	N	20	N	10	15
26	67 29 38	160 52 56	.70	1.0	5.0	.10	50	100	70	10	100	100	300	30
27	67 29 41	160 52 54	1.50	5.0	5.0	.10	200	30	50	10	200	70	150	100
28	67 29 48	160 54 9	2.00	7.0	10.0	.20	70	20	1,000	5	200	200	300	150
29	67 29 50	150 53 55	1.00	7.0	10.0	.20	70	100	100	15	50	(0	20	30
30	67 31 5	160 53 59	.50	5.0	3.0	.03	70	15	(20	N	20	N	10	15
31	67 31 1	160 53 49	.70	3.0	5.0	.05	150	20	20	N	20	N	20	10
32	67 30 56	160 53 32	.50	5.0	3.0	.03	100	10	(20	N	15	N	7	10
33	67 30 40	160 53 55	3.00	3.0	2.0	.15	200	50	20	50	150	10	100	50
34	67 29 37	160 54 3	.30	3.0	3.0	.02	50	10	(20	N	15	N	7	15
35	67 29 37	160 53 47	1.00	5.0	5.0	.30	200	150	200	15	150	30	100	50
36	67 29 37	160 53 42	.50	10.0	5.0	.05	100	10	N	N	30	N	10	(10
37	67 29 44	160 52 43	.70	.5	.1	.07	70	15	(20	5	50	30	200	70
38	67 29 48	160 52 43	.70	1.0	5.0	.05	30	30	200	7	70	15	100	70
39	67 29 51	160 52 40	2.00	5.0	5.0	.15	500	50	100	20	150	5	50	70
40	67 29 55	160 52 57	1.00	3.0	3.0	.07	700	50	N	5	50	10	20	100
41	67 29 55	160 52 59	.70	.5	1.0	.10	150	50	70	7	50	20	100	30
42	67 29 29	160 53 59	.70	15.0	7.0	.10	200	30	100	7	50	N	20	20
43	67 29 29	160 53 55	.70	.5	.1	.15	30	20	70	N	150	30	70	100
44	67 29 30	160 53 45	3.00	10.0	5.0	.20	200	70	N	15	150	N	100	70
45	67 29 31	160 53 35	1.50	5.0	2.0	.10	200	100	70	N	70	N	50	100
46	67 29 20	160 53 41	.50	7.0	10.0	.10	500	20	100	15	50	7	30	30
47	67 29 20	160 53 39	.70	1.0	1.0	.20	100	100	150	7	100	50	200	30
48	67 29 20	160 53 6	1.00	1.5	2.0	.10	500	30	100	N	150	30	70	50
49	67 29 50	160 51 41	.50	5.0	7.0	.10	70	(10	50	10	30	(0	15	30
50	67 29 50	160 51 42	.50	7.0	5.0	.07	100	N	20	5	20	N	10	20

APPENDIX A. OMAR SOIL SAMPLES--Continued

Sample	Sc	V	Y	Zr	La	Sr	As	Zn	Ag	Cd	Sb	Cu
1	N	(10	10	N	N	(100	90	1,100	.55	2.2	2	3,000
2	(5	50	N	N	N	N	20.	1,000	.20	5.8	2	420
3	15	200	15	70	N	100	40	500	.30	1.0	4	860
4	(5	15	15	(10	N	(100	80	270	.35	1.3	4	2,000
5	5	70	20	20	N	N	130	900	.75	1.7	6	2,000
6	5	100	N	20	N	N	220	1,300	4.10	3.4	10	1,100
7	7	30	15	30	N	N	10	25	(.05	.2	N	35
8	(5	15	N	15	N	N	10	20	N	N	N	10
9	5	20	15	70	N	N	N	30	.30	.2	N	10
10	30	200	15	15	N	N	20	60	.25	.2	N	170
11	(5	10	(10	(10	N	(100	(10	30	N	.1	N	15
12	20	150	10	30	N	N	20	55	.10	.3	N	130
13	7	20	20	50	N	100	(10	30	N	.2	N	10
14	7	15	15	30	N	150	10	50	N	.3	N	25
15	5	10	15	15	N	100	(10	120	N	.3	N	15
16	15	50	10	100	N	N	30	130	.20	1.0	2	60
17	(5	100	(10	50	N	N	30	370	N	.7	2	85
18	5	20	10	20	N	N	10	110	.10	.4	(2	30
19	10	50	15	50	N	N	(10	60	N	.2	N	80
20	10	190	15	150	N	N	20	80	N	.2	N	65
21	20	150	30	100	N	N	10	75	N	.4	N	65
22	20	300	50	150	50	N	20	160	.15	.3	(2	100
23	7	1,000	50	50	50	200	20	370	.30	2.7	4	70
24	10	2,000	70	70	100	100	30	460	.40	2.7	6	100
25	7	30	N	20	N	N	10	20	N	.2	N	20
26	7	1,500	70	70	70	700	20	390	.15	4.4	4	110
27	5	500	70	100	N	N	20	120	.60	.7	4	150
28	5	1,500	70	50	30	(0	40	350	.40	3.8	23	150
29	7	20	20	50	N	N	(10	45	(.05	.4	N	15
30	N	20	N	10	N	N	10	15	N	.1	N	10
31	N	20	N	50	N	N	10	30	N	.2	N	15
32	N	20	(10	15	N	N	10	25	N	.2	N	15
33	15	150	10	15	N	N	20	110	.10	.4	N	140
34	N	20	N	10	N	N	10	15	N	.1	N	15
35	10	500	50	(10	50	(0	20	190	.20	1.8	4	30
36	N	50	N	(10	N	N	(10	20	N	N	N	15
37	7	1,000	100	30	50	N	30	700	.90	4.8	4	220
38	5	300	50	10	50	(0	50	150	.60	2.4	2	160
39	7	150	20	70	N	N	40	280	.30	1.0	2	300
40	5	150	10	20	N	N	30	300	.20	.8	2	130
41	5	700	50	70	30	N	40	660	.50	6.3	4	140
42	7	100	N	20	N	N	10	45	N	.2	N	20
43	7	1,500	50	70	50	150	30	180	.80	3.0	2	120
44	10	150	15	70	N	N	20	20	.20	.2	2	30
45	5	100	N	30	N	N	20	65	N	.2	N	60
46	5	50	15	20	N	N	N	70	(.05	1.0	N	15
47	7	1,500	70	100	70	(0	20	410	.50	5.9	6	80
48	5	500	30	50	N	N	20	510	.50	6.8	4	100
49	5	20	10	30	N	N	(10	25	(.05	.2	N	10
50	7	15	10	15	N	N	(10	50	N	.1	N	10

APPENDIX A. OMAR SOIL SAMPLES--Continued

Sample	Latitude	Longitude	Fe	Mg	Ca	Ti	Mn	B	Ba	Co	Cr	Mo	Ni	Pb
51	67 29 52	160 51 55	.50	10.0	15.0	.10	100	(10	20	10	30	(0	50	20
52	67 29 54	160 52 8	.70	5.0	5.0	.10	700	200	100	50	150	10	70	70
53	67 29 57	160 52 35	.50	10.0	15.0	.10	100	(10	20	10	30	(0	50	20
54	67 29 59	160 52 40	.30	7.0	5.0	.03	300	N	(20	7	10	N	10	20
55	67 30 3	160 52 43	7.00	15.0	15.0	.07	500	N	30	5	15	N	20	(10
56	67 30 6	160 52 43	.50	15.0	15.0	.05	300	N	(20	N	30	N	10	(10
57	67 30 13	160 52 54	.15	3.0	3.0	.05	100	(10	(20	N	10	N	N	15
58	67 30 10	160 53 14	2.00	1.5	2.0	.20	300	70	100	20	100	N	70	20
59	67 30 7	160 53 30	3.00	3.0	3.0	.20	150	70	200	10	100	N	50	30
60	67 30 32	160 52 41	.30	10.0	5.0	.02	100	(10	N	N	10	N	N	10
61	67 30 32	160 52 45	.50	7.0	7.0	.03	70	(10	20	20	15	5	20	30
62	67 30 30	160 52 53	.50	5.0	3.0	.03	100	10	(20	N	20	N	5	10
63	67 30 27	160 52 59	2.00	2.0	3.0	.15	200	70	300	15	70	N	50	30
64	67 29 25	160 53 5	1.00	2.0	3.0	.07	200	70	150	N	50	N	20	20
65	67 30 15	160 52 57	2.00	2.0	3.0	.10	200	100	500	15	70	7	30	30
66	67 30 13	160 52 32	.20	7.0	5.0	.01	200	N	20	15	(10	N	10	20
67	67 30 13	160 52 31	1.00	.7	.2	.15	150	50	100	10	50	30	300	30
68	67 30 16	160 52 8	.30	5.0	5.0	.02	100	10	(20	N	20	N	20	(10
69	67 30 20	160 51 49	3.00	3.0	1.5	.30	150	100	50	15	150	10	30	50
70	67 30 22	160 51 38	.50	7.0	5.0	.05	100	10	(20	N	30	N	5	(10
71	67 30 23	160 51 37	.50	3.0	3.0	.02	100	10	(20	N	20	N	5	(10
72	67 30 32	160 51 13	2.00	1.5	5.0	.20	500	100	150	10	100	N	50	30
72	67 30 32	160 51 12	.70	3.0	3.0	.02	50	20	(20	N	20	N	(5	(10
74	67 29 30	160 52 36	5.00	7.0	10.0	.02	1,000	(10	20	300	20	15	70	300
75	67 29 31	160 52 35	1.00	5.0	5.0	.05	700	20	30	70	20	10	30	150
76	67 29 32	160 52 34	2.00	5.0	3.0	.15	700	70	100	50	50	15	50	70
77	67 29 32	160 52 32	1.50	5.0	7.0	.10	500	50	70	30	70	N	30	100
78	67 29 34	160 52 33	1.50	3.0	2.0	.10	200	30	(20	15	50	N	30	70
79	67 29 54	160 51 9	1.00	3.0	2.0	.07	150	.30	70	N	70	N	50	10
80	67 29 51	160 51 7	1.50	.7	.2	.15	200	50	100	7	50	N	20	15
81	67 30 7	160 53 31	.70	.3	.5	.07	100	20	100	N	50	10	70	15

APPENDIX A. OMAR SOIL SAMPLES--Continued

Sample	Sc	V	Y	Zr	La	Sr	As	Zn	Ag	Cd	Sb	Cu
51	5	15	10	20	N	N	N	120	(.05	.2	4	10
52	7	100	20	20	20	N	200	450	1.10	2.3	6	370
53	5	15	10	20	N	N	20	65	.10	.2	N	30
54	7	10	20	10	N	(100	(10	35	N	.1	N	20
55	5	70	30	30	N	N	(10	30	N	N	N	15
56	7	50	10	10	N	N	10	30	N	N	N	15
57	7	10	11	20	N	N	20	250	N	N	N	35
58	15	150	20	100	N	N	20	140	N	.5	N	60
59	15	150	20	70	N	N	10	10	N	N	N	80
60	N	20	11	10	N	N	10	160	N	.7	N	5
61	5	15	(10	10	N	N	10	50	(.05	.3	N	25
62	N	15	N	10	N	N	10	15	N	N	2	10
63	10	150	20	70	N	N	10	130	.10	.5	2	100
64	7	30	10	30	N	200	10	25	N	.1	N	40
65	10	100	10	50	N	N	20	250	N	1.0	N	180
66	15	10	10	(10	N	N	10	80	N	.3	N	20
67	10	1,000	100	100	70	N	30	600	.70	1.0	2	130
68	15	30	N	10	N	N	10	40	N	.3	N	15
69	10	100	20	70	(20	N	20	45	N	.2	N	25
70	15	20	N	50	N	N	10	15	N	N	N	5
71	15	15	N	10	N	N	10	15	N	N	N	5
72	15	70	20	70	N	200	10	40	N	.3	N	35
73	15	20	N	(10	N	N	10	20	N	.1	N	15
74	15	50	15	20	N	N	130	3,000	1.20	6.6	6	16,000
75	N	30	N	20	N	N	50	900	.40	2.3	2	2,500
76	10	100	20	70	N	N	30	400	.40	1.5	2	500
77	5	100	10	20	N	N	20	500	.20	.8	2	1,500
78	5	30	(10	50	N	N	20	250	.10	.6	N	520
79	5	200	11	15	N	N	10	80	.20	.6	N	30
80	10	100	10	70	N	N	10	35	N	.3	N	20
81	7	500	50	50	50	N	10	270	1.10	7.2	2	60

APPENDIX A. OMAR STREAM SEDIMENT SAMPLES

(N, not detected; (, detected but below the limit of determination shown); , determined to be greater than the value shown.)

Sample	Latitude	Longitude	Fe	Mg	Ca	Ti	Mn	B	Ba	Co	Cr	Cu
1	67 29 46	160 53 17	.7	7	10	.100	100	30	20	20	30	100
2	67 29 43	160 53 19	.5	15	10	.050	70	10	N	N	20	15
3	67 29 44	160 53 52	.5	7	5	.070	100	15	N	N	20	20
4	67 29 6	160 53 37	.2	15	5	.015	30	N	N	N	10	5
5	67 30 40	160 52 10	.5	7	7	.030	70	N	(20	7	15	5
6	67 30 42	160 52 3	.3	7	10	.015	100	N	(20	5	15	15
7	67 30 48	160 52 52	.5	15	25	.050	150	N	N	N	(10	N
8	67 30 50	160 52 42	.3	15	5	.020	30	N	N	N	10	5
9	67 30 46	160 53 52	.2	10	7	.020	70	(10	(20	N	10	10
10	67 30 41	160 53 50	.5	15	15	.050	150	(10	N	N	20	7
11	67 30 40	160 53 59	.7	7	7	.070	150	30	30	5	50	70
12	67 30 52	160 53 59	.5	10	7	.050	70	15	N	N	20	10
13	67 30 14	160 54 7	1.0	5	7	.150	300	100	200	5	70	50
14	67 30 0	160 53 19	1.0	10	10	.100	300	20	30	15	30	70
15	67 30 1	160 53 21	1.3	3	3	.150	200	70	150	20	70	70
16	67 29 59	160 53 25	2.0	7	3	.150	300	50	70	30	100	200
17	67 29 55	160 53 31	1.0	5	10	.200	200	(10	50	20	50	30
18	67 29 27	160 51 46	2.0	2	5	.200	150	70	200	20	100	15
19	67 29 36	160 52 18	2.0	3	5	.200	150	100	200	20	150	30
20	67 29 50	160 53 5	2.0	7	10	.150	300	50	100	10	100	50
21	67 29 54	160 53 15	1.5	5	7	.100	150	10	70	15	70	50
22	67 29 8	160 53 49	1.0	7	7	.100	200	50	30	N	70	20
23	67 29 13	160 53 56	.5	5	7	.070	100	(10	50	10	50	20
24	67 29 22	160 54 1	1.0	15	10	.070	150	15	20	N	30	10
25	67 29 34	160 54 6	.7	15	7	.070	100	20	(20	N	50	10
26	67 29 39	160 52 33	5.0	10	10	.300	700	100	500	70	100	1,500
27	67 29 33	160 52 23	1.5	7	5	.150	200	20	150	50	50	700
28	67 29 32	160 52 21	1.5	5	10	.100	300	10	150	50	50	700
29	67 29 44	160 52 22	2.0	7	7	.070	700	20	70	100	70	1,000
30	67 29 46	160 52 12	1.0	7	3	.050	300	(10	(20	30	30	300
31	67 29 49	160 52 14	2.0	15	7	.100	300	30	50	50	100	500
32	67 29 43	160 52 11	.7	10	10	.100	150	30	20	15	30	30
33	67 29 48	160 52 15	.5	2	2	.070	200	10	20	30	50	200
34	67 29 33	160 51 57	.2	5	5	.020	50	(10	(20	7	10	20
35	67 29 38	160 51 32	.3	7	7	.030	70	N	(20	5	20	10
36	67 29 38	160 51 27	.7	10	15	.100	200	10	50	7	30	15
37	67 30 0	160 52 6	.3	5	3	.010	100	N	N	N	15	30
38	67 30 2	160 52 5	1.5	15	15	.100	300	20	20	10	100	30
39	67 30 0	160 51 37	1.0	15	10	.070	100	20	N	N	50	10
40	67 29 59	160 51 27	.5	7	7	.070	70	10	20	10	30	10
41	67 29 12	160 50 16	1.5	7	10	.100	100	20	300	15	50	10
42	67 29 31	160 50 40	1.0	15	10	.150	300	30	(20	5	70	15
43	67 29 37	160 50 51	.7	7	7	.100	500	70	100	N	70	30
44	67 29 51	160 50 54	3.0	10	7	.200	300	150	30	20	150	20

APPENDIX A. OMAR STREAM SEDIMENT SAMPLES--Continued

Sample	Ni	Pb	Sc	Sr	V	Y	Zr	As	Zn	Ag	Cd
1	50	50	5	150	70	15	20	10	95	N	.7
2	10	10	N	N	<10	N	10	10	20	N	.1
3	20	30	N	N	70	N	10	10	45	N	.3
4	5	<10	N	N	20	N	<10	<10	10	N	N
5	10	20	5	<100	10	<10	10	N	20	N	.2
6	5	10	5	150	<10	N	<10	<10	10	N	.3
7	5	N	N	N	20	N	10	<10	10	N	N
8	15	<10	N	N	<10	N	N	10	10	N	N
9	10	15	5	<100	20	10	<10	N	20	N	.2
10	15	10	N	N	30	N	10	N	15	N	N
11	50	15	5	<100	200	N	<10	10	130	.10	1.8
12	7	<10	N	N	30	N	<10	10	20	N	N
13	50	15	5	150	150	15	50	<10	65	N	.1
14	20	50	N	N	100	10	20	20	130	N	.3
15	50	50	7	100	150	20	30	20	210	N	1.9
16	70	70	7	N	200	30	30	20	190	.15	1.2
17	15	30	7	100	50	20	30	10	100	N	.5
18	50	20	10	150	70	15	50	N	70	N	.4
19	50	20	10	200	70	15	50	<10	65	N	.3
20	50	20	10	200	150	15	50	10	100	N	.5
21	50	30	7	300	70	20	20	10	130	N	.8
22	50	20	N	N	200	15	15	10	110	.20	1.6
23	50	20	5	150	150	20	20	10	100	N	1.3
24	20	10	N	100	150	N	20	10	45	N	.3
25	30	15	N	N	200	N	10	10	70	N	.7
26	100	150	15	N	200	30	100	40	800	.40	2.7
27	20	70	7	N	20	15	20	50	360	.30	.7
28	30	100	7	150	20	15	20	40	370	.35	1.5
29	70	70	5	150	200	20	10	100	32	.35	1.5
30	20	50	5	N	30	15	15	60	200	.15	1.0
31	100	100	5	N	700	15	30	80	350	.30	1.5
32	15	30	N	N	100	<10	20	10	40	N	N
33	30	50	5	N	100	10	15	50	370	.20	1.6
34	10	20	5	N	15	<10	<10	<10	50	N	.3
35	15	20	5	<100	30	10	<10	<10	40	N	.3
36	15	20	5	150	50	20	20	<10	40	N	.5
37	10	10	N	N	50	N	N	10	55	N	.1
38	70	30	5	N	500	20	20	10	140	.10	1.3
39	20	15	N	N	50	N	15	<10	30	N	N
40	15	20	5	<100	15	10	20	<10	20	N	1.1
41	20	30	7	150	30	20	50	<10	60	N	.4
42	20	10	5	N	100	<10	50	10	10	N	N
43	20	30	7	100	150	15	50	20	80	N	.5
44	20	20	15	N	300	30	70	10	65	N	.2

Appendix B.

Analytical Procedure and Equipment for ROCK-EVAL Pyrolysis by EXLOG Laboratories, Anchorage, Alaska

Sample Preparation

Samples were washed with cold, clean water and dried. Three to four grams of sample were crushed and prepared for analysis. One gram of sample was heated for three hours at 600 C in approximately 3M hydrochloric acid to remove any carbonates (inorganic carbon source). Residual mixture was vacuum filtered onto a glass fiber mat. The solid residue and mat were washed with approximately 100 ml of clean water to remove any excess acid. Samples were then dried in a warm (800 C) oven for one hour.

Analytical Equipment

1. Leco CR12 Carbon Determinator
2. Geocom Source Rock Analyzer

Analytical Cycle

Carrier Gas--Helium

Initial Isothermal Temperature--300o C

Isothermal Hold--3 minutes

Temperature Ramp--25o/minute

Final Isothermal Temperature--550o C

CO2 Trap Close--390o C

The Rock-Eval was calibrated using EXLOG's EL-5 standard. Standard and blank calibrations were run every 10 samples.